VOLUME 33 MARCH 1955 NUMBER 3

Canadian Journal of Chemistry

Editor: LÉO MARION

Associate Editors:

HERBERT C. BROWN, *Purdue University*
A. R. GORDON, *University of Toronto*
C. B. PURVES, *McGill University*
Sir ERIC RIDEAL, *King's College, University of London*
J. W. T. SPINKS, *University of Saskatchewan*
E. W. R. STEACIE, *National Research Council of Canada*
H. G. THODE, *McMaster University*
A. E. VAN ARKEL, *University of Leiden*

Published by THE NATIONAL RESEARCH COUNCIL

OTTAWA CANADA

CANADIAN JOURNAL OF CHEMISTRY

(Formerly Section B, Canadian Journal of Research)

Under the authority of the Chairman of the Committee of the Privy Council on Scientific and Industrial Research, the National Research Council issues THE CANADIAN JOURNAL OF CHEMISTRY and six other journals devoted to the publication, in English or French, of the results of original scientific research. Matters of general policy concerning these journals are the responsibility of a joint Editorial Board consisting of: members representing the National Research Council of Canada; the Editors of the Journals; and members representing the Royal Society of Canada and four other scientific societies.

The Chemical Institute of Canada has chosen the Canadian Journal of Chemistry and the Canadian Journal of Technology as its medium of publication for scientific papers.

EDITORIAL BOARD

Representatives of the National Research Council

A. N. Campbell, *University of Manitoba*
G. E. Hall, *University of Western Ontario*
E. G. D. Murray, *McGill University*
D. L. Thomson, *McGill University*
W. H. Watson (Chairman), *University of Toronto*

Editors of the Journals

D. L. Bailey, *University of Toronto*
J. B. Collip, *University of Western Ontario*
E. H. Craigie, *University of Toronto*
G. A. Ledingham, *National Research Council*
Léo Marion, *National Research Council*
R. G. E. Murray, *University of Western Ontario*
G. M. Volkoff, *University of British Columbia*

Representatives of Societies

D. L. Bailey, *University of Toronto*
Royal Society of Canada
J. B. Collip, *University of Western Ontario*
Canadian Physiological Society
E. H. Craigie, *University of Toronto*
Royal Society of Canada
R. G. E. Murray, *University of Western Ontario*
Canadian Society of Microbiologists
H. G. Thode, *McMaster University*
Chemical Institute of Canada
T. Thorvaldson, *University of Saskatchewan*
Royal Society of Canada
G. M. Volkoff, *University of British Columbia*
Royal Society of Canada; Canadian Association of Physicists

Ex officio

Léo Marion (Editor-in-Chief), *National Research Council*

Manuscripts for publication should be submitted to Dr. Léo Marion, Editor-in-Chief, Canadian Journal of Chemistry, National Research Council, Ottawa 2, Canada.
(For instructions on preparation of copy, see **Notes to Contributors** (inside back cover).)

Proof, correspondence concerning proof, and orders for reprints should be sent to the Manager, Editorial Office (Research Journals), Division of Administration, National Research Council, Ottawa 2, Canada.

Subscriptions, renewals, requests for single or back numbers, and all remittances should be sent to Division of Administration, National Research Council, Ottawa 2, Canada. Remittances should be made payable to the Receiver General of Canada, credit National Research Council.

The journals published, frequency of publication, and prices are:

Canadian Journal of Biochemistry and Physiology	Bimonthly	$3.00 a year
Canadian Journal of Botany	Bimonthly	$4.00 a year
Canadian Journal of Chemistry	Monthly	$5.00 a year
Canadian Journal of Microbiology*	Bimonthly	$3.00 a year
Canadian Journal of Physics	Monthly	$4.00 a year
Canadian Journal of Technology	Bimonthly	$3.00 a year
Canadian Journal of Zoology	Bimonthly	$3.00 a year

The price of single numbers of all journals is 75 cents.

*Volume 1 will combine three numbers published in 1954 with six published in 1955 and will be available at the regular annual subscription rate of $3.00.

Reprinted in entirety by photo-offset from the original issue.

Canadian Journal of Chemistry

Issued by THE NATIONAL RESEARCH COUNCIL OF CANADA

VOLUME 33 MARCH 1955 NUMBER 3

ORGANIC FLUORINE COMPOUNDS

I. AN IMPROVED SYNTHESIS OF HEXAFLUOROACETONE[1]

BY A. T. MORSE, P. B. AYSCOUGH, AND L. C. LEITCH

ABSTRACT

The synthesis of hexafluoroacetone reported recently by Brice, Lazerte, Hals, and Pearlson has been improved in several particulars. Teflon was depolymerized to tetrafluoroethylene which was then dimerized to give a 50% yield of perfluoroisobutene in one step. Oxidation of the latter at 35–40°C. with aqueous potassium permanganate gave a 75% yield of hexafluoroacetone hydrate. The vapor pressure of hexafluoroacetone was measured between −60° and −28°C.

Hexafluoroacetone was first obtained by Fukuhara and Bigelow (2) among the products of the direct fluorination of acetone. It was subsequently prepared by Henne, Shepherd, and Young (3) by the oxidation of the chlorofluoroolefin $(CF_3)_2C=CCl_2$. While the yield of ketone is satisfactory, the preparation of the olefin is tedious and involves hydrofluorination at one stage. Brice, Lazerte, Hals, and Pearlson (1) recently obtained a 26% yield of hexafluoroacetone by the oxidation of perfluoroisobutene prepared by the thermal isomerization of perfluorocyclobutane. The latter was presumably prepared by polymerization of tetrafluoroethylene at 500°C. as reported by Miller (5).

It occurred to us that perfluoroisobutene might be obtained in one step from tetrafluoroethylene. The use of teflon was later suggested to us in a letter from Dr. W. H. Pearlson of the Minnesota Mining and Manufacturing Company, St. Paul, Minn. A furnace, described by one of us in an earlier paper (4), having three independent elements which permit the temperature to be controlled at different points appeared to be suitable for the preparation of perfluoroisobutene. Teflon was depolymerized at 450°C. to tetrafluoroethylene in the first section of the furnace and then dimerized to a mixture of perfluorobutenes by heating the monomer to 700°C. in the second and third sections. A 62% yield of fluorobutenes consisting of 85% perfluoroisobutene was thus obtained; the 2-isomer was formed to the extent of only 15%. These figures were arrived at by comparing the infrared spectrum of our product with the spectra of the pure compounds reported in the paper by Pearlson and co-workers (1).

The perfluorobutenes were oxidized with alkaline permanganate in the apparatus illustrated in the experimental part at 35 to 40°C. instead of in an auto-

[1]*Manuscript received November 16, 1954.*
Contribution from the Division of Pure Chemistry, National Research Council, Ottawa, Ontario, Canada. Issued as N.R.C. No. 3512.

clave at 100°C. as reported by Pearlson and co-workers. The yield of hexafluoroacetone hydrate was 70 to 80% of the theoretical amount. The dehydration to hexafluoroacetone was carried out according to the directions of Henne and co-workers (3). These authors reported the formation of a white solid during the dehydration of hexafluoroacetone hydrate which gave a semicarbazone melting very near hexafluoroacetone semicarbazone prepared from the hydrate. In the present work this substance was also detected when the hexafluoroacetone was fractionated on the vacuum line. It gives a mass spectrum identical with that of hexafluoroacetone. When sealed in a glass tube it can be sublimed by merely applying the heat of the hand. The sub-

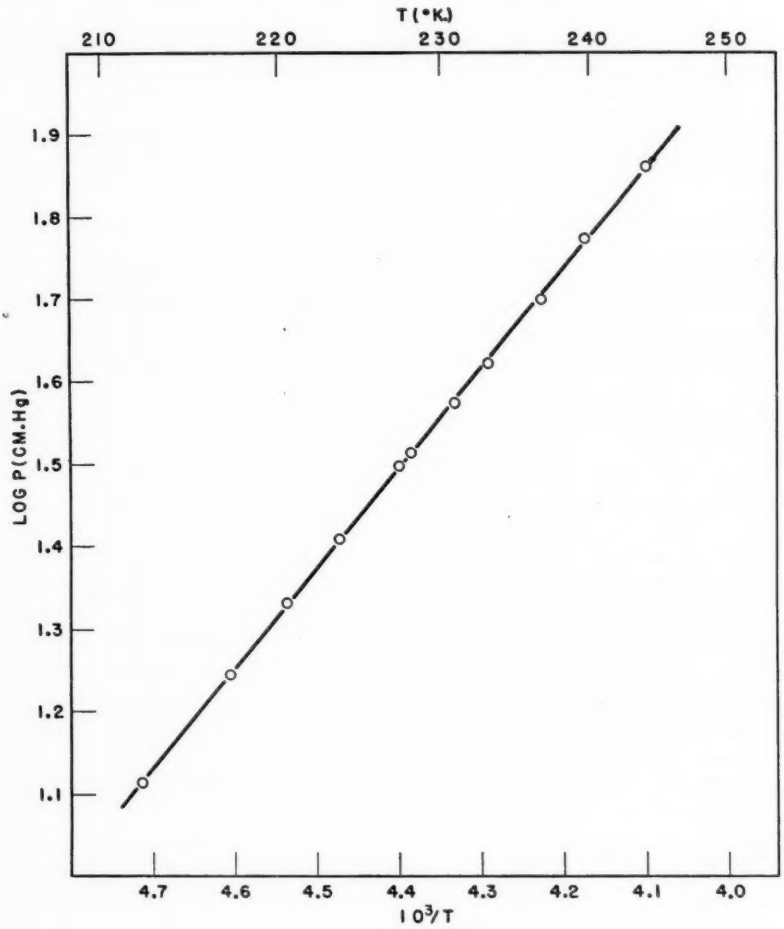

FIG. 1. Vapor pressure of hexafluoroacetone.

stance is considered to be a polymeric form of hexafluoroacetone and is provisionally assigned the structure I.

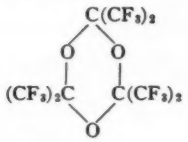

I

The vapor pressure of a sample of hexafluoroacetone purified by fractionation on the vacuum line was measured by the static method described in an earlier paper (4). The line shown in Fig. 1 gives the expression

$$\log p \text{ (mm.)} = 6.8060 - [(1.2074 \times 10^3)/T]$$

for the vapor pressure of hexafluoroacetone between -60°C. and -28°C.

EXPERIMENTAL

Perfluoroisobutene

The furnace used in this experiment was referred to in the Introduction. Teflon (200 gm.) cut into small pieces was placed at one end of the reactor while the other end was connected to a 150 ml. spiral trap cooled to -78°C. The section of the furnace containing the teflon was slowly heated to 450°C. while the temperature of the other two units was kept at 700–725°C. After two hours the temperature of the first section was raised to 550°C. to complete the depolymerization of the teflon. At the end of the experiment the trap contained 110 ml. of yellow liquid which was fractionated on the vacuum line. Forty milliliters of material with a very high vapor pressure, consisting chiefly of perfluoropropene, were distilled off. The remainder (70 ml.), which had a vapor pressure of 40 mm. at -78°C., was collected in another trap. Yield: 125 gm. By infrared analysis this product was found to contain 85% perfluoroisobutene, i.e. 106 gm., and 15% perfluorobutene-2.

Hexafluoroacetone Hydrate

The apparatus used in the oxidation is shown in Fig. 2. Potassium permanganate (300 gm.) and 1200 ml. of water were placed in the 3-liter reaction flask *B*. The fluoro-olefin (95 ml., 165 gm.) was condensed into the trap *A* which was then connected to the bubbler immersed in the permanganate solution. The contents of the flask were agitated by means of a magnetic stirrer. The temperature of the fluoro-olefin was raised to about 10°C. and maintained there while the vapor bubbled slowly into the permanganate solution. The rate of flow could be readily controlled by varying the temperature of the bath surrounding the olefin. Hexafluoroacetone hydrate produced by the oxidation remained in solution while unchanged perfluoroisobutene was returned to the flask by the cold finger *C* which was kept at -80°C. The carbon dioxide which was produced simultaneously passed into the atmosphere, any fluoro-olefin which it carried over being condensed in a second trap (*D*)

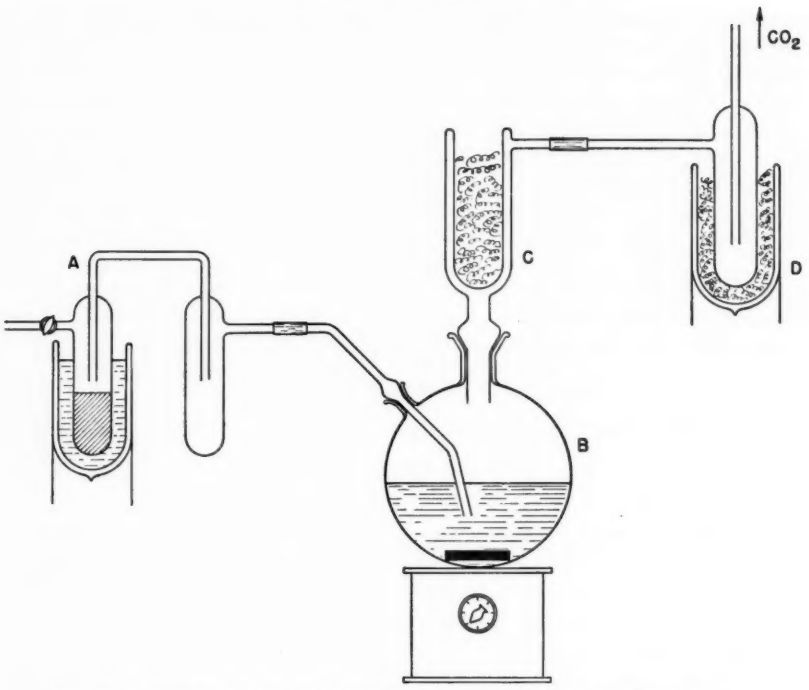

FIG. 2. Apparatus for the oxidation of perfluoroisobutene to hexafluoroacetone.

maintained at −80°C. Reaction was slow at first but became more rapid as the temperature increased to 35–40°C. The fluoro-olefin was absorbed at the rate of 20–25 gm. per hour.

The reaction mixture was then treated with sulphur dioxide to remove excess permanganate and the mixture filtered with suction. The precipitate on the filter was washed with 500 ml. of water and discarded. The combined filtrates were extracted with ether in a continuous extraction apparatus for 24 hr. The ether extract was separated, dried over sodium sulphate, and freed of solvent. The residue was fractionated under reduced pressure. The yield of hexafluoroacetone hydrate, b.p. 55–6°C. at 80 mm., n_D^{20} 1.3179 was 108 gm. (72% of the theoretical amount).

Hexafluoroacetone

The hydrate was treated with phosphorus pentoxide as directed by Henne, Shepherd, and Young (3). A middle fraction of 5.0 ml. from a total of 7.5 ml. of hexafluoroacetone was collected separately on the vacuum line. It distilled at a constant pressure of 32.6 mm. at −78°C. The vapor pressure of this fraction was measured at several temperatures, between −60°C. and −28°C. by the static method (4), and the values plotted logarithmically in

Fig. 2. The mass spectrum of the product was identical with that of Pearlson and co-workers (1).

ACKNOWLEDGMENT

The authors are extremely grateful to Dr. W. H. Pearlson of the Minnesota Mining and Manufacturing Company for a generous sample of hexafluoroacetone and suggestions.

REFERENCES

1. BRICE, T. J., LAZERTE, J. D., HALS, L. J., and PEARLSON, W. H. J. Am. Chem. Soc. 75: 2698. 1953. U.S. Patent No. 2,617,836. November, 1952.
2. FUKUHARA, N. and BIGELOW, L. A. J. Am. Chem. Soc. 63: 788. 1941.
3. HENNE, A. L., SHEPHERD, J. W., and YOUNG, E. J. J. Am. Chem. Soc. 72: 3577. 1950.
4. LEITCH, L. C. and RENAUD, R. Can. J. Chem. 30: 79. 1952.
5. MILLER, W. T. Chap. 32, p. 592. SLESSER, C. and SCHRAM, S. R. *In* Preparation, properties and technology of fluorine and organic fluoro compounds. Natl. Nuclear Energy Ser. Div. VII, Vol. I. McGraw-Hill Book Company, Inc., New York. 1951.

THE SYNTHESIS OF HEMOPYRROLE-DICARBOXYLIC ACID AND OF SOME DIPYRROMETHENES[1]

By S. F. MacDonald and R. J. Stedman[2]

ABSTRACT

The pyrrole II*e* was obtained through the known II*c* and hydrolyzed to III*b*. This last could be partially decarboxylated to hemopyrrole-dicarboxylic acid III*c* or, with formic acid, converted into the dipyrromethene VII*b*. The isomeric dipyrromethene VII*a* was obtained analogously.

Of the two key pyrroles related to the uroporphyrins, cryptopyrrole-dicarboxylic acid I*a* has already been synthesized (10). The synthesis of the second of these, hemopyrrole-dicarboxylic acid III*c*, is now reported.

With ethyl cyanoformate and hydrogen chloride, the pyrrole II*c* (10), for which an improved preparation is given, gave the glyoxylic ester II*d*. Consistently high yields were obtained only when the usual conditions (cf. (6)) were modified to ensure that the intermediate ketimine hydrochloride crystallized. The glyoxylic ester was catalytically reduced in acetic–sulphuric acid over palladium black (cf. (9)) to II*e*, which Treibs and Ott have obtained from II*c* by a different route (13). When this reduction was attempted with W-6 Raney nickel in refluxing ethanol (cf. (12)), with hydrogen (cf. (15)) at 130–150° and 3000 to 4000 lb. per sq. in. in ethanol over copper chromite (1), or with zinc dust in boiling acetic acid, the only product isolated was II*c* identified by melting point and mixed melting point, the positive Ehrlich's reaction in the cold, and, in the first case, by analysis for C, H, and N. The loss of an acyl group on catalytic reduction was unexpected but is not without analogy (cf. (8)).

Alkaline hydrolysis of II*e* resulted in III*a* or in III*b*, differing in their Ehrlich's reactions. These structures were confirmed by decarboxylating the latter to the known hemopyrrole-carboxylic acid IV*a*. With water at 100°, III*b* gave a dicarboxylic acid which could not be directly shown to be III*c* rather than IV*b*, for the latter is known only as a half-ester (7*b*). Under these conditions I*a* had been obtained from I*b* (10) and IV*b* would be expected to lose its α-carboxy group. Further, the dimethyl ester of the dicarboxylic acid gave a strongly positive Ehrlich's reaction in the cold, behavior consistent with III*c* but not with IV*b*. However, the dicarboxylic acid was shown definitely to be hemopyrrole-dicarboxylic acid III*c* by conversion of its dimethyl ester into V*e* (see below) with phosgene and methanol (cf. (7*c*)).

As the preparation of the intermediates might have proved more convenient using the higher-melting methyl esters, methyl α-oximino-β-ketoadipate and benzyl acetoacetate were combined in the Knorr synthesis to give V*a*, which

[1]*Manuscript received November 8, 1954.*
Contribution from the Division of Pure Chemistry, National Research Council, Ottawa, Canada. Issued as N.R.C. No. 3513. Reported in part at the Seminar in the Chemistry of Natural Products, University of New Brunswick, August, 1953, and in a preliminary communication (11).
[2]*National Research Council of Canada Postdoctorate Fellow.*

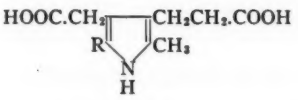

I*a*, R = H
b, R = COOH

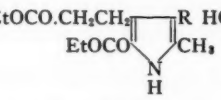

II*a*, R = $COOCH_2.C_6H_5$
b, R = COOH
c, R = H
d, R = CO.COOEt
e, R = CH_2.COOEt

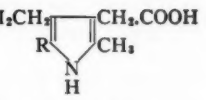

III*a*, R = COOEt
b, R = COOH
c, R = H

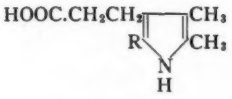

IV*a*, R = H
b, R = COOH

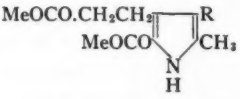

V*a*, R = $COOCH_2.C_6H_5$
b, R = COOH
c, R = H
d, R = CO.COOMe
e, R = CH_2.COOMe

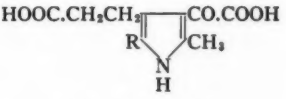

VI*a*, R = COOEt
b, R = COOH

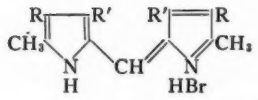

VII*a*, R = $CH_2CH_2.COOH$; R′ = CH_2.COOH
b, R = CH_2.COOH; R′ = CH_2CH_2.COOH

was converted into V*b*, V*c*, V*d*, and V*e*. The structures of these were confirmed by relating V*d* and V*e* to the ethyl esters for which there was independent analytical proof. Thus II*d* could be hydrolyzed either to VI*a* or VI*b*, and the latter gave V*d* with diazomethane; similarly II*e* was hydrolyzed to III*b*, which was converted into V*e* with diazomethane.

Two better methods were found for converting ethyl β-keto-α-carbethoxy-adipate into ethyl β-ketoadipate (cf. (5, 14)), an intermediate in the preparation of II*a*: the triester was allowed to stand with sulphuric acid, and alcohol added to the mixture, or the triester was boiled with water (cf. (4, 2)). To obtain the methyl β-ketoadipate of Bardhan (3) required in the synthesis of V*a*, β-carbomethoxy-propionyl chloride and the ethoxymagnesium derivative of ethyl malonate gave methyl δ,δ-dicarbethoxylevulinate, which was converted into β-ketoadipic acid with hydrochloric acid (cf. (5)), and the acid esterified.

Both the pyrroles I*b* and III*b* reacted normally with formic acid and hydrogen bromide at 100° (cf. (7*d*)) to give the dipyrromethenes VII*a* and VII*b* respectively. At lower temperatures, the hydrobromides of I*a* and III*c* were the predominant products (16).

EXPERIMENTAL

2-Methyl-5-carboxypyrrole-4-(propionic acid) Diethyl Ester, IIc

Up to 500 gm. of the benzyl ester II*a* have been hydrogenated in 1 liter of ethanol in a 3 liter autoclave as previously described (10). The mixture of crude acid II*b* and catalyst (277 gm.) from 378 gm. of the benzyl ester II*a* was dry distilled in two lots at 230° rising to 260° (air bath temperatures) under the water-pump vacuum (initially and finally 15 mm.). The pyrrole II*c* rapidly

solidified in the air condenser. It was recrystallized from pentane by extraction (Soxhlet) giving 155 gm. (63% from the benzyl ester), m.p. 67-67.5° (cf. (10)).

2-Methyl-5-carboxypyrrole-3-(glyoxylic acid)-4-(propionic acid) Triethyl Ester, IId

The pyrrole II*c* (45 gm.) in ethyl cyanoformate (45 ml.), dry ether (150 ml.), and chloroform (50 ml., dry and alcohol free) was stirred in an ice–salt bath and protected from moisture while dry hydrogen chloride was passed in for three hours. Dry air was then passed through without cooling until the mixture was largely crystalline. Ether (100 ml.) was added, the mixture kept at 0° overnight, the ketimine hydrochloride filtered off, washed with ether, dried *in vacuo*, and dissolved in ice-water (3 liters). After several hours, the glyoxylic ester was filtered off and washed with water. It was dissolved in alcohol, filtered with charcoal, and the charcoal washed with alcohol. After the filtrate and washings (110 ml.) were diluted with 85 ml. of water and allowed to stand at 25° then at 0°, 53 gm., m.p. 78–79°, were collected. The mother liquors diluted with 100 ml. of water and allowed to stand as above gave 4.8 gm., m.p. 77–78° (total, 92% as used for reduction). For analysis, the ester was recrystallized twice and dried *in vacuo*, forming colorless needles, m.p. 78.5°–79°. Ehrlich's reaction slowly positive hot. Found: C, 57.64; H, 6.72; N, 4.01%. Calc. for $C_{17}H_{23}O_7N$: C, 57.78; H, 6.56; N, 3.96%.

2-Methyl-5-carboxypyrrole-3-(acetic acid)-4-(propionic acid) Triethyl Ester (Ethyl α-Carbethoxyhemopyrrole-dicarboxylate), IIe

The glyoxylic ester II*d* (24 gm.) in acetic acid (100 ml.) and sulphuric acid (3.75 ml.) was shaken for six hours with palladium black (1.2 gm., freshly prepared (17)) under hydrogen (60 lb. per sq. in.) at 27°. After the theoretical uptake in two hours, absorption nearly ceased. The filtrate and washings from the catalyst were added to ice-water (3 liters) containing sodium bicarbonate (70 gm.), seeded, and left at 0° overnight. The solid was filtered off, washed, and dried. The acidified filtrate was extracted once with ether, and the ether evaporated from the extract.

Three reductions, using 57.8 gm. glyoxylic ester, were worked up together. When the solid was extracted with pentane (Soxhlet) most of the product crystallized from the pentane. More was obtained by combining the partially hydrolyzed pentane-insoluble material with the residue from the ether extract, esterifying it with 5% ethanolic hydrogen chloride at 25° overnight, pouring it into ice water, and extracting the dried solid with pentane (Soxhlet). Yield 44 gm. (79%), long colorless needles, m.p. 63–64°, or prisms, m.p. 64–65°. Ehrlich's reaction negative cold but positive hot. For analysis, it was recrystallized three times from aqueous ethanol and dried *in vacuo*, needles m.p. 63–64°. Found: C, 59.98; H, 7.26; N, 4.26%; mol. wt. (Rast) 333. Calc. for $C_{17}H_{25}O_6N$: C, 60.16; H, 7.43; N, 4.13%; mol. wt. 339.

When less active palladium black was used, the yield fell to about 50%.

This pyrrole and the isomeric ethyl α-carbethoxycryptopyrrole-dicarboxylate (10) were not clearly distinguished by their melting points or by their infrared

spectra in carbon disulphide. However, their mixed melting point showed a depression.

α-Carboxyhemopyrrole-dicarboxylic Acid, IIIb

The triethyl ester IIe (2 gm.) in ethanol (25 ml.) and 10% sodium hydroxide (25 ml.) was heated for two and a half hours on the steam bath in an open flask. The solvent was removed *in vacuo*, the residual gum dissolved in water (25 ml.), warmed, and filtered with charcoal, and the product (1.27 gm., 84%), a yellow powder m.p. 144–145° (decomp.), precipitated with sulphur dioxide at 0° and washed with ice-water. After three recrystallizations from acetone (dried over potassium carbonate) (thimble) it formed small very pale violet needles, m.p. 155–156° (decomp.), Ehrlich's reaction strongly positive cold. Found in material dried *in vacuo*: C, 51.29; H, 5.36; N, 5.54%. Calc. for $C_{11}H_{13}O_6N$: C, 51.76; H, 5.13; N, 5.49%. It is stable when kept under nitrogen, or *in vacuo* over phosphorus pentoxide.

Hemopyrrole-dicarboxylic Acid, IIIc

The crude tricarboxylic acid IIIb (0.802 gm., m.p. 148°) in water (3 ml.) was heated under nitrogen on the steam bath to solution and cessation of effervescence (*ca.* 15 min.). After the solution was cooled to 0°, the product (0.544 gm., 84%) was collected and washed with a little ice-water, as very pale pink prisms, m.p. 150–150.5° (decomp.), Ehrlich's reaction positive cold, no insoluble picrate was formed in wet ether. After three recrystallizations from water (4 ml.) the melting point was unchanged. Found in material dried *in vacuo* and stored over nitrogen: C, 56.78; H, 6.26; N, 6.82%. Calc. for $C_{10}H_{13}O_4N$: C, 56.86; H, 6.20; N, 6.63%.

Dimethyl Hemopyrrole-dicarboxylate[3]

Hemopyrrole-dicarboxylic acid IIIc (3.05 gm.) was allowed to stand overnight with a cooled ethereal solution of diazomethane. After removing the ether *in vacuo*, the crystalline residue was distilled (135°, 5×10^{-5} mm.). The ester (3.33 gm., 96%) formed yellow crystals, m.p. 50–51°, raised to 51°–52.5° by resublimation, Ehrlich's reaction strongly positive cold. Found: C, 60.39; H, 7.35; N, 6.03%. Calc. for $C_{12}H_{17}O_4N$: C, 60.23; H, 7.16; N, 5.86%.

Unless protected from light and stored *in vacuo* or under nitrogen, the product turns red.

Conversion of Dimethyl Hemopyrrole-dicarboxylate to 2-Methyl-5-carboxypyrrole-3-(acetic acid)-4-(propionic acid) Trimethyl Ester, Ve

Dimethyl hemopyrrole-dicarboxylate (2.11 gm., distilled in high vacuum at 110–115°) was dissolved in dry ether (70 ml.), cooled in ice-water, and treated with a rapid stream of phosgene for 15 min. The solution initially became cloudy, but rapidly cleared and darkened. After one and a quarter hours at room temperature the ether and excess phosgene were removed by a stream of dry air, and the crystalline residue was briefly dried *in vacuo* and dissolved in dry methanol (50 ml.). Evaporation under reduced pressure after 60 hr. gave a

[3]*This preparation is due to Dr. K. H. Michl.*

dark gum which rapidly crystallized and was freed from hydrogen chloride by drying *in vacuo* over potassium hydroxide. Recrystallization from 15 ml. of methanol and 30 ml. of water (charcoal) gave the trimethyl ester (2.30 gm., 87%) as light brown crystals, m.p. 91°–91.5°.

A further crystallization from methanol–water gave light yellow plates, melting point unchanged, undepressed by authentic V*e* (see below), and indistinguishable from it by its infrared spectrum in carbon disulphide. The Ehrlich's reaction was positive hot. Found, in material recrystallized from pentane (thimble) and dried at 60° *in vacuo*: C, 56.77; H, 6.55; N, 4.83%. Calc. for $C_{14}H_{19}O_6N$: C, 56.56; H, 6.44; N, 4.71%.

Hemopyrrole-carboxylic Acid, IVa, from α-Carboxyhemopyrrole-dicarboxylic Acid, IIIb

The tricarboxylic acid III*b* (0.583 gm., m.p. 155°) in glycerol was heated under nitrogen at 200° for 15 min. After the mixture was poured into water (100 ml.) and extracted with ether (4 × 25 ml.), the extract was washed with water (25 ml.), dried over sodium sulphate, and the ether evaporated. The crystalline residue on sublimation (100°, 5×10^{-4} mm.) gave cream colored crystals (0.224 gm., 58%), m.p. 120–125°. After three crystallizations from water it formed cream colored rectangular plates, m.p. 127–128° (lit. 130–131° (7*a*)), Ehrlich's reaction positive cold. Found in material stored under nitrogen: C, 64.60; H, 8.06; N, 8.65%. Calc. for $C_9H_{13}O_2N$: C, 64.65; H, 7.83; N, 8.38%.

Methyl Hemopyrrole-carboxylate

Hemopyrrole-carboxylic acid (77 mgm., m.p. 128–129°, from III*b*) was added to ethereal diazomethane (from 2 gm. nitrosomethylurea) under nitrogen. After one hour the ether solution was washed with dilute hydrochloric acid, the acid neutralized with sodium bicarbonate and washed with ether, the ether washed twice with water and dried over sodium sulphate. The dark crystalline residue left after evaporation of the ether was sublimed (50–60°, 10^{-3} mm.) giving methyl hemopyrrole-carboxylate as colorless prisms (31.5 mgm., 38%), m.p. 48–51°; after recrystallization from aqueous methanol, colorless plates, m.p. 49–51°, were obtained.

The methyl ester picrate, long chocolate-brown prisms, m.p. 118.5–120° (lit. 121–122° (7*a*)) was obtained from the ester with picric acid in wet ether.

The methyl ester, regenerated from the picrate with ether and aqueous sodium bicarbonate, melted at 50–53° (lit. 57° (7*a*)) after sublimation.

α-Carbethoxyhemopyrrole-dicarboxylic Acid, IIIa

The triethyl ester II*e* (1.94 gm.) in 20 ml. of ethanol and 14.2 ml. of 0.889 *N* sodium hydroxide (2.2 equiv.) was heated for two hours in an open flask on the steam bath. After it was taken to dryness *in vacuo*, the residual gum was dissolved in 9 ml. of water and the product precipitated with sulphur dioxide at 0° and washed with ice-water. After it was suspended in 12 ml. of water at 100° for 15 min., filtered at 0° and washed, the cream colored product (1.16 gm., 72%) melted at 232–234° (decomp.). For analysis, it was recrystallized four times from acetone (thimble) giving very light brown elongated prisms, m.p. 237–238° (decomp.), Ehrlich's reaction very weak cold but strongly

positive hot. Found in material dried *in vacuo* at 60°: C, 55.49; H, 5.82; N, 5.09%. Eq. wt. 140.6. Calc. for $C_{13}H_{17}O_6N$: C, 55.12; H, 6.05; N, 4.94%. Eq. wt. 141.6.

2-Methyl-3-carbobenzoxy-4-(2-carbomethoxyethyl)-5-carbomethoxypyrrole, Va

Sodium nitrite (45 gm.) in water (75 ml.) was slowly added at ⩽8° with stirring to methyl β-ketoadipate (101.3 gm.) in acetic acid (350 ml), and the excess nitrite was destroyed with ammonium sulphamate. This solution and zinc dust (300 gm.) were added slowly with stirring and cooling to benzyl acetoacetate (121 gm.) and ammonium acetate (100 gm.) in acetic acid (250 ml.) at 60–70°. After one hour at 90° the solution was decanted into ice-water (6 liters) and the zinc washed with hot acetic acid (50% then glacial). After the oil which separated had solidified, it was filtered off, well washed with water, and dried *in vacuo*, m.p. 120–126°. Recrystallization from ethanol (400 ml.) gave the product as pale yellow crystals (118 gm., 61%), m.p. 128–130°. For analysis, it was recrystallized three times from ethanol giving nearly colorless rectangular plates, m.p. 130–130.5°, Ehrlich's reaction positive hot. Found in material dried at 60° *in vacuo*: C, 63.71; H, 5.56; N, 3.74%. Calc. for $C_{19}H_{21}O_6N$: C, 63.50; H, 5.89; N, 3.90%.

2-Methyl-3-carboxy-4-(2-carbomethoxyethyl)-5-carbomethoxypyrrole, Vb

The benzyl ester V*a* (112 gm.) in 800 ml. of ethanol was hydrogenated for eight hours at 130° and 1100 lb. per sq. in. over 10 ml. of Raney nickel. When filtered off and washed with ethanol, the product (87 gm., containing nickel) was suitable for decarboxylation. A portion (14 gm.) was ground and filtered with 1 liter of ice-cold *N*/10 sodium carbonate, the product precipitated from the filtrate with carbon dioxide, filtered, and washed, giving 9 gm., m.p. 243–244° (decomp.). After two recrystallizations from ethanol and one from methanol, it formed colorless plates, melting point unchanged, Ehrlich's reaction positive hot. Found in material dried *in vacuo*: C, 53.76; H, 5.87; N, 5.36%. Calc. for $C_{12}H_{15}O_6N$: C, 53.53; H, 5.62; N, 5.20%.

2-Methyl-4-(2-carbomethoxyethyl)-5-carbomethoxypyrrole, Vc

The crude acid V*b* (73 gm., containing nickel) was distilled in two portions under the vacuum of a water pump at 230° rising to 245° (air-bath temperature) into an air condenser. The pale yellow waxy product was recrystallized from pentane (thimble) to give pink prisms (39 gm. 66% from the benzyl ester), m.p. 71–72°. This was suitable for the next stage. Two further recrystallizations gave the pyrrole as cream colored prisms, m.p. 72.5–73.5°. Ehrlich's reaction was slowly positive in the cold. Found in material dried *in vacuo*: C, 58.64; H, 6.86; N, 6.45%. Calc. for $C_{11}H_{15}O_4N$: C, 58.65; H, 6.71; N, 6.22%.

2-Methyl-5-carboxypyrrole-3-(glyoxylic acid)-4-(propionic acid), VIb

The ethyl ester II*d* (5.295 gm.) was heated in an open flask on the steam bath for two and one-half hours with 60 ml. of ethanol and 60 ml. of 10% sodium hydroxide. After removal of the residual solvent *in vacuo*, the gum was dissolved in 50 ml. of water, filtered, and the product precipitated with excess hydrochloric acid at 0°. The tricarboxylic acid VI*b* (2.81 gm., 70%) obtained

as a white powder by washing the precipitate with water and drying it *in vacuo* had a melting point of 197–198° (decomp.), which was depressed by admixture of 2-methyl-5-carbethoxypyrrole-3-(glyoxylic acid)-4-(propionic acid) VI*a* (see below). Ehrlich's reaction was slowly positive in the cold.

Precipitation by sulphur dioxide instead of hydrochloric acid gave a product containing sodium.

2-Methyl-5-carboxypyrrole-3-(glyoxylic acid)-4-(propionic acid) Trimethyl Ester, Vd

(*i*) *From the Triethyl Ester IId by Hydrolysis and Re-esterification*

The glyoxylic acid VI*b* (2 gm.) was added in portions to diazomethane (from 14 gm. of nitrosomethylurea) in ether. After it had stood for three hours, the ethereal solution was washed with dilute hydrochloric acid, with aqueous sodium bicarbonate, and with water, dried over sodium sulphate, and evaporated to dryness. The residue, which crystallized slowly at 0°, was recrystallized from methanol (12 ml.) – water (18 ml.), and had the melting point 106–107.5° (1.82 gm., 78%). After three recrystallizations from aqueous methanol, it formed long colorless prisms, m.p. 108–109° or, with slow heating, 114–115°. The Ehrlich's reaction was positive hot. Found in material dried *in vacuo* at 60°: C, 53.63; H, 5.10; N, 4.57%. Calc. for $C_{14}H_{17}O_7N$: C, 54.01; H, 5.51; N, 4.50%.

Subsequent preparations gave only the higher melting form, colorless rectangular plates, m.p. 114.5–115°, and undepressed by admixture of the lower melting form. Ehrlich's reaction was positive hot. Found: C, 54.22; H, 5.48; N, 4.69%.

(*ii*) *From 2-Methyl-4-(2-carbomethoxyethyl)-5-carbomethoxypyrrole, Vc (Preparative Method)*

The pyrrole V*c* (32.6 gm.) was dissolved in 35 ml. of methyl cyanoformate (b.p. 97.5–98.5°), 38 ml. of chloroform (dry and alcohol free), and 120 ml. of dry ether, cooled in ice-salt with the exclusion of moisture, stirred, and treated with a rapid stream of dry hydrogen chloride for three hours. Solid separated during the reaction; the mixture was evaporated to dryness by a stream of dry air passed into the mixture, without cooling, for four hours. Dry ether (120 ml.) was added and, after 12 hr. at 0°, the ketimine hydrochloride was collected as a yellow powder, washed with ether, and dried under water pump vacuum. The hydrochloride was powdered and added portionwise, with stirring, to ice-water (3 liters). The glyoxylic ester was collected, washed with water, and dried *in vacuo* after the initially clear yellow solution had been allowed to stand for four hours at 0°. The crude product was dissolved in methanol (160 ml.), warmed with charcoal, filtered, and recrystallized by the addition of water, giving colorless plates (39.0 gm., 86.5%) m.p. 111°-113°, sufficiently pure for hydrogenation.

2-Methyl-5-carboxypyrrole-3-(acetic acid)-4-(propionic acid) Trimethyl Ester, Ve

(*i*) *By Reduction of the Glyoxylic Ester (Preparative Method)*

The glyoxylic ester V*d* (36.4 gm., m.p. 111–113°, prepared by method (*ii*))

in acetic acid (120 ml.) and sulphuric acid (6.49 ml.) with palladium black (2.3 gm., freshly prepared) was shaken at 28° under hydrogen (60 lb. per sq. in.) for four hours. After the theoretical uptake in two hours, absorption nearly ceased. The filtrate and acetic acid washings from the catalyst were evaporated to dryness under reduced pressure on the steam bath after the addition of anhydrous sodium carbonate (13.5 gm.). The residue was taken up in dry benzene (320 ml.), which was distilled, initially at atmospheric pressure, and finally to dryness under water pump vacuum. The rapidly solidifying gum was dissolved in dry methanolic hydrogen chloride (160 ml. of 10%), warmed to 55° in a water bath, and allowed to cool in the bath overnight. The crystals that rapidly separated when the solution was poured into ice-water (2.5 liters) were collected after one hour at 0°, well washed with water, and dried *in vacuo*. The crude product was recrystallized from methanol (180 ml.) – water (320 ml.) to give the pyrrole (27.0 gm., 78%) as pale pink plates, m.p. 92°.

(*ii*) A sample prepared in the same way by reducing glyoxylic ester (m.p. 114–115°, prepared by method (*i*)) and recrystallized twice from aqueous methanol formed colorless plates, m.p. 92°, giving a positive Ehrlich's reaction (hot). Found in material dried *in vacuo*: C, 56.32; H, 6.41; N, 4.93%. Calc. for $C_{14}H_{19}O_6N$: C, 56.56; H, 6.44; N, 4.71%.

The melting point of this specimen was not depressed by admixture of material prepared by method (*i*).

(*iii*) *From the Ethyl Ester IIe Via the Tricarboxylic Acid IIIb*

The tricarboxylic acid III*b* (0.116 gm., m.p. 144–145°) was esterified with diazomethane (from 2 gm. of nitrosomethylurea). After one hour the ether was washed with dilute hydrochloric acid, with aqueous sodium bicarbonate, and with water, and dried over sodium sulphate. The gum which remained after evaporation of the ether rapidly crystallized. Recrystallization from methanol (2 ml.) – water (9 ml.) gave the product (64 mgm., 47%), m.p. 91–92°. The melting point was unchanged after recrystallizations from aqueous ethanol and aqueous methanol. Found, in material dried *in vacuo*: N, 4.81%. The identity of this product and the analytical sample of (*ii*) above was confirmed by their mixed melting point and by their infrared spectra in carbon disulphide.

2-Methyl-5-carbethoxypyrrole-3-(glyoxylic acid)-4-(propionic acid), VIa

The triethyl ester II*d* (7 gm.) in ethanol (45 ml.) and 0.889 *N* sodium hydroxide (50 ml., 2.23 equiv.) was heated in an open flask on the steam bath for 35 min. The solvent was removed *in vacuo* and the partially crystalline residue dissolved in water (25 ml.) and made strongly acid with hydrochloric acid at 0°. The crude product was filtered off and washed with ice-water. Two recrystallizations from water (20 ml.) gave 2.17 gm. (37%), m.p. 195–196° (decomp.), eq. wt. 148.0 (calc. 148.6). Large pale pink prisms, m.p. 198–199°, Ehrlich's reaction positive hot, were obtained after two further recrystallizations. Found in material dried *in vacuo*: C, 52.20; H, 5.16; N, 5.03%. Calc. for $C_{13}H_{15}O_7N$: C, 52.52; H, 5.09; N, 4.71%.

As in the case of VI*b*, the crude product contained sodium when precipitated by sulphur dioxide.

Diethyl β-Ketoadipate

(*i*) To diethyl β-keto-α-carbethoxyadipate (809.5 gm.) (14) cooled in an ice–salt bath, sulphuric acid (810 ml.) was added at $\leqslant 20°$ with stirring. After 12 hr. at 27°, absolute ethanol (1500 ml.) was added with stirring, together with solid carbon dioxide to keep the temperature at $\leqslant 10°$. After 20 hr. at room temperature, the solution was poured into ice-water (8 liters) and extracted with benzene (3 × 500 ml.). The extracts were washed twice with dilute sulphuric acid, thrice with dilute sodium bicarbonate, twice with water, and dried over sodium sulphate. Distillation through a Vigreux column gave the diester (330 gm. 54%), b.p. (0.4 mm.) 112–120°, η_D^{25} 1.4390.

(*ii*) Three liters of water and 1406 gm. of ethyl β-keto-α-carbethoxyadipate were gently boiled with vigorous stirring under a 12 in. Vigreux column for four and one-half hours. A hydrometer showed 180 gm. (theory 225 gm.) of ethanol in the 1.8 liters of distillate. The undistilled residues from two such runs were combined. The ester was separated and combined with the ether wash (1 liter) of the water layers, washed with saturated sodium bicarbonate, four times with water, and with 4 × 250 cc. of cold saturated sodium carbonate which was then back-washed with ether. The organic layer was clarified with anhydrous sodium sulphate, washed three times with water, three times with dilute sulphuric acid, and four times with water, clarified with an anhydrous sodium sulphate, filtered, the ether removed on the steam bath, and the residue distilled to 150° at 0.2 mm. The fractionation of the distillate at 0.2 mm. with a 12 in. lagged Vigreux column was followed refractometrically; the product (1367 gm., 65%, η_D^{26} 1.4390) consisted of the main fraction (1280 gm., b.p. 108–119°, nearly all 117–119°) together with that obtained by refractionating the 95–108° cut.

Methyl δ,δ-Dicarbethoxylevulinate

The ester (214 gm., 81%) b.p. 140° (0.4 mm.) was obtained according to the method used for the triethyl ester (14) from 145.5 gm. of β-carbomethoxypropionyl chloride, 162 gm. of malonic ester, and 23.4 gm. of magnesium. For analysis, it was slowly distilled through a 3 in. Vigreux column and collected at 115° (0.25 mm.), as a colorless liquid, η_D^{27} 1.4486, giving a violet-brown color with ferric chloride. Found: C, 52.60; H, 6.51%. Calc. for $C_{12}H_{18}O_7$: C, 52.55; H, 6.61%.

Dimethyl β-Ketoadipate

β-Ketoadipic acid (281.5 gm.) from the above ester and hydrochloric acid (cf. (5)) gave the dimethyl ester (3) (126 gm., 38%) b.p. (0.6 mm.) 100–104°, η_D^{27} 1.4416, when esterified with 250 ml. of methanol containing 93 gm. of hydrogen chloride.

5,5′-Dimethylpyrromethene-3,3′-(diacetic acid)-4,4′-(dipropionic acid) Hydrobromide, VIIa

The tricarboxylic acid I*b* (1 gm., crude m.p. 143°) (10) was heated on the steam bath with 98% formic acid (5 ml.) and 30% hydrogen bromide in acetic acid (2.5 ml.) under reflux for 40 min. After two hours at 10° the product

was filtered off and washed with cold formic acid. The brown powder, 0.535 gm. (53%), m.p. 200–201° (decomp.), gave orange-yellow micro needles (0.385 gm.), melting point unchanged, on recrystallizing from formic acid (8 ml.). Found in material dried *in vacuo*: C, 49.22; H, 5.08; N, 5.45; Br, 15.39%. Calc. for $C_{21}H_{25}O_8N_2Br$: C, 49.13; H, 4.91; N, 5.46; Br, 15.57%.

It is stable when kept *in vacuo* over phosphorus pentoxide and protected from light.

5,5'-Dimethylpyrromethene-3,3'-(dipropionic acid)-4,4'-(diacetic acid) Hydrobromide, VIIb

The crude tricarboxylic acid III*b* (1.02 gm., m.p. 145°) was heated under reflux on the steam bath with 98% formic acid (5 ml.) and 30% hydrogen bromide in acetic acid (2.5 ml.) for one hour. The reaction mixture was evaporated to dryness under reduced pressure and acetic acid (15 ml.) added to the rapidly crystallizing brown residue. After one hour at 0°, the methene hydrobromide was collected, washed with cold acetic acid, and dried *in vacuo*. The orange-powder (0.641 gm., 62%), m.p. 217°–218° (decomp.), was recrystallized from formic acid (4 ml.) to give small orange elongated prisms (0.405 gm.), m.p. 218–218.5° (decomp.). The melting point was unchanged by further recrystallization. Found in material dried *in vacuo*: C, 49.38; H, 4.95; N, 5.36; Br, 15.55%. Calc. for $C_{21}H_{25}O_8N_2Br$: C, 49.13; H, 4.91; N, 5.46; Br, 15.57%.

The hydrobromide was stored *in vacuo* over phosphorus pentoxide, and protected from light.

REFERENCES

1. ADKINS, H., BURGOYNE, E. E., and SCHNEIDER, H. J. J. Am. Chem. Soc. 72: 2626. 1950.
2. BAKER, B. R., SCHAUB, R. E., and WILLIAMS, J. H. J. Org. Chem. 17: 116. 1952.
3. BARDHAN, J. C. J. Chem. Soc. 1851. 1936.
4. BERNHARD, A. Ann. 282: 166. 1894.
5. EISNER, U., ELVIDGE, J. A., and LINSTEAD, R. P. J. Chem. Soc. 2223. 1950.
6. FISCHER, H. and ANDERSAG, H. Ann. 458: 117. 1927.
7. FISCHER, H. and ORTH, H. Chemie des Pyrrols. Leipzig. 1934. Band I: (*a*) p. 282. (*b*) p. 289. (*c*) p. 235. Band II/i: (*d*) p. 3.
8. FISCHER, H., WEISS, B., and SCHUBERT, M. Ber. 56: 1194. 1923.
9. KINDLER, K., METZENDORF, W., and DSCHI-YIN-KUOK. Ber. 76: 308. 1943.
10. MACDONALD, S. F. Chemistry & Industry, 759. 1951. J. Chem. Soc. 4176, 4184. 1952.
11. MACDONALD, S. F. and STEDMAN, R. J. J. Am. Chem. Soc. 75: 5448. 1953.
12. MOZINGO, R., SPENCER, C., and FOLKERS, K. J. Am. Chem. Soc. 66: 1859. 1944.
13. OTT, W. Thesis, Technische Hochschule, Munich. 1953. p. 51. TREIBS, A. and HINTERMEIER, K. Chem. Ber. 87: 1167. 1954.
14. RIEGEL, B. and LILIENFELD, W. M. J. Am. Chem. Soc. 67: 1273. 1945.
15. SINAIGO, F. K. and ADKINS, H. J. Am. Chem. Soc. 58: 709. 1936.
16. STEDMAN, R. J. and MACDONALD, S. F. Can. J. Chem. 33: 468. 1955.
17. TAUSZ, J. and VON PUTNOKY, M. Ber. 52: 1573. 1919.

SIMPLE PYRROLES AS BASES[1]

By R. J. Stedman[2] and S. F. MacDonald

ABSTRACT

Some simple pyrroles form stable hydrobromides. Their formation may interfere with some reactions, but offers analytical possibilities.

Although the basic nature of dipyrromethenes and of porphyrins is well-known, that of simple pyrroles has been largely ignored. Discussions have been limited to rationalizing the instability of salts of pyrrole itself (1, 10). However, the acidic (7) and basic properties of simple pyrroles are very dependent on the substituents present. Solubility in mineral acid has been noted (13), shown spectroscopically to be due to salt formation (3), and used to separate mixtures by partition (9). Chloroaurates and chloroplatinates (13, 2) as well as picrates are known, but apparently only two salts of simple pyrroles with mineral acids have been described: the deliquescent or unstable hydrochloride of cryptopyrrole (2,4-dimethyl-3-ethylpyrrole) (6), and an unstable hydrobromide of 2-bromomethyl-3-methyl-4-ethyl-5-carbethoxypyrrole (8).

When the preparation of a dipyrromethene from I*b* was attempted with formic acid and hydrogen bromide at 55° (12), the product which separated was the hydrobromide of I*a*, cryptopyrrole-dicarboxylic acid. The hydrobromide could also be prepared directly from I*a* in ether, to which it again reverted with aqueous pyridine. α-Carboxy-hemopyrrole-dicarboxylic acid, II*b*, behaved like I*b*, and both hemopyrrole-dicarboxylic acid, II*a*, and cryptopyrrole-carboxylic acid, III, behaved like I*a*. The hydrobromides were stable to recrystallization and to drying in vacuum. The behavior of other pyrroles with hydrogen bromide has not been studied.

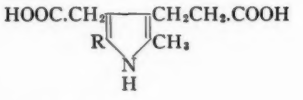

I*a*, R = H
b, R = COOH

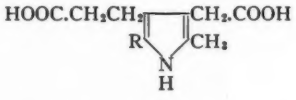

II*a*, R = H
b, R = COOH

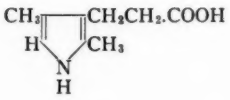

III

These hydrobromides should prove useful analytically, for pyrroles such as I*a* are very soluble in water and neither the acids nor the methyl esters are

[1]*Manuscript received November 8, 1954.*
Contribution from the Division of Pure Chemistry, National Research Council of Canada, Ottawa. Issued as N.R.C. No. 3507.
[2]*National Research Council of Canada Postdoctorate Fellow, 1952–1954.*

precipitated by picric acid, the classical reagent for separating pyrrole mixtures. In a preliminary experiment the pyrrole mixture resulting on the reduction of uroporphyrin, previously obtained as an oil (5), was readily precipitated from ether with hydrogen bromide in acetic acid, and the hydrobromides converted into a solid mixture of pyrroles.

EXPERIMENTAL

Hydrobromide of Cryptopyrrole-dicarboxylic Acid

(*i*) *From Cryptopyrrole-dicarboxylic Acid, Ia*

The pyrrole (0.192 gm.) was dissolved in acetic acid (2 ml.) and dry ether (5 ml.). The addition of hydrogen bromide (0.5 ml. of a 30% solution in acetic acid) caused the separation of an oil which crystallized on scratching. More ether was added, and the product (0.231 gm., 87%), m.p. 134–136° (decomp.), filtered off and washed with ether. By recrystallization from acetic acid (2 ml.) – ether (2 ml.), it was obtained as pale pink plates, m.p. 137–138° (decomp.), unchanged on further recrystallization. Ehrlich's reaction was strongly positive cold. Found in material dried *in vacuo*: C, 41.11; H, 4.61; N, 4.70; Br, 27.59%. Calc. for $C_{10}H_{14}O_4NBr$: C, 41.11; H, 4.83; N, 4.80; Br, 27.36%.

(*ii*) *From α-Carboxycryptopyrrole-dicarboxylic Acid, Ib*

The crude tricarboxylic acid (4 gm., m.p. 140.5°) was suspended in 98% formic acid (8 ml.) and warmed at 55° with hydrogen bromide (4 ml. of a 30% solution in acetic acid) to solution and cessation of effervescence (*ca.* 20 min.) (cf. (12)). The solvent was removed *in vacuo* at 50°, the partially crystalline residue shaken with acetic acid (140 ml.) at 50° and, after two hours at 25°, some dipyrromethene removed by filtration and washed with acetic acid. The pyrrole hydrobromide (3.18 gm., 69%), a yellow powder m.p. 136–138° (decomp.), was precipitated from the combined filtrate and washings by dry ether (200 ml.) and washed with acetic acid – ether (1:1). After recrystallization from acetic acid (25 ml.) – ether (25 ml.) it formed pale tan plates (2.71 gm.), m.p. 137–138° (decomp.), undepressed by admixture with the hydrobromide obtained under (*i*). Ehrlich's reaction was strongly positive cold. Found in material dried *in vacuo*: C, 41.24; H, 4.87; N, 4.67; Br, 27.27%. The infrared spectra in Nujol mull of the products obtained under (*i*) and (*ii*) confirmed their identity.

The material (0.246 gm., 6%), insoluble in acetic acid, was recrystallized from formic acid to give the yellow 5,5′-dimethyl pyrromethene-3,3′-diacetic acid-4,4′-dipropionic acid hydrobromide, m.p. 200–200.5° (decomp.), undepressed by admixture with authentic material (12).

Cryptopyrrole-dicarboxylic Acid, Ia, from its Hydrobromide

The pyrrole hydrobromide (292 mgm., 1 millimole) was dissolved in aqueous pyridine (0.5 ml. of a 16.5% w/v solution, 1.05 millimole). After one hour at 0°, the pale pink plates (86 mgm., 41%) were filtered off and washed with a little ice cold water. The m.p. (128–129°) was undepressed by authentic cryptopyrrole-dicarboxylic acid of m.p. 128–129° (11), and identity was confirmed by infrared spectra in Nujol mull.

Hydrobromide of Hemopyrrole-dicarboxylic Acid

(*i*) *From Hemopyrrole-dicarboxylic Acid, IIa*

This hydrobromide (0.716 gm., 95%) m.p. 158–159°, was obtained as a gray powder from 0.545 gm. of the pyrrole II*a* in 5 ml. of acetic acid with 1 ml. of hydrogen bromide in acetic acid, as was the isomer above. After two recrystallizations from 7 ml. of acetic acid it formed violet prisms, m.p. 160–161°. Ehrlich's reaction was strongly positive cold. Found in material dried *in vacuo*, C, 41.18; H, 5.01; N, 4.57; Br, 24.81%. Calc. for $C_{10}H_{14}O_4NBr.\frac{1}{2}CH_3.COOH$: C, 41.01; H, 5.01; N, 4.35; Br, 24.81%.

The distillate from a solution of the hydrobromide (30 mgm., subjected to prolonged drying *in vacuo*) in 0.75 ml. of water gave a positive test for acetic acid when treated with lanthanum nitrate, iodine, and ammonia (4).

(*ii*) *From α-Carboxyhemopyrrole-dicarboxylic Acid, IIb*

The crude tricarboxylic acid II*b* (0.5 gm., m.p. 149°) was heated at 70° for a few minutes with 1 ml. of formic acid and 0.5 ml. of hydrogen bromide in acetic acid. The solvent was removed *in vacuo* at 25°, leaving a gum which rapidly crystallized. Recrystallization from 7 ml. of acetic acid gave a yellow powder (0.278 gm., 48%), m.p. 157–159°. After two further crystallizations it formed pale yellow prisms, m.p. 159–160.5°. Contamination by dipyrromethene was detected by the visible spectrum. Ehrlich's reaction was strongly positive in the cold. Found in material dried *in vacuo*: C, 41.40; H, 5.04; N, 4.66; Br, 24.64%. The melting point was undepressed by the product of (*i*) above, and the infrared spectra in Nujol mull confirmed their identity.

Hydrobromide of Cryptopyrrole-carboxylic Acid

Cryptopyrrole-carboxylic acid, III, (0.501 gm., m.p. 140–141°) in 10 ml. of dry ether was treated with hydrogen bromide (1 ml. of a 30% solution in acetic acid). The oil which was immediately deposited rapidly crystallized and the product (0.716 gm., 96%) was collected after one hour at room temperature, washed with dry ether, and dried *in vacuo*. The crude material, a greenish powder, m.p. 148–150° (decomp.) was recrystallized from 7 ml. of acetic acid, giving small green prisms (0.365 gm.), m.p. 151–151.5°. The color persisted after two further recrystallizations and the melting point was unchanged. The Ehrlich's reaction was strongly positive in the cold. Found in material dried *invacuo*: C, 43.86; H, 5.90; N, 5.83; Br, 32.28%. Calc. for $C_9H_{14}O_2NBr$: C, 43.56; H, 5.69; N, 5.65; Br, 32.21%.

Cryptopyrrole-carboxylic Acid, III, from its Hydrobromide

The pyrrole hydrobromide (193 mgm.; 0.78 millimole) was dissolved in 1 ml. of water and treated with pyridine (0.80 ml. of a 7.9% w/v aqueous solution, 0.80 millimole). The free pyrrole was immediately deposited and was collected after one hour at 0° as a brown powder (95.5 mgm., 73%), washed with cold water, and dried *in vacuo*. Sublimation at 100° in a high vacuum gave a colorless product, m.p. 141–142°, undepressed by admixture of authentic cryptopyrrole-carboxylic acid.

REFERENCES

1. BAMBERGER, E. Ber. 24: 1758. 1891.
2. CIAMICIAN, G. Ber. 37: 4200. 1904.
3. COOKSON, G. H. J. Chem. Soc. 2789. 1953.
4. FEIGL, F. Spot tests. Vol. 2. 4th English ed. Elsevier Publishing Co., Inc., Amsterdam. 1954. p. 247.
5. FISCHER, H. Z. physiol. Chem. 95: 58. 1915; 98: 78. 1916. FISCHER, H. and ANDERSAG, H. Ann. 458: 117. 1927. FISCHER, H. and ZERWICK, W. Z. physiol. Chem. 137: 243. 1924.
6. FISCHER, H., BAUMANN, E., and RIEDL, H. J. Ann. 475: 205. 1929.
7. FISCHER, H. and ELHARDT, E. Z. physiol Chem. 257: 61. 1939. FISCHER, H. and ERNST, P. Ann. 447: 139. 1926.
8. FISCHER, H. and STANGLER, G. Ann. 459: 53. 1927.
9. FISCHER, H. and TREIBS, A. Ann. 450: 132. 1926.
10. INGOLD, C. K. Structure and mechanism in organic chemistry. Cornell Univ. Press, Ithaca, N.Y. 1953. pp. 160, 174.
11. MACDONALD, S. F. J. Chem. Soc. 4184. 1952.
12. MACDONALD, S. F. and STEDMAN, R. J. Can. J. Chem. 33: 458. 1955.
13. ZANETTI, C. U. and LEVI, E. Ber. 27. Ref. 585. 1894.

PHOTOLYSIS OF ACETONE IN THE PRESENCE OF MERCURY DIMETHYL[1]

By H. G. Oswin, R. Rebbert, and E. W. R. Steacie

ABSTRACT

The reactions between $CH_3+CH_3—Hg—CH_3$ were investigated in a system in which acetone was used as the source of CH_3 radicals. Similarly d_6-acetone was used to investigate the reactions of CD_3 radicals and $CH_3—Hg—CH_3$. Activation energies for the hydrogen abstraction reactions were calculated, and no significant difference was found between the CD_3 and CH_3 reactions, being respectively 10.0 and 10.2 kcal./mole. Under conditions of constant intensity and acetone concentration, reaction rates appear to be dependent on mercury dimethyl concentrations. In the case of the acetone-d_6 system, quantities of $C_2D_3H_3$ were found in the reaction products. This is discussed as possible evidence of such a reaction as:

$$CD_3+CH_3—Hg—CH_3 \rightarrow CD_3—CH_3+Hg+CH_3.$$

INTRODUCTION

The photolysis of mercury dimethyl was recently investigated (4) and an activation energy for the reaction

$$CH_3+Hg(CH_3)_2 \rightarrow CH_4+CH_3—Hg—CH_2 \qquad [1]$$

was derived. The work presently described was carried out to determine whether this value is in fact independent of the source of methyl radicals.

Acetone and deuterated acetone are suitable sources of methyl radicals, and can be photolyzed in a wavelength region above 2800 Å, where mercury dimethyl does not absorb. Under these conditions there will be two competing reactions producing methane,

$$CH_3+Hg(CH_3)_2 \rightarrow CH_4+CH_3—Hg—CH_2 \qquad [1]$$

$$CH_3+CO(CH_3)_2 \rightarrow CH_4+CH_3—CO—CH_2. \qquad [2]$$

To obtain the rate of reaction [1], the rate of reaction [2] is subtracted from the over-all rate of formation of methane. The disadvantage of this method is that the rate constant of reaction [2] is considerably larger than [1], and consequently contributes far more to the over-all methane formation rate.

Deuterated acetone has been used successfully to investigate similar reactions (3, 6), and under the circumstances should give a clearer picture of the two competing reactions; in this case:

$$CD_3+Hg(CH_3)_2 \rightarrow CD_3H+CH_3—Hg—CH_2 \qquad [3]$$

$$CD_3+CO(CD_3)_2 \rightarrow CD_4+CD_3—CO—CD_2. \qquad [4]$$

Hence the ratio of CD_4 to CD_3H (determined mass spectrometrically) should give a more accurate measure of the relative rates. A correction can be made for CD_3H formed by reactions of the type

[1]*Manuscript received November 9, 1954.*
Contribution from the Division of Pure Chemistry, National Research Council, Ottawa, Canada. Issued as N.R.C. No. 3508.

$$CD_3+HCD_2—CO—CD_3 \rightarrow CD_3H+CD_2—CO—CD_3 \quad [4a]$$

and $$CD_2H+CD_3—CO—CD_3 \rightarrow CD_3H+CD_2—CO—CD_3 \quad [4b]$$

from the rates found in the photolysis of the deuterated acetone sample alone.

EXPERIMENTAL TECHNIQUE

A conventional high-vacuum apparatus was employed, containing a suitable cell, mixing bulb, and micro-gas analysis equipment. All stopcocks were lubricated with silicone grease to minimize the amount of mercury dimethyl dissolving.

A suitable filter (Corning 0/53) was used to absorb radiation of shorter wavelength than 2800 Å. This eliminates direct energy absorption by mercury dimethyl, a fact which was established by carrying out a few preliminary blank runs with only mercury dimethyl present.

Mercury dimethyl was prepared in the previously described manner (4). Reagent grade acetone was first dried and distilled *in vacuo* before using.

A sample of deuterated acetone was prepared (3) and analyzed mass spectrometrically. It was found that the total hydrogen content of the sample consisted of 96% of the deuterium isotope.

In the case of the experiments with deuterated acetone, the various fractions of the reaction products were analyzed mass spectrometrically. By this method, CO, CD_4, and CD_3H can be determined in the C_1 fraction. In the C_2 fraction only C_2D_6 can be analyzed accurately, estimates of the succeeding compounds C_2D_5H, $C_2D_4H_2$ etc. becoming progressively less accurate.

RESULTS

(*a*) *"Light" Acetone and Mercury Dimethyl*

The case of "light" acetone will be considered first.

The temperature range investigated here was restricted between 433° and 511°K., the lower limit being imposed by small rates of reaction [1] at low

TABLE I

No.	Temp., °C.	Acetone (mm.)	Mercury dimethyl (mm.)	Rates of formation of products (molecules/cc./sec. × 10^{11}) CH_4	C_2H_6	CO	$(k_2/k_5^{\frac{1}{2}}) \times 10^{13}$
Photolysis of acetone alone							
174	126	41.7		5.65	15.0	20.1	4.57
176	144	42.4		8.24	13.8	21.4	7.18
172	178	46.0		17.5	11.0	25.2	17.0
175	212	49.3		27.0	6.1	25.8	35.4
177	238	52.6		34.4	3.74	27.4	56.5
Photolysis of acetone in presence of mercury dimethyl							
186	160	43.3	42.3	11.4	8.69	16.5	1.81
180	178	45.6	45.0	18.9	9.71	22.3	2.63
185	195	48.1	47.7	22.6	6.42	19.6	4.26
184	212	49.2	48.2	29.4	5.18	20.6	6.59
181	238	51.4	50.9	45.5	4.92	24.2	10.4

temperatures. The upper limit is determined by the increased thermal decomposition of mercury dimethyl above this temperature range.

Table I lists the reaction rates for pure acetone and acetone–mercury dimethyl mixtures. Values of log $(k_1/(k_5)^{\frac{1}{2}})$ were calculated where k_5 is the rate constant for methyl recombination.

$$CH_3+CH_3 \rightarrow C_2H_6 \qquad [5]$$

These values are shown plotted against $10^3/T°K.$ in Fig. 1.

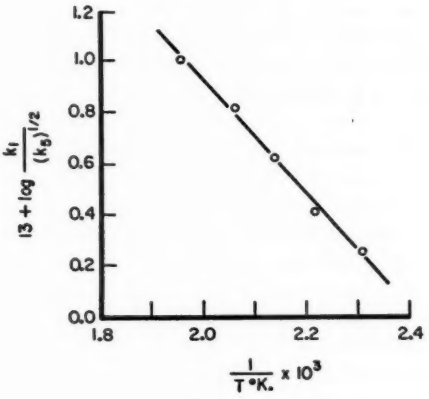

FIG. 1

The regression equation of log $(k_1/(k_5)^{\frac{1}{2}})$ on T is

$$\log (k_1/(k_5)^{\frac{1}{2}}) = -(2238/T°K.)-7.59$$

from which it is found that

$$E_1-\tfrac{1}{2}E_5 = 10.2\pm1.0 \text{ kcal. per mole.}$$

TABLE II

EFFECT OF MERCURY DIMETHYL ON PRODUCTS AT CONSTANT INTENSITY

No.	Temp., °C.	Pressure of acetone (mm.)	Pressure of $Hg(CH_3)_2$ (mm.)	R_{CO}	$\frac{1}{2}R_{C_1}+R_{C_2}$
176	144	42.4	0	2.32	1.94
182	144	41.5	40.7	2.12	1.84
187	144	40.9	41.4	2.08	1.83
172	178	46.0	0	2.71	2.12
180	178	45.6	45.0	2.44	2.09
175	212	49.3	0	2.85	2.18
184	212	49.2	48.2	2.57	2.49
177	238	52.6	0	2.99	2.27
181	238	51.4	50.9	2.73	3.11

Table II shows various rates measured under conditions of constant intensity at different temperatures. The apparent dependence of these rates on mercury dimethyl concentrations will be discussed later.

(*b*) *Deuterated Acetone and Mercury Dimethyl*

The rates of formation of the various reaction products are listed in Table III. The column headed R_{CD_3H} lists the corrected values allowing for the CD_3H formation from acetone.

TABLE III

No.	Temp., °C.	d_6-acetone (mm.)	Mercury dimethyl (mm.)	Rates of formation of products (molecules/cc./sec. × 10^{11}) CD_4	CD_3H	C_2D_6	$C_2D_3H_3$
18	202	84	25	7.63	3.66	3.29	4.39
17	200	79	46	5.81	4.08	1.78	3.38
16	200	89	—	16.7	1.50	11.6	—
6	200	75	26	10.2	4.77	11.3	5.72
5	197	87	49	10.9	9.88	8.58	7.38
7	182	82	54	7.92	7.63	9.45	7.18
13	172	83	—	8.84	1.01	11.6	0.2
14	172	71	44	3.85	4.64	6.72	4.4
15	172	89	22	8.08	3.19	15.6	5.08
12	155	76	52	3.23	4.48	10.5	5.07
2	153	80	—	6.95	1.53	39.8	—
3	153	69	45	4.64	4.19	20.9	6.06
4	148	77	30	4.04	2.26	20.7	3.34
11	135	89	25	3.36	1.59	13.8	1.57
10	134	85	44	2.99	2.74	10.0	2.0
19	126	88	—	2.44	0.33	11.8	—
20	125	85	33	1.81	1.09	11.0	4.39
21	125	78	49	1.10	1.29	7.58	6.24
8	125	88	53	2.08	2.05	18.8	4.97

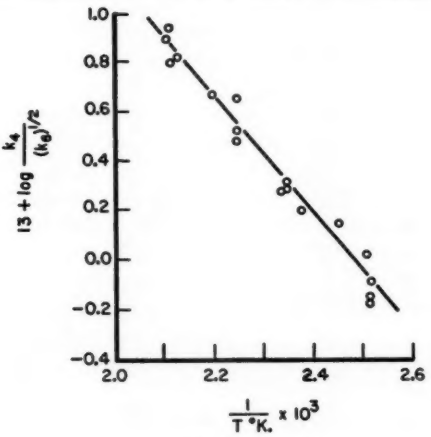

FIG. 2

Very small quantities of C_3 products were found, but these were too small to allow accurate analysis, and would probably contain appreciable proportions

of C_2 compounds. By volume this fraction usually amounted to between one per cent and three per cent of the C_2 fraction.

A preliminary check on the conditions of the experiment can be obtained from a calculation of the activation energy for the reaction:

$$CD_3 + (CD_3)_2CO \rightarrow CD_4 + CD_3—CO—CD_2. \qquad [4]$$

Fig. 2 shows a plot of log $(R_{CD_4}/(R_{C_2D_6})^{\frac{1}{2}})$ [acetone] against $10^3/T°K$.

The regression equation of this relationship is given by

$$\log (k_4/(k_6)^{\frac{1}{2}}) = -(2373/T°K.) - 9.254,$$

where k_6 is the rate constant for the methyl recombination:

$$2CD_3 \rightarrow C_2D_6. \qquad [6]$$

From the above expression

$$E_4 - \tfrac{1}{2}E_6 = 10.9 \pm 1.0 \text{ kcal. per mole.}$$

The activation energy for reaction [3]

$$CD_3 + CH_3—Hg—CH_3 \rightarrow CD_3H + CH_3—Hg—CH_2$$

was calculated from a plot of

$$\log (R_{CD_3H}/(R_{C_2D_6})^{\frac{1}{2}}) \text{ [mercury dimethyl] versus } 10^3/T°K.$$

The plot shown in Fig. 3 may be represented by

$$\log (k_3/(k_6)^{\frac{1}{2}}) = -(2196/T°K.) - 7.336.$$

Hence $E_3 - \frac{1}{2}E_6 = 10.0 \pm 1.0$ kcal. per mole.

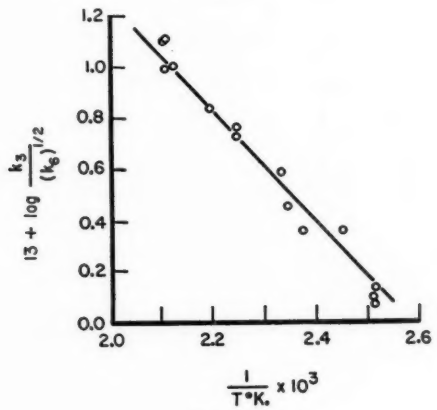

FIG. 3

Also listed in Table III are the rates of formation of $C_2D_3H_3$. Although the accuracy of these figures may be no better than $\pm 50\%$, the quantities are still

too large to be accounted for by such reactions as

$$CD_2H + CH_2D \rightarrow C_2D_3H_3.$$

The presence of $C_2D_3H_3$ will be discussed later.

DISCUSSION

The value of 10.9 kcal./mole found for E_4 lies between the previous values of 10.6 and 11.6 kcal./mole obtained respectively by Majury and Steacie (3) and Whittle and Steacie (6). In view of the different experimental conditions, the present value of 10.9 is probably not as accurate as these others. However, Whittle and Steacie in support of the higher value suggest that the lower value of 10.6 kcal./mole is due to non-linearity of the Arrhenius plot at lower temperatures; since the present work was carried out at the lower temperatures also, it is not surprising that it agrees more with the value of 10.6 kcal./mole.

The recent figures of McNesby and Gordon (2) for the acetone–acetone-d_6 photolysis indicate that there is no measurable difference in activation energy for the abstraction of hydrogen from acetone by CH_3 and CD_3 radicals. It seems reasonable to assume therefore that there should be no significant difference between the activation energies for reactions [1] and [3], as is indicated by the values of 10.2 ± 1.0 and 10.0 ± 1.0 kcal./mole presently obtained.

Activation energies previously obtained (5) for hydrogen abstraction reactions, using mercury dimethyl as a source of methyl radicals, are generally in good agreement with those obtained in acetone systems. It was assumed in this work that the only sources of CH_4 and C_2H_6 were by hydrogen abstraction and recombination of methyl radicals. However, several features of the present work with acetone and mercury dimethyl must be considered in this respect.

(1) In the presence of an equal amount of mercury dimethyl, the rate of formation of CO from acetone is reduced by 10% over the range 144°–238°C. (see Table II).

(2) Table II also indicates that the quantum yield of methyl radicals recovered as CH_4 and C_2H_6, in the presence of mercury dimethyl, is decreased at the lower temperatures and increased at the higher temperatures, eventually exceeding two CH_3 radicals per CO formed.

(3) Mixtures of deuterated acetone and mercury dimethyl yield appreciable quantities of $C_2D_3H_3$ (see Table III), although only CD_3 radicals are formed in appreciable amount by direct light absorption.

Holroyd and Noyes (1), investigating the photolysis of mercury dimethyl alone at 2600 Å, established these points:

(4) At 175°C., there is an increase in $R_{CH_4}/R_{C_2H_6}^{\frac{1}{2}}[DM]$ with increasing light absorption.

(5) At 175°C., more than two methyls appear as methane and ethane per quantum absorbed.

(6) The quantum yield of ethane formation is nearly independent of the amount of methane formed, and is approximately the same at 30°C. and 175°C. There is a slight increase with decreasing light absorption.

In reference to point (1), there are two possible causes of a decrease in CO formation:

(*a*) decreasing extinction coefficient of acetone, in the presence of mercury dimethyl; but in view of the pressures used, it is unlikely that this effect would be appreciable;

(*b*) transfer of energy from an excited acetone molecule or CH_3CO radical; this may or may not induce decomposition of the mercury dimethyl molecule.

Both of these possibilities would result in an increased or decreased primary production of methyl radicals, but would not affect the modes of formation of methane and ethane. If the transfer of energy to mercury dimethyl resulted in subsequent decomposition, it would explain the presence of CD_3–CH_3 in the reaction products, but could not account for all of it.

Observation (5), that more than two methyls appear per quantum absorbed, has been offered by Holroyd and Noyes as evidence of the reaction:

$$CH_3+CH_3—Hg—CH_3 \rightarrow C_2H_6+CH_3+Hg. \qquad [7]$$

The observed formation of CD_3–CH_3 in the present work also indicates that reaction [7] may occur. This reaction together with the suggested explanations of the R_{CO} decrease could explain qualitatively the reported observations. In view of the possibility of energy transfer, the quantities of CD_3–CH_3 formed cannot be used for an accurate estimation of the importance of reaction [7].

If reaction [7] is an additional mode of formation of ethane, then the relation holds

$$\frac{k_1}{k_5^{\frac{1}{2}}}[DM] = \frac{R_{CH_4}}{R_{C_2H_6}^{\frac{1}{2}}\beta^{\frac{1}{2}}} - \frac{k_8}{k_5^{\frac{1}{2}}}[RH]$$

$$= 1-\frac{k_7}{k_1}\frac{R_{CH_4}}{R_{C_2H_6}}\left(1+\frac{k_8}{k_1}\frac{[RH]}{[DM]}\right)$$

where k_8 is the rate constant for the abstraction of hydrogen from an added hydrocarbon RH. Hence from the photolysis of mercury dimethyl alone, it is possible to determine the two parameters $k_1/k_5^{\frac{1}{2}}$ and k_7/k_1 from variations in the formation of CH_4 and C_2H_6 over an extensive range of light absorption. From Holroyd and Noyes data, k_7/k_1 would be between zero and unity at 175°C. At room temperature no methane is formed and

$$C_2H_6 = 1+\frac{k_7}{k_5^{\frac{1}{2}}}\frac{[DM]}{I_a^{\frac{1}{2}}}$$

which is in qualitative agreement with the drift with light absorption observed by Holroyd and Noyes.

Inasmuch as reaction [7] does occur, it should have a very low activation energy and an unusually small steric factor; unfortunately no more than these qualitative conclusions can be drawn.

Analysis of the present and previous (4) data, assuming reaction [7] occurs, shows that in view of the amounts of CH_4 and C_2H_6 found at higher temperatures, k_7 can have no more than a slight temperature coefficient. Arbi-

trarily taking $E_1 - E_7 = 10$ kcal. and $k_7/k_1 = 0.37$ at 175°C., it is found that values of $k_1/k_5^{\frac{1}{2}}$ and $E_1 - \frac{1}{2}E_5$ become practically identical for mercury dimethyl alone, and the present experiments with acetone – mercury dimethyl mixtures. Other values for hydrogen-abstraction reactions remained virtually unaffected by this treatment.

Although this treatment has no more than a qualitative significance, it would seem that a second mode of ethane formation could exist in the mercury dimethyl photolysis without affecting the observed agreement with the acetone work.

ACKNOWLEDGMENT

We should like to thank Miss F. Gauthier, Miss J. Fuller, and Dr. F. P. Lossing for the mass-spectrometer analysis, and Dr. R. J. Cvetanovic for very helpful discussions.

REFERENCES

1. HOLROYD, R. A. and NOYES, W. A., JR. J. Am. Chem. Soc. 76: 1583. 1954.
2. MCNESBY, J. R. and GORDON, A. S. J. Am. Chem. Soc. 76: 1416. 1954.
3. MAJURY, T. and STEACIE, E. W. R. Can. J. Chem. 30: 800. 1952.
4. REBBERT, R. E. and STEACIE, E. W. R. Can. J. Chem. 31: 631. 1953.
5. REBBERT, R. E. and Steacie, E. W. R. J. Chem. Phys. 21: 1723. 1953.
6. WHITTLE, E. and STEACIE, E. W. R. J. Chem. Phys. 21: 993. 1953.

STUDIES ON CARRAGEENIN: COMPARISON OF FRACTIONS OBTAINED WITH POTASSIUM CHLORIDE AND BY SUCCESSIVE EXTRACTION AT ELEVATED TEMPERATURES[1]

By D. A. I. Goring and E. Gordon Young

ABSTRACT

Carrageenin was fractionated with potassium chloride and by successive extractions at elevated temperatures. Measurements were made of sulphate content, optical rotation, gel strength, intrinsic viscosity, sedimentation rate, and ionic mobility. The results indicated three components extractable at 30°C., 60°C., and 100–120°C. The 60°C. extract had a high gel strength while the components extracted at 30°C. and 100–120°C. showed low gelling tendencies. The two non-gelling components were concentrated in the supernatant liquid when fractionated with potassium chloride.

INTRODUCTION

Carrageenin, the polysaccharide extractable from the red alga Irish moss (*Chondrus crispus*), has been shown to consist mainly of D-galacto-4-sulphate residues joined in the 1–3 position (11). Other monosaccharides have been found in carrageenin as usually prepared (2, 9, 11, 19, 24). The chemical individuality of these preparations however was not established. Cook, Rose, and Colvin (3) observed in the ultracentrifuge two components in commercial carrageenin. Smith and Cook (21) and Smith, Cook, and Neal (22) were able to separate these components in aqueous solution with potassium chloride. They applied the term κ-carrageenin to the precipitated component and λ-carrageenin to the component remaining in solution. These components differed in sulphate content, optical activity, rates of sedimentation and of diffusion, and intrinsic viscosity. Neither Cook *et al.* (3) nor Goring (6) could detect any clear separation of components electrophoretically.

Rose (18) found no evidence for chemically distinct components but cold and hot water extracts have been reported to differ in optical rotation and gelling tendencies (15). The usual hot water extract of carrageenin will act as a suspending agent in milk only when mixed at 60°–70°C. Hess and Siehrs (10) noted that when the residues of a hot water extraction were re-extracted with steam at 105°–120°C., a substance was obtained which suspended cocoa in milk when mixed at 10°–20°C.

These observations indicated that fractionation of the polysaccharides in Irish moss was feasible and that these fractions differed in certain properties. The purpose of the present work was to compare the properties of fractions separated by (*a*) potassium chloride and (*b*) re-extraction of the plant at increasing temperatures. Measurements were made of sulphate content, optical rotation, gel strength, intrinsic viscosity, sedimentation rate, and electrophoretic mobility.

[1]*Manuscript received October 4, 1954.*
Contribution from the Maritime Regional Laboratory, National Research Council, Halifax, Nova Scotia. Issued as N.R.C. No. 3515.

PREPARATION AND FRACTIONATION

All preparations were made from one lot of *Chondrus crispus* harvested at Prospect, Nova Scotia, in September, 1952. The plants were washed, air-dried, and milled to pass a 40-mesh screen. Manipulations were carried out as quickly as possible and toluene was added as a preservative when necessary. Samples were stored at −13°C. No excessive bacterial contamination was found at any time either microscopically or by plating.

The solvent used throughout for extraction and fractionation was aqueous sodium acetate of ionic strength (*I*) 0.02.

The various fractions were studied exclusively as the sodium salt. A 0.5% solution of the crude polysaccharide was dialyzed with internal mechanical stirring against aqueous sodium acetate for 24 hr. at 10°C. The acetate was then removed by dialysis against a solution of 50–100 mgm./liter sodium hydroxide in distilled water. If the concentration of sodium hydroxide was 1% of the concentration of carrageenin in the solution, the final pH of the dialyzate was 8–9. Dialysis against distilled water caused the pH to fall and degradation to occur which brought about a marked drop in viscosity.

Sodium carrageenate was obtained by freeze-drying the dialyzed solution. The water content of this material was 1–4%.

Fractionation with Potassium Chloride

Following the method of Smith *et al.* (21, 22), potassium chloride was added to the solutions of carrageenin. On centrifugation a gel separated and the supernatant liquid was decanted. These fractions are subsequently termed *gel* and *sol* respectively. Fractionation was difficult with carrageenin of high intrinsic viscosity because of more or less complete gelation. A more effective fractionation was possible after the solutions had been heated to 90°C. for 15 min. and cooled. The intrinsic viscosity of the purified polysaccharide was unchanged by this treatment.

Preliminary fractionations confirmed in general the results of Smith and co-workers (21, 22). The fractionation with potassium chloride, which was studied in detail, is shown in Fig. 1. Dried, ground *Chondrus crispus* was extracted with 0.02 *M* aqueous sodium acetate at 100°C. for five minutes in a Servall Dumore blendor. The solution was clarified by centrifugation and the crude polysaccharide was precipitated by pouring into five volumes of ethanol. The yield on the basis of dry weight was 65%.

The crude polysaccharide was redissolved at a concentration of 0.5% and the solution heated to 90°C. for 15 min. Part of the solution was dialyzed and freeze-dried to give the unfractionated material (Fig. 1). The remainder was fractionated by adding a 10% solution of potassium chloride dropwise with vigorous stirring until a concentration of 0.4% was established. This caused the separation of a *sol* fraction, S1, and a *gel* fraction, G1. Part of G1 was dialyzed and refractionated to give S2 and G2. Fractions were finally dialyzed and freeze-dried to give the sodium salt. The ratio G1/S1 was 2.36 and G2/S2 was 2.43. These *gel*/*sol* ratios were considerably larger than the values reported by Smith *et al.* (21, 22). The higher concentration of carrageenin used by us

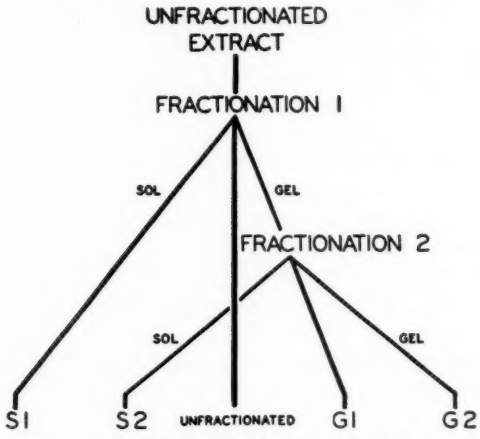

FIG. 1. Fractionation with potassium chloride.

(0.5% compared to 0.05–0.2%) could account for this difference. The equality of G1/S1 and G2/S2 showed that the fractionation was not as clean-cut as that obtained by Smith *et al.* (22) with more dilute solutions.

Successive Extraction at Increasing Temperature

Two series of extractions were made. These are designated Extraction E and Extraction F.

Extraction E.—Forty grams of dried, ground *Chondrus crispus* were stirred in 1400 cc. of aqueous sodium acetate at 30°C. for two hours. After centrifuging the clear supernatant liquid was dialyzed and freeze-dried. The residue was re-extracted at 60°C. for 15 min. After separation, a further extraction was made at 120°C. for 15 min. The final residue was discarded. As controls, portions of the 30°C. and 60°C. extracts were subjected to identical treatment at 120°C. Notation of the extracts and yields expressed as percentages of the total yield are given in Table I.

TABLE I

EXTRACTION E. SUCCESSIVE EXTRACTIONS OF IRISH MOSS AT 30°C., 60°C., AND 120°C.

	Temp., °C.	Time, min.	Yield, % of total	Notation of fraction
	30	120	25	E 30
	60	15	55	E 60
	120	15	20	E 120
Controls	30–120	15	—	EC 30–120
	60–120	15	—	EC 60–120

Extraction F.—Extraction F was similar to Extraction E except that temperatures were 60°C., 100°C., and 120°C. Portions of the 60°C. extract were subjected to the higher temperatures to provide controls. Notation and yields are given in Table II.

TABLE II

EXTRACTION F. SUCCESSIVE EXTRACTIONS OF IRISH MOSS AT 60°C., 100°C., AND 120°C.

	Temp., °C.	Time, min.	Yield, % of total	Notation of fraction
	60	60	77.5	F 60
	100	60	16.0	F 100
	120	25	4.2	F 120-A
	120	60	2.3	F 120-B
Controls	100	60	—	FC 100
	120	25	—	FC 120-A

ANALYTICAL PROCEDURES

Measurement of Concentration

The concentration, c, was based on the weight of purified material dried at 50°C. *in vacuo*. For sulphate content, gel strength, optical rotation, and refractive increment, concentrations were computed by direct weighing. For viscosity, sedimentation, and electrophoresis a refractometric determination was made with a Bellingham and Stanley refractometer. The mean value of dn/dc at 5461 Å for six different samples was 0.132 ($\pm$0.002) gm.$^{-1}$ cm.^{3}

Optical Rotation

The specific rotation was measured at a concentration of 0.3% in a 20 cm. tube at room temperature (23°C.) in a Rudolph polarimeter with a sodium lamp.

Sulphate

Sodium carrageenate was hydrolyzed by refluxing for three hours in 6 *N* hydrochloric acid. The solution was diluted and filtered. Sulphate was determined in the filtrate as barium sulphate. Measurements were done in duplicate and the mean deviation was $\pm$0.7%.

Ionic Mobility

Electrophoresis was observed at 25°C. in a Tiselius apparatus fitted with the Longsworth scanning device. The buffer was sodium acetate (pH = 5.5, I = 0.05) made up according to Green (7). The usual technique was modified as previously described (6). The mobility, U, was the mean for the rates of migration of ascending and descending boundaries.

Viscosity

The intrinsic viscosity, $[\eta]$, was determined with Ubbelohde capillary viscometers as previously described (6). A correction for degradation on storage was not necessary because it was found that the viscosity was constant over long periods for the sodium salt obtained from a solution at pH 8–9. Measurements were made at 25°C. in acetate buffers (pH = 5.5; I = 0.05).

Some variation of intrinsic viscosity with rate of shear has been observed in carrageenin of high molecular weight (14). The intrinsic viscosity observed must, therefore, be considered to obtain only for the mean rate of shear for solvent flow (1100 sec.$^{-1}$) in the viscometers used.

Gel Strength

Gel strength was measured with the apparatus shown in Fig. 2. A motor-driven cylindrical plunger (0.8 cm. in diameter) descended at 0.15 cm./sec. on the surface of the gel contained in a 5 ml. beaker as used in the Beckman

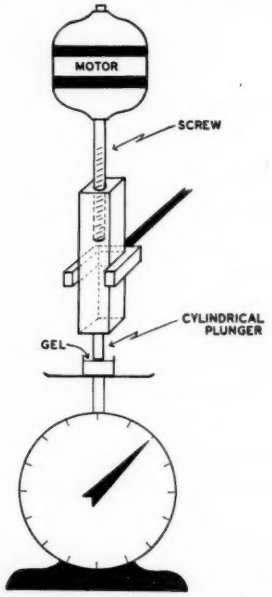

FIG. 2. Apparatus for measurement of gel strength.

pH meter. The beaker rested on a 500 gm. dietary spring balance. The breaking point was the maximum reading of the balance before penetration. This point was quite sharp and readily determined.

The solvent was a solution of potassium chloride ($I = 0.05$) in acetate buffer (pH = 5.5; $I = 0.05$). Gels were made by allowing a 2% solution of the polysaccharide to set overnight at a temperature of 20°C. Immediately before measurement the gel was inverted in the beaker, exposing a fresh surface. A stainless steel disk placed initially in the bottom of the beaker facilitated this operation. Measurements were done in triplicate and the mean deviation was $\pm 5\%$.

Sedimentation

Sedimentation was observed in an analytical Spinco ultracentrifuge at 42°C. to inhibit gelation. The rotor and cells were kept at 50°C. overnight. The filled cells and the rotor were then equilibrated at 50°C. for one hour. In the machine, the rotor was equilibrated under vacuum for one hour. At intervals during the run the temperature was taken with the fixed couple. The difference between the readings for the fixed and free couples was taken at

the end of the run. On an average the free couple reading exceeded the fixed couple reading by 0.6°C. By this method excellent temperature control was achieved. The range of fixed couple readings in any one run was 0.8°C. and the average temperature was 42.3 (±0.4)°C. for 66 runs. Thus, the range during any one run was small and the temperature for a series of runs was essentially constant.

As shown in Fig. 3, the graphs of $\log_{10} r$ vs. time were linear for all concentrations studied. Although the concentrated solutions were gel-like, no variation of the sedimentation constant, s, with time occurred as reported for thymus nucleoprotein (20).

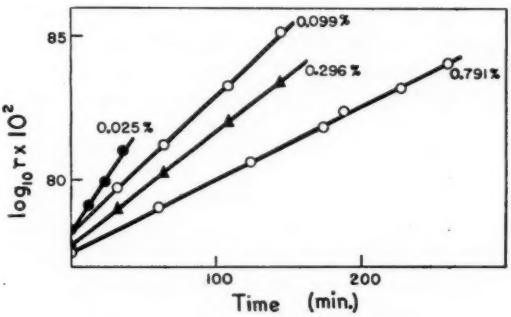

FIG. 3. Graphs of $\log_{10} r$ vs. time for S1.

Sedimentation constants were corrected (1) to water at 40°C. This correction implies that the molecular shape in the buffer is unaltered in water. With a polyelectrolyte such as sodium carrageenate this is not the case. Therefore the s°_{40} value gives the rate of sedimentation in water for a molecule having the same shape as sodium carrageenate in the buffer used.

Areas of the peaks were measured on enlargements with a planimeter. For the two components observed, dn/dc was assumed equal and relative concentrations were assumed to be proportional to areas. The relative area of the fast "shoulder" varied with the total concentration of carrageenin and was sometimes difficult to estimate. To permit comparison, all measurements of area were done on runs at the same concentration of carrageenin (0.007 gm. cm.$^{-3}$).

The variation of s°_{40} with c was studied for the fractions shown in Fig. 1 and Table II. As may be seen in Fig. 6, s°_{40} usually increased rapidly for low values of the concentration. Graphs of $\sqrt{s}$, $1/s$, and $\log_{10} s$ vs. c and sc vs. s failed to give a straight line. The graph of $\sqrt{(1/s)}$ vs. c was linear but the intercept was too near the origin to permit interpretation. The method of Jullander as used by Greenwood (8) was found to be applicable. On the same graph s°_{40} vs. c and $s^\circ_{40}\,\eta_{rel}$ vs. c are plotted. As shown in Fig. 4, the double extrapolation permits a reasonably unambiguous determination of $(s^\circ_{40})_{c=0}$. For these fractions the values of $(s^\circ_{40})_{c=0}$ were also obtained by the method of Newman, Loeb, and Conrad (16). Agreement between the two methods was ±1%.

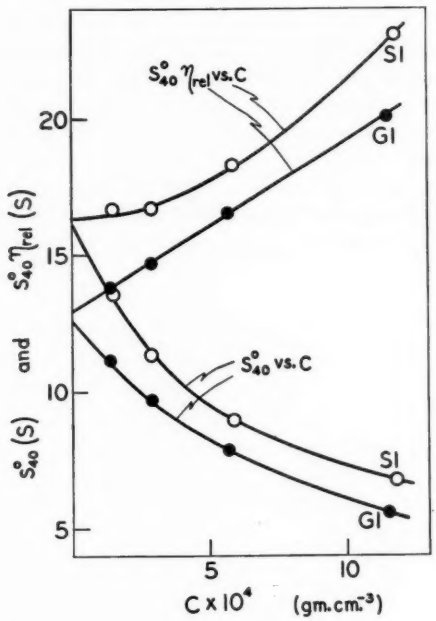

FIG. 4. Graphs of s°_{40} vs. c and $s^\circ_{40}\,\eta_{rel}$ vs. c for S1 and G1.

The molecular weight, M, was computed by the method of Mandelkern and Flory (12) from

$$[1] \qquad M = \left(\frac{(s^\circ_{40})_{c=0}\,[\eta]^{\frac{1}{2}}\,\eta_0 N}{2.5 \times 10^6(1-\bar{v}\rho)}\right)^{3/2}$$

where η_0 is the viscosity of the solvent, N is Avogadro's number, $\bar{v}$ is the partial specific volume of the solute, and ρ is the density of the solvent. The partial specific volume determined by Cook *et al.* was used (3).

Certain experimental factors limited the validity of the absolute values of M. The intrinsic viscosity was measured at 25°C. in an ionic strength of 0.05 whereas sedimentation was observed at 40°C. in an ionic strength of 0.2. Cook *et al.* (3) have noted that $[\eta]$ does not change markedly for such a range in ionic strength and temperature. Also, for one of the undegraded fractions studied, the decrease in $[\eta]$ for rates of shear from 100 sec.$^{-1}$ to 1000 sec.$^{-1}$ was 13%. However since $[\eta]$ occurs in Equation 1 only as a cube root such errors are small.

As noted by Smith *et al.* (22) a more serious discrepancy lies in the assumption of a random, uncharged coil implicit in the Mandelkern-Flory treatment. The carrageenin molecule is charged and although its shape in solution is not known with certainty, viscometric (13) and light scattering (4) results suggest

that it is rod-like. However, experimental conditions were identical for all fractions and therefore the relative values of M were considered to indicate the approximate changes in molecular weight from fraction to fraction.

RESULTS

Fractionation with Potassium Chloride

The electrophoretic and ultracentrifugal diagrams of the fractions (Fig. 1) are shown in Tables III and IV respectively. The corresponding values for the sulphate content, $[\eta]$, gel strength, M, and $[\alpha]_D$ are given in Table V. Included in Table IV are the relative concentrations of the minor component observed in sedimentation.

Successive Extraction at Increasing Temperature

The ultracentrifugal data for Extractions E and F (Tables I and II) are given respectively in Tables VI and VIII. The corresponding values of $[\alpha]_D$, gel strength, $[\eta]$, and sulphate content are given in Tables VII and IX.

TABLE III

ELECTROPHORESIS FOR THE FRACTIONS OBTAINED WITH POTASSIUM CHLORIDE SHOWN IN FIG. 1. IN THE DIAGRAMS, THE MEAN TIME AND DISTANCE OF MIGRATION OF THE ASCENDING BOUNDARIES WERE RESPECTIVELY 110 (±3) MIN. AND 63 (±3) MM.; THESE WERE 58 (±5) MIN. AND 28 (±2.5) MM. FOR THE DESCENDING BOUNDARIES

Fraction	Diagram	$U \times 10^4$, cm.^{2} sec.$^{-1}$ volt^{-1}
	ASCENDING → DESCENDING ←	
S1	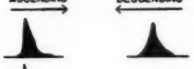	3.1
S2		3.0
Unfrac.		2.9
G1		2.9
G2	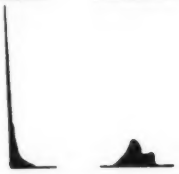	2.8

TABLE IV

SEDIMENTATION CONSTANTS AND DIAGRAMS FOR THE FRACTIONS OBTAINED WITH POTASSIUM CHLORIDE SHOWN IN FIG. 1. IN THE DIAGRAMS THE BAR ANGLE WAS 70° AND THE MEAN DISTANCE OF SEDIMENTATION WAS 6.9 (±0.8) MM.

Fraction	Diagram $c = 0.007$ gm. cm.$^{-3}$	Percentage of minor component	$(s^{\circ}_{40})_{c=0}$ S
S1		16	16
S2		10	13
Unfrac.		7	14
G1		4	13
G2		0	11

TABLE V

DATA FOR FRACTIONATION WITH POTASSIUM CHLORIDE SHOWN IN FIG. 1
ELECTROPHORESIS AND ULTRACENTRIFUGE DIAGRAMS ARE IN TABLES III AND IV RESPECTIVELY

Fraction	Sulphate, % SO_4	$[\eta] \times 10^{-2}$, gm.$^{-1}$ cm.^{3}	Gel strength, gm. cm.$^{-2}$	$[\alpha]_D$	$M \times 10^{-5}$
S1	24.1	15	<20	+29.0	14
S2	24.9	18	60	+41.3	11
Unfrac.	23.6	18	150	+48.5	12
G1	22.9	16	290	+50.7	10
G2	22.6	18	470	+60.3	8

TABLE VI

SEDIMENTATION CONSTANTS AND DIAGRAMS FOR SUCCESSIVE EXTRACTIONS AT INCREASING TEMPERATURE SHOWN IN TABLE I. IN THE DIAGRAMS THE BAR ANGLE WAS 70° AND THE MEAN DISTANCE OF SEDIMENTATION WAS 6.9 (±0.6) MM.

Extract	Diagram c = 0.007 gm. cm.$^{-3}$	Percentage of minor component
E 30		9
E 60		10
E 120		18
EC 30–120		0
EC 60–120		5

TABLE VII

DATA FOR SUCCESSIVE EXTRACTIONS AT INCREASING TEMPERATURE DESCRIBED IN TABLE I. ULTRACENTRIFUGE DIAGRAMS ARE SHOWN IN TABLE VI

Extract	Sulphate, % SO_4	$[\eta] \times 10^{-2}$, gm.$^{-1}$ cm.^{3}	Gel strength, gm. cm.$^{-2}$	$[\alpha]_D$
E 30	26.4	10	0	+45.7
E 60	25.9	14	240	+47.9
E 120	25.0	11	50	+32.4
EC 30–120	25.9	8	0	+45.1
EC 60–120	24.7	11	210	+46.2

TABLE VIII

SEDIMENTATION CONSTANTS AND DIAGRAMS FOR SUCCESSIVE EXTRACTIONS AT INCREASING TEMPERATURE SHOWN IN TABLE II. IN THE DIAGRAMS THE BAR ANGLE WAS 70° AND THE MEAN DISTANCE OF SEDIMENTATION WAS 7.0 (±0.5) MM.

Extract	Diagram c = 0.007 gm. cm.$^{-3}$	Percentage of minor component	$(s^{\circ}_{40})_{c=0}$ S
F 60		9	13
F 100		14	13
FC 100		8	12
F 120-A		6	10
FC 120-A		0	8
F 120-B		0	8

TABLE IX

DATA FOR SUCCESSIVE EXTRACTIONS AT INCREASING TEMPERATURE DESCRIBED IN TABLE II. ULTRACENTRIFUGE DIAGRAMS ARE SHOWN IN TABLE VIII

Extract	Sulphate, % SO_4	$[\eta] \times 10^{-2}$, gm.$^{-1}$ cm.^{3}	Gel strength, gm. cm.$^{-2}$	$[\alpha]_D$	M $\times 10^{-5}$
F 60	25.3	13	210	+50.4	10
F 100	22.8	11	50	+47.3	8
FC 100	25.4	12	210	+49.0	8
F 120-A	18.4	8	10	+40.3	5
FC 120-A	24.7	7	150	+49.1	3
F 120-B	—	5	—	+25.1	3

DISCUSSION

In families of polymeric substances there are two major categories of molecular differences. In the first the molécules of any single polymer may differ in chain length to give a polydispersity of molecular weight. In the second the difference is of molecular type. For example, sulphated polysaccharides may differ in type of linkage, sugar residues, branching, or degree of sulphation. In the present work we are concerned mainly with the second category, i.e. with components rather than polydispersity of molecular weight. Therefore

properties independent of molecular weight were most important in identifying components.

As mentioned previously, the fractionations were probably not sharp and it is likely that all the fractions were, to some extent, mixtures of components. However, marked differences were noted in some of the properties from fraction to fraction. It was therefore possible to infer that in some fractions a component with certain physical properties predominated. The results indicated three components. The differences in the various properties of these components are discussed in detail in the sections below.

Gel Strength

Large differences were noted in the gel strengths of different fractions compared with the relatively small decrease in the controls (EC 60–120 in Table VII and FC 100 and FC 120-A in Table IX). Further S1, with a molecular weight twice as great as the strongly gelling G2, had nearly zero gel strength. Thus it appeared that the gel strength depended more on structural factors than on molecular weight.

For successive extractions at increasing temperatures (Tables VII and IX) a pronounced maximum in gel strength was noted in the 60°C. extracts. This supports the early reports (15) of a non-gelling cold extract. The decrease in gel strength for re-extractions at 100–120°C. agrees with the findings of Hess and Siehrs (10). These results suggest that there are three components extractable at approximately 30°C., 60°C., and 100–120°C., the 60°C. extract having a strong gelling tendency.

The extract fractionated with potassium chloride was made at 100°C. and therefore would contain some of each of the three components. The fractionation would be expected to concentrate the single gelling component in the *gel* fractions while the *sol* fractions would contain the two non-gelling components. Provisionally the components extractable at 30°C., 60°C., and 100–120°C. will be called respectively Components A, B, and C.

Sedimentation

In nearly all the fractions (Tables IV, VI, and VIII) a varying proportion of a minor fast-moving component was noted. A similar component has been noted by Cook *et al.* (3) and Smith *et al.* (21, 22). Usually the minor component was more concentrated in extracts made at 100°–120°C. (Tables VI and VIII) and, as later discussed, F 120-B was composed largely of this material. Its proportion was not increased in the controls and thus it probably did not originate from heat treatment of the other components.

The minor component was probably the non-gelling Component C. This is supported by the increased concentration of the minor component in the sol fractions (Table IV). However, its proportion was small. Thus, the main component of the *sol* fractions would be A.

Differences in the three components are further illustrated by the concentration dependence of s°_{40}. As shown in Fig. 5, the graphs of s°_{40} vs. c for F 60 and F 120-A were coincident from $c = 0.002$ to $c = 0.01$ gm. cm.$^{-3}$ despite the marked decrease in $[\eta]$ and M on degradation. Below $c = 0.002$ gm. cm.$^{-3}$

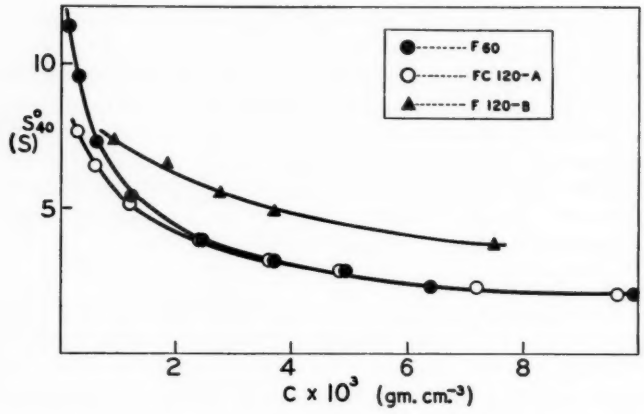

FIG. 5. Graphs of s°_{40} vs. c for F 60, FC 120-A, and F 120-B (Table IX).

the heavier molecule sedimented more quickly. However, F 120-B shows a faster sedimentation over most of the concentration range with a smaller dependence of s°_{40} on c. A similar though smaller effect was noted for F 120-A. These results suggest that F 120-A and F 120-B are composed largely of the quickly sedimenting Component C. The molecular weight of F 120-B is considerably less than that of F 60. The difference in sedimentation behavior must therefore be associated with a difference in shape or intermolecular interaction.

A lesser distinction in sedimentation is noted for G1 and the main component of S1, as shown in Fig. 6. The concentration dependence is similar but

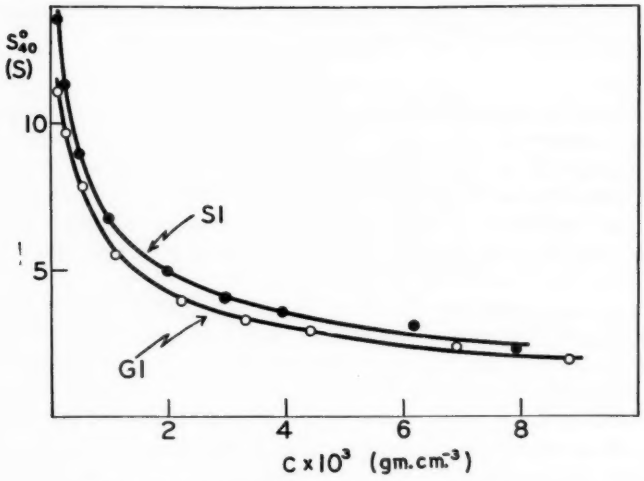

FIG. 6. Graphs of s°_{40} vs. c for S1 and G1 (Fig. 1).

s°_{40} for S1 is higher than that for G1. This small increase in s°_{40} occurred in all fractions rich in Component A. This might be expected since the molecular weights for the *sol* fractions (Table V) were greater than those for the *gel* fractions in agreement with the data of Smith *et al.* (21, 22). However, the coincidence of s°_{40} vs. c for F 60 and FC 120-A shows that a change in chain length alone does not alter s°_{40} at $c \geqslant 0.002$ gm. cm.$^{-3}$ Therefore, the slightly greater value of s°_{40} for Component A probably arises from a small structural variation in the polysaccharide rather than a difference in chain length.

Sulphate Content

The sulphate content was remarkably constant for most fractions at 23–26%. Also, the controls (Tables VII and IX) showed that a negligible loss in sulphate occurred on heating to 100–120°C. A decrease in sulphate content was noted for F 100 and F 120-A (Table IX). This suggests that a lower sulphate content was a property of Component C.

The sulphate contents of the *sol* fractions were higher than those of the *gel* fractions (Table V). This effect was smaller but in the same direction as that observed by Smith and Cook (21). The low sulphate content of Component C concentrated in the *sol* fractions could have masked the difference in sulphate between Components A and B.

Optical Rotation

On heating, the change in $[\alpha]_D$ for the controls was negligible (Tables VII and IX). But low values of $[\alpha]_D$ were observed in all fractions in which the quickly sedimenting component was concentrated (e.g. S1 in Table V or F 120-B in Table IX) indicating a low rotation for Component C.

The equality of $[\alpha]_D$ for E 30 and E 60 (Table VII) suggested that the rotations of Components A and B were essentially equal. The low rotation of the *sol* fractions could then be due to the increased concentration of Component C.

Electrophoresis

As observed by previous workers (3, 6) the electrophoretic diagrams (Table III) showed no clear indication of separate components. The peak asymmetry increased with gel strength. This effect was due to a non-classical distribution of concentration at the boundaries (described in detail elsewhere (5)) and could not definitely be associated with polydispersity. Because of the uncertainty in interpretation of the patterns, electrophoresis was not attempted on all the fractions.

The mobility of the *sol* fractions was slightly greater than that of the *gel* fractions. This trend was probably due to the smaller sulphate content (Table V) of the *gel* fractions.

Viscosity

The intrinsic viscosity of E 60 (Table VII) was greater than that of E 30 and a marked decrease in $[\eta]$ occurred for the extracts and controls of Extraction F at 100–120°C. (Table IX). As noted by Rose (18) this decrease is probably due to the degradation of the polysaccharide by the high tempera-

tures used. Because of the ease of degradation of carrageenin (6, 13) the intrinsic viscosity could not be used as a means of identifying components.

CONCLUSIONS

The results of the potassium chloride fractionation agree well with those of Smith *et al.* considering the different sources of material in the two investigations. In both, the *sol* fractions showed a higher molecular weight, sedimentation constant, and sulphate content and a lower specific rotation (Tables IV and V). The small divergences in detail from the results of these workers could be due to either (*a*) different degrees of degradation on preparation of the carrageenin or (*b*) different proportions of the two non-gelling components in the sol fractions.

The significant properties of the three components are summarized in Table X. Sulphate content and $[\alpha]_D$ were found to be independent of the

TABLE X

A SUMMARY OF THE PROPERTIES OF THE THREE COMPONENTS EXTRACTABLE FROM *Chondrus crispus*

Component	Temp. of extraction, °C.	Relative conc., % of extractable material*	Gelling tendency	$[\alpha]_D$	Sulphate content (%)
A	30	35	Nil	45–50	26
B	60	50	Strong	45–60	22–26
C	100–120	15	Weak	<30	<20

**The proportion of Component C was derived from the areas of the quickly sedimenting components in Extraction F. The remainder was assumed to consist entirely of Components A and B. An approximate A/B ratio was obtained by assuming the main component of S1 and S2 to be entirely A.*

decrease in molecular weight which occurred on extraction at higher temperatures. The gel strength showed some decrease on degradation but this was small compared with the large differences between the gelling and non-gelling extracts. These properties therefore pertain to the molecular *type* of the component. The figures given for the proportion of a component, $[\alpha]_D$, or the sulphate content obtain only for the sample of Irish moss examined although the trends noted may be general.

From the results it is clear that Components A and B made up the bulk of the extractable polysaccharide. The marked distinction between the two components lies in the ability of B to form a gel. The gelling tendency might be related to different degrees of branching in the molecules. An appreciable change in the concentration dependence of the sedimentation would then be expected. As shown in Fig. 6, the sedimentation behavior of the two components was similar. On the other hand, O'Neill (17) has recently discovered 24% of 3,6-anhydro-D-galactose in a *gel* fraction whereas the corresponding *sol* fraction contained considerably less (23). The gelling tendency may therefore be associated with this structural difference in the chain rather than a difference in shape due to branching.

The minor component, C, comprised only a small percentage of the extractable material although a greater proportion may be available with prolonged extraction. The low sulphate content suggests that it was a desulphated product of one of the major components. This could give rise to the small concentration dependence of s°_{40} due to the decrease in interaction (Fig. 5). However, the controls showed no loss in sulphate, which indicated that the material differed in this respect from Component A or B.

ACKNOWLEDGMENTS

The authors wish to thank Dr. A. N. O'Neill for his help in the measurements of optical rotation, and H. F. Roberts, F. G. Mason, and Miss M. C. Chepeswick for technical assistance.

REFERENCES

1. ALEXANDER, A. E. and JOHNSON, P. Colloid science. Oxford University Press, London. 1949.
2. BUCHANAN, J., PERCIVAL, E. E., and PERCIVAL, E. G. V. J. Chem. Soc. 51. 1943.
3. COOK, W. H., ROSE, R. C., and COLVIN, J. R. Biochim. et Biophys. Acta, 8: 595. 1952.
4. GORING, D. A. I. Can. J. Chem. 31: 1078. 1953.
5. GORING, D. A. I. Nature, 173: 734. 1954.
6. GORING, D. A. I. J. Colloid Sci. 9: 141. 1954.
7. GREEN, A. A. J. Am. Chem. Soc. 55: 2331. 1933.
8. GREENWOOD, C. T. Biochem. J. (London), 57: 151. 1954.
9. HAAS, P. and RUSSELL-WELLS, B. Biochem. J. (London), 23: 425. 1929.
10. HESS, M. P. and SIEHRS, A. E. U.S. Patent No. 2,462,398. 1949.
11. JOHNSTON, R. and PERCIVAL, E. G. V. J. Chem. Soc. 1994. 1950.
12. MANDELKERN, L. and FLORY, P. J. J. Chem. Phys. 20: 212. 1952.
13. MASSON, C. R. and CAINES, G. W. Can. J. Chem. 32: 51. 1954.
14. MASSON, C. R. and GORING, D. A. I. To be published.
15. MORI, T. Advances in Carbohydrate Chem. 8: 315. 1953.
16. NEWMAN, S., LOEB, L., and CONRAD, C. M. J. Polymer Sci. 10: 463. 1953.
17. O'NEILL, A. N. Abstr. of papers presented before the Div. of Carbohydrate Chem., Am. Chem. Soc. September, 1954.
18. ROSE, R. C. Can. J. Research, F, 28: 202. 1950.
19. RUSSELL-WELLS, B. Biochem. J. (London), 16: 578. 1922.
20. SHOOTER, K. V., DAVISON, P. F., and BUTLER, J. A. V. Biochim. et Biophys. Acta, 13: 192. 1954.
21. SMITH, D. B. and COOK, W. H. Arch. Biochem. and Biophys. 45: 233. 1953.
22. SMITH, D. B., COOK, W. H., and NEAL, J. L. Arch. Biochem. and Biophys. 53: 192. 1954.
23. SMITH, D. B., O'NEILL, A. N., PERLIN, A. S., and COOK, W. H. To be published.
24. YOUNG, E. G. and RICE, F. A. H. J. Biol. Chem. 164: 35. 1946.

THE PHOTO-OXIDATION OF AZOMETHANE[1]

By G. R. Hoey[2] and K. O. Kutschke

ABSTRACT

The photo-oxidation of azomethane has been studied at low oxygen pressures (0.02 to 1 mm.) in the temperature range *ca.* 25°C. to 161°C. The primary process in the normal photolysis of azomethane is essentially unaffected by the presence of oxygen. Carbon monoxide is probably a secondary product of the oxidation of methyl radicals. Carbon dioxide formation is quite small, and therefore neither methyl radicals nor $CH_3N{=}N{-}CH_2$ radicals are oxidized appreciably to carbon dioxide. Nitrous oxide, which is a major product of the oxidation, is most likely formed from the oxidation of $CH_3N{=}NCH_2$ radicals. The suggested mechanism of N_2O formation is:

$$CH_3N{=}N{-}CH_2+O_2 = CH_3N{=}NCH_2O_2$$
$$CH_3N{=}N{-}CH_2O_2 = CH_3+N_2O+H_2CO.$$

The reaction of methyl radicals with oxygen was found to proceed with a negligible activation energy and a steric factor of the order of 10^{-3}. Evidence for the occurrence of the reactions

$$2CH_3O_2 = 2CH_3O+O_2$$
$$2CH_3O = CH_3OH+H_2CO$$

at room temperature was obtained.

INTRODUCTION

The photolysis of azomethane has been studied extensively, and the mechanism appears to be well established. The main reactions involved in the photolysis are (15, 23):

$$CH_3N{=}NCH_3+h\nu = 2CH_3+N_2$$
$$CH_3+CH_3N{=}NCH_3 = CH_4+CH_3N{=}NCH_2$$
$$CH_3+CH_3N{=}NCH_3 = (CH_3)_2N{-}NCH_3$$
$$CH_3+CH_3 = C_2H_6$$
$$CH_3+CH_3N{=}NCH_2 = CH_3N{=}NC_2H_5$$
$$CH_3+(CH_3)_2N{-}NCH_3 = (CH_3)_2N{=}N(CH_3)_2.$$

The quantum yield of nitrogen formation is close to unity at the longer wavelengths, and independent of temperature. Since Φ_{N_2} is independent of the pressure of azomethane, and unaffected by the presence of carbon dioxide, the possibility of an excited molecule mechanism is unlikely (23). There is no evidence for a stable $CH_3N{=}N$ radical. Azomethane has been shown to be a convenient source of radicals for reactions of the type

$$CH_3+RH = CH_4+R$$

where RH is a hydrogen donor compound (1, 15). In view of these features of the photolysis, azomethane would be expected to be a convenient source of radicals for a study of the reaction of methyl radicals with oxygen.

Marcotte and Noyes (18) have investigated the photolysis of acetone in the presence of oxygen at low oxygen pressures and low light intensities. Their

[1]*Manuscript received November 18, 1954.*
Contribution from the Division of Pure Chemistry, National Research Council, Ottawa, Canada. Issued as N.R.C. No. 3514.
[2]*National Research Laboratories Postdoctorate Fellow 1952–1954.*

results indicated that the reaction between a methyl radical and oxygen, which they assumed to yield a formyl radical and a water molecule, proceeds with negligible activation energy and a low steric factor (*ca.* 10^{-4}). Christie (8), working in Noyes' laboratories, has since shown that, for experimental conditions similar to those of Marcotte and Noyes, methyl radical oxidation leads to formaldehyde and water with a further acetone molecule supplying the additional hydrogen. On the basis of Christie's results, the earlier scheme must be considered oversimplified; in particular the products of methyl radical interaction with oxygen postulated by Marcotte and Noyes seem rather doubtful.

Martin and Noyes (19) have extended the study to mixtures of mercury dimethyl and oxygen, and methyl iodide and oxygen. The relative amounts of CO and CO_2 were different than for acetone. Formaldehyde is a major product with methyl iodide – oxygen mixtures at room temperature (2, 19) and with acetone at temperatures above 120°C. (8, 14), whereas with mercury dimethyl with temperatures above 100°C., it does not seem to be a major product (19). It would be interesting to compare results obtained with azomethane and oxygen with those obtained by Noyes and co-workers using similar experimental conditions.

There has been no study reported in the literature on the thermal oxidation of azomethane. Scheer and Taylor (22) photolyzed azomethane in the presence of propane and oxygen. They observed a slow oxidation of propane in the temperature range 35° to 200°C., and cool flames at 250°C.

EXPERIMENTAL

Part I

The azomethane was prepared by Mr. R. Renaud of these laboratories (21). It was purified by a trap to modified Ward still (16) distillation, and the fraction collected between −78°C. and −110°C. was stored as a gas in a blackened flask behind a mercury cutoff. The oxygen was prepared by heating potassium permanganate and purified by passage through two traps at liquid nitrogen temperature. Commercial carbon dioxide was degassed at −196°C. Carbon monoxide was prepared by heating a $ZnO–CaCO_3$ mixture (27) and purified by passage through a trap at −196°C.

A Hanovia S-500 mercury arc was used as the light source. The beam, which was collimated by a quartz lens, completely filled the reaction cell. A Corning violet ultra filter No. 586, 6 mm. in thickness, was used in all the experiments. This filter limited the incident intensity mainly to the 3340 Å and 3660 Å wavelengths. The relative extinction coefficients of these wavelengths are such that the absorbed light intensity is effectively the 3660 Å wavelength (15). The incident light intensity was varied by the use of neutral density filters.

The quartz cell was 10 cm. long and 5 cm. in diameter with a volume of 180 cc. The cell was surrounded by an aluminum block furnace, and the temperature was controlled manually to ±1°C. The total volume of the reaction system, including reaction cell, U-tube manometer, stirrer, and McLeod gauge, was 400 cc.

Oxygen pressures as low as 0.02 mm. were used in this work. An oxygen consumption of at least 0.15 mm. was necessary for analysis of the products. Since constant oxygen pressures were desired at pressures less than 0.15 mm., small oxygen doses (0.003 mm.) were added during the run as frequently as necessary to maintain constancy of pressure. The number of doses required was determined in trial runs.

The run was interrupted at regular intervals (two to five minutes), at which time a premeasured oxygen dose was pumped into the reaction mixture through an iron, glass-enclosed float, and sufficient time allowed for mixing of the gases. The rate of oxygen disappearance was found to depend on the temperature and on the oxygen pressure. To compensate for this, the number of doses per run, and consequently the exposure time per dose (rather than the size of the oxygen dose), was varied. Mixing of the gases was effected by a glass propeller type stirrer with a glass-enclosed copper core at the bottom; the stirrer was driven by an induction motor. At oxygen pressures greater than 0.15 mm., 0.02 mm. doses were added during the exposure without interrupting the run.

Gas analyses were carried out for N_2, CH_4, CO, O_2, CO_2, and N_2O. After each run the reaction mixture was passed through a modified Ward still at $-196°C$. The non-condensables, N_2, CH_4, CO, and O_2, were analyzed by means of a Cu–CuO furnace at a temperature of about 230°C. The oxygen formed CuO. The CO was oxidized to CO_2 and was frozen out at a cold finger. The remainder, N_2 and CH_4, was collected and analyzed for N_2 and CH_4 mass spectrometrically. The CO_2 and the N_2–CH_4 mixture were measured directly, and the oxygen was determined by difference. The CO_2 and N_2O were distilled from the Ward still at $-160°C$., and were collected for mass spectrometric analysis. Ethane was not detected in any of the experiments in which oxygen was present.

Azomethane was used as an actinometer. A value of unity (23) for the quantum yield of nitrogen formation in the absence of oxygen was used for the temperature range 25° to 161°C. The data in the literature are in accord (4, 7, 15) with such a value although the individual values are quite often less than unity and nearer 0.9. If, in fact, $\Phi_{N_2} < 1$ in the absence of oxygen, the values of the quantum yields quoted here are too large by about 10%.

Formaldehyde was not detectable at the Ward still or by mass spectrometric analysis. This, however, is not conclusive evidence that formaldehyde is not a major product of the oxidation as the formaldehyde may have polymerized. To check this point, an amount of formaldehyde roughly comparable to that expected in the experiments described in Part II was introduced into the reaction system in the presence of azomethane. Polymerization of the formaldehyde evidently occurred as formaldehyde was not detected by the two methods mentioned above. Analysis of formaldehyde in the presence of azomethane in aqueous media was not accomplished since an acid catalyzed hydrolysis forms formaldehyde and methyl hydrazine from azomethane (28). Methods which were unsuccessful owing to this interference by azomethane were Lebbin's resorcinol test, Schiff's test, and the polarographic method (25). Thus, it

cannot be stated whether or not formaldehyde is a major product of the reaction.

The products remaining after distilling off the azomethane at −90°C. were analyzed mass spectrometrically. Water and methanol were identified positively and formed most of the fraction.

PART II

Experiments of long duration were performed at room temperature in order to collect sufficient products for chemical analysis. Large oxygen pressures were used and oxygen was not added during the run. The azomethane pressure was maintained constant during the run at 6.6 mm. by circulating the gases through two traps in the reaction system held at the temperature of dry ice.

After the run, the gases were passed to the Ward still. The non-condensables and CO_2 were analyzed as described in Part I. N_2O was not detected by mass spectrometric analysis. The azomethane was separated from the Ward still at −90°C.; no product was detected between these fractions. This fraction was shown to be azomethane with trace quantities of methanol and water by mass spectrometric analysis. These results were verified by the infrared absorption of the fraction. The remainder, which will be designated as the "liquid products", was separated from the Ward still at room temperature.

The liquid products were analyzed by the following methods. Mass spectrometric analysis showed the presence of methanol and water only. The methanol was analyzed by the method of Elving and Warshowsky (10) and by infrared analysis. The two methods agreed to within 20%. The acid, which was shown to be formic acid by its infrared absorption, was titrated directly using phenolphthalein as the indicator. Peroxides were determined by the method of Nozaki (20).

The liquid products were also placed in contact with metallic sodium. The hydrogen given off was a measure of the total active hydrogen present (amount of H_2 = ½ × amount of active hydrogen). The quantum yield of water formation was assumed to be

$$\Phi_{H_2O} = (\Phi_{\text{active hydrogen}}) - (\Phi_{CH_3OH} + \Phi_{HCOOH} + \Phi_{\text{peroxides}}).$$

RESULTS AND DISCUSSION

The lack of variation of Φ_{N_2} with the experimental conditions of temperature and oxygen pressure (Fig. 1) and of azomethane pressure (Table I) strongly suggests that nitrogen is formed solely in a primary process. Since ethane was not detected at any temperature at an oxygen pressure as low 0.02 mm., the possibility of a direct molecular rearrangement into ethane and nitrogen (6) may be discounted. This is in agreement with the conclusion reached by Davis, Jahn, and Burton (9) who observed complete suppression of hydrocarbon products and no inhibition of the nitrogen yield when the photolysis was carried out in the presence of nitric oxide (10 mm.). On the basis of this evidence, the primary process is taken as [1], proceeding with a quantum efficiency close to unity in the presence of oxygen.

$$CH_3N_2CH_3 + h\nu \rightarrow 2CH_3 + N_2. \qquad [1]$$

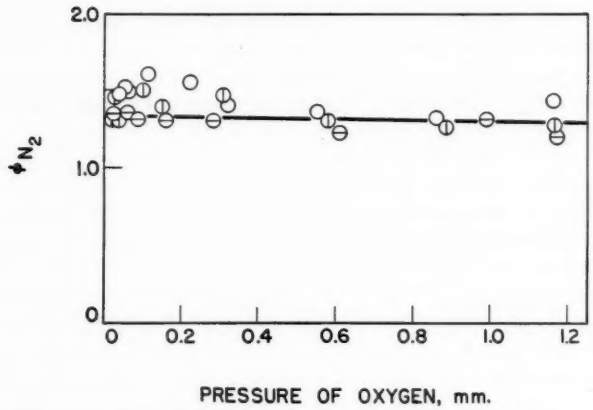

FIG. 1. Dependence of Φ_{N_2} on oxygen pressure:
$I_a = 5 \times 10^{11}$ quanta/cc./sec.; pressure of azomethane, 101 mm.; ○, 161°C.; ⊕, 123°C.; ⊖, *ca.* 25°C.

TABLE I

EFFECT OF AZOMETHANE PRESSURE ON THE REACTION

Pressure (mm.) Azomethane	Total	Φ_{N_2}	Φ_{CO}	Φ_{N_2O}	$-\Phi_{O_2}$
102	103	1.25	0.22	0.51	3.0
6.6	100[a]	1.21	0.36	—	2.2
6.6	100[b]	—	—	0.10	—
6.6	8	1.11	0.31	0.06	2.0

Pressure of oxygen = 0.9±0.1 mm.; temp. = 123°C.; $I_a = 10^{12}$ quanta/cc./sec.
[a]*CO_2 added.*
[b]*CO added.*

The photo-oxidation, under conditions such that methane is found, is postulated to proceed in part through the following steps:

$$CH_3 + A \rightarrow CH_4 + CH_3N_2CH_2 \quad [2]$$
$$CH_3 + A \rightarrow CH_3A \quad [3]$$
$$CH_3 + O_2 \rightarrow CH_3O_2 \quad [4]$$
$$CH_3A + O_2 \rightarrow CH_3AO_2 \quad [5]$$
$$CH_3N_2CH_2 + O_2 \rightarrow CH_3N_2CH_2O_2. \quad [6]$$

Reaction [2] has been well substantiated (1, 15, 23) and reaction [3] has been shown to proceed at a somewhat greater rate (15). Reaction [5] has been included to account for $-\Phi_{O_2} \geqslant 2$ at low oxygen pressure Fig. 2; i.e. every methyl radical must, directly or indirectly, lead to the consumption of one molecule of oxygen. The sole fate of methyl radicals produced in the primary process must be reaction with oxygen when Φ_{CH_4} is negligible. This condition is met at all oxygen pressures studied at room temperature, and at a progressively higher oxygen pressure as the temperature is increased (Fig. 3). A similar phenomenon is observed in the photo-oxidation of acetone (8, 14, 18).

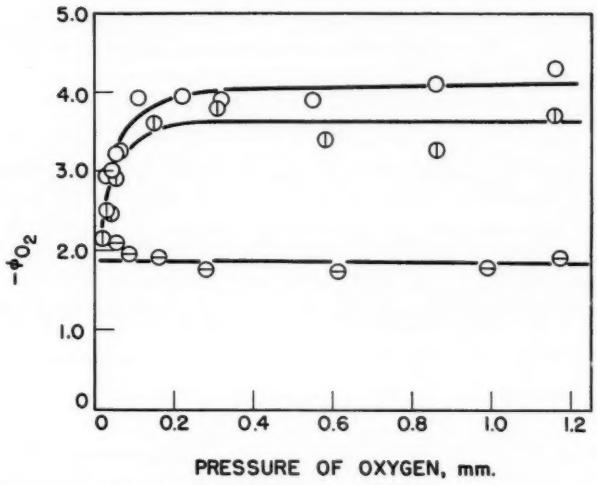

FIG. 2. Dependence of $-\Phi_{O_2}$ on oxygen pressure:
$I_a = 5 \times 10^{11}$ quanta/cc./sec.; pressure of azomethane, 101 mm.; ○, 161°C.; ◑, 123°C.; ⊖, *ca.* 25°C.

Nitrous oxide is a major product at the higher temperatures employed. An upper limit to Φ_{N_2O} is attained at oxygen pressures such that Φ_{CH_4} is negligible (Figs. 3 and 4); the value of this limit is temperature dependent (Fig. 3). At

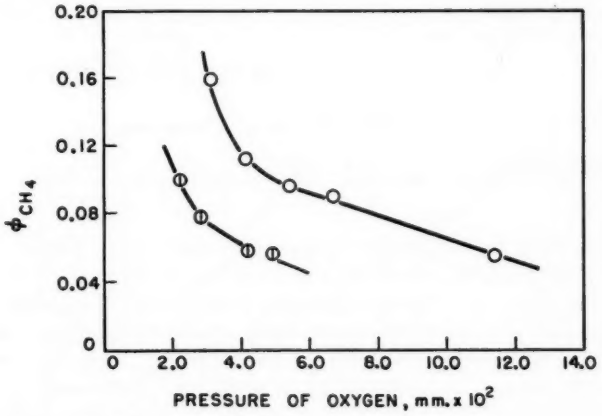

FIG. 3. Dependence of Φ_{CH_4} on oxygen pressure:
$I_a = 5 \times 10^{11}$ quanta/cc./sec.; pressure of azomethane, 101 mm.; ○, 161°C.; ◑, 123°C.

oxygen pressures such that this limit is attained, a radical resulting from the oxidation of a methyl radical must initiate a sequence of reactions which eventually produces nitrous oxide. A plausible scheme is

$$CH_3O_2 \rightarrow R+? \quad [7]$$
$$R+CH_3N_2CH_3 \rightarrow RH+CH_2N_2CH_3 \quad [8]$$
$$CH_3N_2CH_2+O_2 \rightarrow CH_3N_2CH_2O_2 \quad [6]$$
$$CH_3N_2CH_2O_2 \rightarrow CH_3+N_2O+H_2CO \quad [9]$$
$$R \rightarrow \text{no } N_2O \quad [10]$$

where R is some oxygenated radical. Reaction [10], a chain termination not involving azomethane or oxygen, is included to account for the dependence of Φ_{N_2O} on the concentration of azomethane (Table I). Insufficient data are available to determine whether [10] is of the first or second order in radical concentration. Since [8] and possibly [9] will probably require an activation energy, the temperature dependence of Φ_{N_2O} is qualitatively explained.

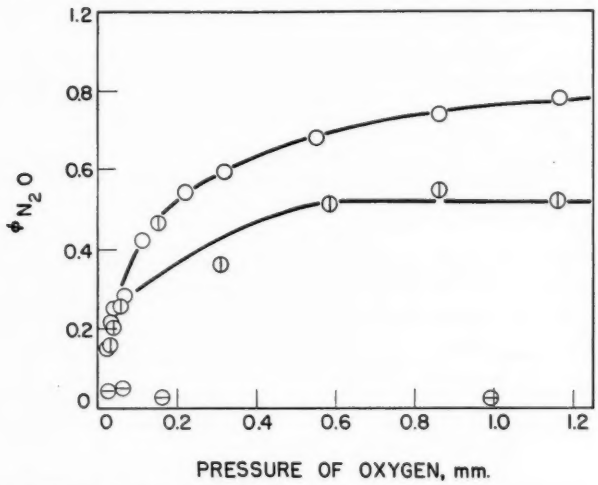

FIG. 4. Dependence of Φ_{N_2O} on oxygen pressure:
$I_a = 5 \times 10^{11}$ quanta/cc./sec.; pressure of azomethane, 101 mm.; ○, 161°C.; ◐, 123°C.; ⊖, *ca.* 25°C.

Although it has been assumed that nitrous oxide is produced in a chain propagating reaction, [9], which may occur in steps, the over-all yield of this product is low, $\Phi_{N_2O} < 1$. Unless fates other than [6] and [9] are postulated for $CH_3N_2CH_2$ and $CH_3N_2CH_2O_2$ respectively, it seems necessary to employ efficient chain termination reactions for the radicals R. Methyl radicals disappear rapidly in a system containing azomethane, presumably by addition to the nitrogen–nitrogen double bond to form tetramethyl hydrazine (15). It is, therefore, conceivable that azomethane acts as a sink for oxygenated radicals in a two stage addition process; the over-all reaction may be written

$$2R+CH_3N_2CH_3 \rightarrow CH_3NRNRCH_3. \quad [11]$$

The correct general form of $-\Phi_{O_2}$, Φ_{CH_4}, and Φ_{N_2O} as a function of (O_2) and of $(CH_3N_2CH_3)$ is obtained from a steady state treatment of the mechanism.

Under conditions such that Φ_{CH_4} is negligible, i.e. Φ_{N_2O} and $-\Phi_{O_2}$ have attained their limiting values, the mechanisms predict that

$$-\Phi_{O_2} = 2+2\Phi_{N_2O}.$$

Substitution of the observed values of Φ_{N_2O} leads, at 123°C., to $-\Phi_{O_2} = 3.1$ (experimental = 3.6), and at 161°C. to $-\Phi_{O_2} = 3.6$ (experimental = 4.0). The proposed mechanism, though obviously oversimplified, is in near accord with the data.

The relative rates of [2] and [4] may be determined from a relationship between Φ_{CH_4} and Φ_{N_2O} derived from the following assumptions: (i) two methyl radicals are produced in the primary process; (ii) methyl radicals are consumed only by [2], [3], and [4]; (iii) each methyl radical formed in other than the primary process is accompanied by the production of one molecule of nitrous oxide.

$$(2+\Phi_{N_2O})/\Phi_{CH_4} = (k_2+k_3)/k_2+k_4(O_2)/k_2(A)$$

In Fig. 6 a linear relation is shown between $(2+\Phi_{N_2O})/\Phi_{CH_4}$ and (O_2) at constant (A) for two temperatures. The slopes of these lines lead to $k_4/k_2 = 6.8 \times 10^4$ at 123°C. and 3.3×10^4 at 161°C. Extrapolation to $(O_2) = 0$ yields $(k_2+k_3)/k_2 = 5.0$ at 123° and 6.5 at 161°C.; the values obtained from the data of Jones and Steacie (15) for these intercepts are 6.2 and 6.0 respectively. This degree of agreement is considered adequate. The Arrhenius activation energy difference, E_2-E_4, is equal to 6.9 kcal./mole and the collision theory steric factor ratio, p_4/p_2, is 17; $E_2 - \frac{1}{2}E_E$ equals 7.3 kcal./mole and $p_2/p_E^{\frac{1}{2}}$ equals 4×10^{-4} (1), where the subscript E refers to the combination of two methyl radicals producing ethane, the latter proceeding with negligible activation energy and approximately unit collision efficiency (11). Hence $E_4 \backsim 0.4$ kcal./mole and $p_4 \backsim 7 \times 10^{-3}$.

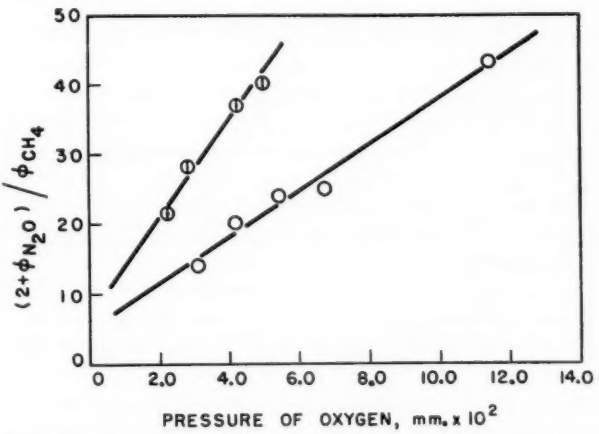

FIG. 6. Dependence of $(2+\Phi_{N_2O})/\Phi_{CH_4}$ on oxygen pressure:
$I_a = 5 \times 10^{11}$ quanta/cc./sec.; pressure of azomethane, 101 mm.; ○, 161°C.; ◑, 123°C.

Using acetone photolysis as a source of methyl radicals, Marcotte and Noyes (18) obtained $E_4 \backsim 0$ and $p_4 \backsim 10^{-1}$ by a method essentially similar to that employed here. The general agreement of the present determination with the earlier work in which more extensive data were reported at four temperatures is taken as support for the over-all reaction [9]. From an investigation of the photo-oxidation of methyl iodide, Blaedel, Ogg, and Leighton (5) estimated $E_4 \sim 3$ kcal./mole, while van Tiggelen (24) obtained an approximate value $E_4 \sim 1.5$ kcal./mole in a study of the acetone photosensitized oxidation of methane. Thus, there is general agreement that reaction [4] is rapid and that both the activation energy and steric factor are low.

The identity of the primary products of the oxidation of methyl radicals is still a matter of conjecture, however; thus [7] has been explicitly written as

$$CH_3O_2 \rightarrow HCO + H_2O \qquad [12]$$
$$\rightarrow HCHO + OH. \qquad [13]$$

Other reactions of peroxymethyl radicals which have been suggested are (12, 17, 26)

$$CH_3O_2 + R'H \rightarrow CH_3O_2H + R' \qquad [14]$$
$$CH_3O_2 + CH_3O_2 \rightarrow 2CH_3O + O_2. \qquad [15]$$

Reaction [12] is now considered unlikely (8, 14, 19) and reaction [15] should not be of great importance in the low concentration range under discussion at present. The positive identification of methanol and water among the liquid products suggests that R radicals may be identified tentatively with CH_3O_2, CH_3O, and OH. Further speculation regarding the detailed reactions of these radicals are, on the basis of the present data, unwarranted.

Small quantities of carbon monoxide and dioxide are found, the latter in almost insignificant amounts and apparently independent of conditions ($\Phi_{CO_2} < 0.1$). The carbon monoxide yield roughly parallels that of nitrous oxide as a function of oxygen pressure (Figs. 4 and 5) but is smaller by a factor

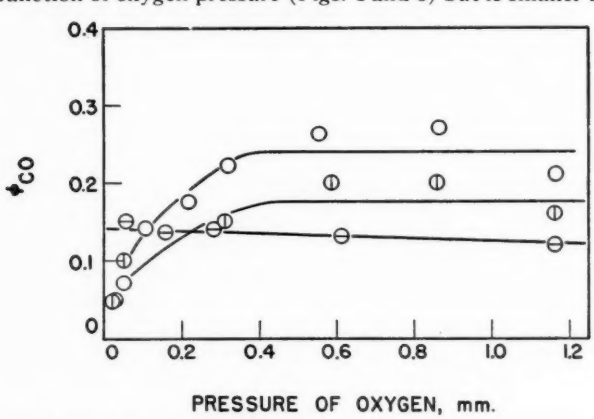

FIG. 5. Dependence of Φ_{CO} on oxygen pressure:
$I_a = 5 \times 10^{11}$ quanta/cc./sec.; pressure of azomethane, 101 mm.; ○, 161°C.; ◑, 123°C.; ⊖, *ca.* 25°C.

of approximately two. The variation of Φ_{CO} as azomethane concentration is decreased by a factor of 15 with a constant rate of production of radicals is small and in the opposite direction to that of Φ_{N_2O} in the same circumstances (Table I). This suggests that carbon monoxide arises from an oxidation of methyl radicals and that the intermediate stages do not involve the substrate. The variability (18, 19) in the CO/CO_2 ratio when various methyl radical sources are used suggests that both these products arise in an indirect manner (14). This is supported by Hentz (13) who observed an induction period for the production of carbon monoxide in the acetone–oxygen system. It might be pointed out that the low yield of carbon dioxide observed here is compensated by the production of nitrous oxide. Indeed, if the acetonyl radical were to react with oxygen in the manner postulated here for $CH_3N_2CH_2$ (i.e. [6] and [9]), the product would be carbon dioxide.

The experiments described in Part II of the Experimental section are reported in Table II as averages taken over a number of experiments. The salient facts are: (i) Φ_{N_2} and $-\Phi_A$ do not differ significantly from unity; (ii) $-\Phi_{O_2}$ lies

TABLE II

PRODUCTS OF AZOMETHANE PHOTO-OXIDATION

	Φ		Φ
N_2	1.1	"Liquid products"	1.1
CO	0.06	HCOOH	0.1
CO_2	0.09	"Peroxides"	0.02
CH_3OH	0.7[a]	O_2 disappearance	1.3
H_2O	0.1–0.2	Azo disappearance[b]	1.1

Partial pressure of azomethane, 6.6 mm.; average pressure of oxygen, 10 mm.; room temperature; $I_a \sim 10^{14}$ quanta/cc./sec.; exposure time, 48 hr.; volume of reaction system, 420 cc.

[a] *Average of the two analytical methods used.*

[b] *About one-half (9 mm.) of the azomethane originally present was reacted.*

between one and two; (iii) methanol, water, and formic acid are major products; (iv) a material balance is not even approximately attained if one nitrogen molecule is accompanied by the production of two single carbon radicals; (v) the oxygen concentration and the absorbed intensity, and hence the radical concentration, were high, while the temperature and azomethane concentration were low.

As pointed out previously, the experimental arrangement was such that formaldehyde probably could not have been detected as a product. If the total apparent decrement in the carbon balance is assumed to be formaldehyde, $\Phi_{H_2CO} \sim 1$. It is not readily apparent how an explanation of the results can be advanced if Φ_{H_2CO} is not at least as great as Φ_{CH_3OH} since the nearly unit yield of azomethane disappearance renders abstraction reactions unimportant. If this assumption is made, however, the mechanism might be expected to reduce to the radical–radical interactions suggested by Vaughan *et al.* (3), viz. [1], [4], and [15] followed by

$$2CH_3O \rightarrow CH_3OH + H_2CO. \qquad [16]$$

This is in qualitative accord with the data if it is noted that small amounts of oxygen will be required to oxidize some of the products of [16] to the water, acid, and carbon oxides found.

ACKNOWLEDGMENTS

The authors are indebted to Dr. E. W. R. Steacie for advice and encouragement throughout this work. They also wish to thank Dr. L. C. Leitch and Mr. R. Renaud for azomethane samples, Miss F. Gauthier and Miss M. J. Fuller for the mass spectrometric analyses, and Mr. R. Lauzon for the infrared absorption measurements.

REFERENCES

1. Ausloos, P. and Steacie, E. W. R. Can. J. Chem. 32: 593. 1954.
2. Bates, J. R. and Spence, R. J. Am. Chem. Soc. 53: 1689. 1931.
3. Bell, E. R., Raley, J. H., Rust, F. F., Seubold, F. H., and Vaughan, W. E. Discussions Faraday Soc. 10: 242. 1950.
4. Blacet, F. E. and Taurog, A. J. Am. Chem. Soc. 61: 3024. 1939.
5. Blaedel, W., Ogg, R. A., and Leighton, P. A. J. Am. Chem. Soc. 64: 2499, 2500. 1942.
6. Burton, M., Davis, T. W., and Taylor, H. A. J. Am. Chem. Soc. 59: 1038. 1937.
7. Cannon, C. V. and Rice, O. K. J. Am. Chem. Soc. 63: 2900. 1941.
8. Christie, M. I. J. Am. Chem. Soc. 76: 1979. 1954.
9. Davis, T. W., Jahn, F. P., and Burton, M. J. Am. Chem. Soc. 60: 10. 1938.
10. Elving, P. J. and Warshowsky, B. Ind. Eng. Chem., Anal. Ed. 19: 1006. 1947.
11. Gomer, R. and Kistiakowsky, G. B. J. Chem. Phys. 19: 85. 1951.
12. Gray, J. A. J. Chem. Soc. 3150. 1952.
13. Hentz, R. R. J. Am. Chem. Soc. 75: 5810. 1953.
14. Hoare, D. E. Trans. Faraday Soc. 49: 1292. 1953.
15. Jones, M. H. and Steacie, E. W. R. J. Chem. Phys. 21: 1018. 1953.
16. LeRoy, D. J. Can. J. Chem. 28: 492. 1950.
17. Lewis, B. and von Elbe, G. Combustion, flames and explosions in gases. Academic Press, Inc., New York. 1951.
18. Marcotte, F. B. and Noyes, W. A., Jr. Discussions Faraday Soc. 10: 236. 1951. J. Am. Chem. Soc. 74: 783. 1952.
19. Martin, R. B. and Noyes, W. A., Jr. J. Am. Chem. Soc. 75: 4183. 1953.
20. Nozaki, K. Ind. Eng. Chem., Anal. Ed. 18: 583. 1946.
21. Renaud, R. and Leitch, L. C. Can. J. Chem. 32: 545. 1954.
22. Scheer, M. D. and Taylor, H. A. J. Chem. Phys. 20: 653. 1952.
23. Steacie, E. W. R. Atomic and free radical processes. 2nd ed. Reinhold Publishing Corporation, New York. 1954. p. 376.
24. van Tiggelen, A. Ann. mines Belg. 43: 117. 1942.
25. Walker, J. F. Formaldehyde. 2nd ed. Reinhold Publishing Corporation, New York. 1953.
26. Walsh, A. D. Trans. Faraday Soc. 43: 297. 1947.
27. Weinhouse, S. J. Am. Chem. Soc. 20: 442. 1948.
28. Whitmore, F. C. Organic chemistry. 2nd ed. D. Van Nostrand Company, Inc., New York. 1951.

THE PREPARATION OF DICYANODIACETYLENE

By F. J. Brockman

ABSTRACT

The preparation of dicyanodiacetylene as reported by Moureu and Bongrand has been investigated more fully and a procedure developed whereby yields as high as 36% have been obtained.

INTRODUCTION

In 1920 Moureu and Bongrand (1) reported what was undoubtedly the first synthesis of dicyanodiacetylene. By the action of aqueous potassium ferricyanide on the cuprous derivative of propriolonitrile (cyanoacetylene) they obtained trace quantities of a solid with characteristic properties. This preparation has been investigated more fully and a procedure developed whereby yields as high as 36% have been obtained. The product was characterized as dicyanodiacetylene (C_6N_2) by elementary analysis and molecular weight determinations and by conversion on hydrogenation to hexamethylenediamine. Although the yield of hexamethylenediamine (isolated as the picrate) was low (8.5%), this low yield appeared to be due to decomposition of the dicyanodiacetylene in the presence of the hydrogenation catalyst (Adams' platinum oxide).

Dicyanodiacetylene is an unstable, volatile, white solid with a marked irritating odor. By sublimation in a stream of carbon dioxide gas it may be obtained as fine, elongated crystals melting at 64.5–65.5°C. X-ray diffraction lines obtained from a single crystal rotation pattern are listed in Table I, together with their estimated relative intensities.

TABLE I

X-RAY* DIFFRACTION PATTERN DATA ON DICYANODIACETYLENE

Spacing, d (Å)	Intensity, I/I_1	Spacing, d (Å)	Intensity, I/I_1
5.10	30	2.62	10
4.09	60	2.57	10
3.98	5	2.39	20
3.52	5	2.35	10
3.43	30	2.16	10
3.24	100	2.09	20
3.19	80	2.05	10
3.10	80	1.88	10
3.05	80	1.84	20
2.88	20	1.76	10
2.83	20	1.58	10

*Wave length 1.5418 Å.

Attention should be drawn to the unusual composition and structure of dicyanodiacetylene. Being composed solely of carbon and nitrogen it can be

[1]*Manuscript received September 27, 1954.*
Contribution from the Central Research Laboratory, Canadian Industries (1954) Ltd., McMasterville, Quebec.

considered as a subnitride of carbon. It is also one of the longest, completely linear molecules described and should be a very interesting compound for structural study.

EXPERIMENTAL

Preparation of Cuprous Propriolonitrile

Cuprous chloride (9.9 gm., 0.10 mole) was dissolved in 10 cc. of 14% aqueous ammonia under an atmosphere of nitrogen and diluted with 900 ml. of water. To this solution at approximately 25°C. was added with agitation propriolonitrile (1) (1.5 gm., 0.029 mole) over a three minute period. After being stirred for an additional five minutes the olive green precipitate was separated by decantation and filtration and washed twice with 30 ml. of 1.5% aqueous ammonia. The product after drying under vacuum, first over sulphuric acid and finally over phosphorus pentoxide, weighed 3.7 gm. (110% yield on propriolonitrile). Cuprous propriolonitrile is subject to detonation by heat and shock.

Preparation of Dicyanodiacetylene

A solution of 7.8 gm. (0.0234 mole) potassium ferricyanide in 20 ml. of water was added over a five minute period to a stirred suspension of cuprous propriolonitrile (1.5 gm., 0.012 mole) in 25 ml. of water and 25 ml. of benzene. The temperature of the reaction mixture was maintained at 5 to 6°C. throughout. Agitation was continued for two minutes after addition was complete and the reaction mixture then centrifuged, the centrifuge bottles and cups being chilled before use in an ice-water bath. After centrifuging for five minutes at 2000 r.p.m., the benzene layer (17 ml.) was removed. The lower aqueous layer and a heavy sludge-like precipitate were again cooled, extracted with a further 20 ml. of benzene, and the centrifuging procedure repeated. Owing to the formation of a fine black precipitate at this stage, only 10 ml. of benzene extract could be separated by this means. By filtration of the residual mixture through filter-aid, a further 15 ml. of extract was obtained. The combined benzene extracts were dried over sodium sulphate and most of the benzene removed by fractionation at atmospheric pressure through a short (8 cm.) Vigreux column. The resulting dark brown concentrate (2 ml.) was taken to dryness in a slow stream of carbon dioxide, the condensate being collected in a small ice-cooled receiver. After removal of all the benzene, dicyanodiacetylene was sublimed from the residue by continuing the volatization procedure. The sublimate was further purified by resublimation in a stream of carbon dioxide. The white crystalline product thus obtained, m.p. 64.5–65.5°C., weighed 0.180 gm. (30.5% yield). Calc. for C_6N_2: C, 72.0; N, 28.0; mol. wt., 100. Found: C, 72.15; N, 27.42; mol. wt. (depression of f.p. of benzene) 97. An additional 0.035 gm. of product, m.p. 64–64.5°C., was obtained by distilling most of the solvent from the benzene distillates using a column packed with glass spirals and working up the concentrate as described above. The total yield isolated was 0.215 gm. (36% yield on cuprous propriolonitrile).

Dicyanodiacetylene gradually turns brown at room temperature, but may be stored at 0°C. This discoloration is more rapid in the presence of water or

in ether solution and occurs at once in alcohol. Petroleum ether, b.p. 28–35°C., may be used as an extraction solvent in place of benzene. Ether is unsatisfactory owing to the instability of dicyanodiacetylene in this medium and chloroform is not recommended since it is difficult to separate from the by-product sludge.

Hydrogenation of Dicyanodiacetylene to Hexamethylenediamine

The hydrogenation was carried out in a small high pressure hydrogenation unit equipped with a 110 ml. glass liner. Dicyanodiacetylene (0.27 gm., 0.0027 mole) was dissolved in 20 ml. of acetic anhydride and Adams' platinum oxide (0.10 gm.) added just prior to the sealing up of the mixture in the hydrogenation unit. (Although dicyanodiacetylene is reasonably stable in acetic anhydride solution, decomposition occurs in the presence of Adams' catalyst as evidenced by the gradual appearance of a dark brown color.) After being flushed out with hydrogen, the apparatus was charged to a pressure of 800 p.s.i. and the shaker started. The pressure fell off to 725 p.s.i. in 15 min. and more slowly to 710 p.s.i. over a three and one-half hour period. No further drop in pressure had occurred at the five hour mark and the reaction was stopped. The reaction temperature remained at approximately 30°C. throughout the hydrogenation. The solvent was removed from the dark brown reaction mixture by vacuum distillation, and the residual oily gum, containing acetylated hexamethylenediamine, was hydrolyzed by refluxing for five hours with 20% aqueous sulphuric acid (5 gm.). The hydrolyzate was made alkaline to a pH of 13–13.5 with 20% aqueous sodium hydroxide to liberate hexamethylenediamine from its salt and the resulting solution distilled to dryness under aspirator vacuum. To the distillate was added 1.4% aqueous picric acid (40 ml.) and the precipitate of hexamethylenediamine picrate removed by filtration. The product, m.p. 219°C., weighed 0.13 gm. (8.5% yield on dicyanodiacetylene). After recrystallization from water, the material melted at 221–222°C. (lit. 220°C.). It was further identified as hexamethylenediamine

TABLE II

X-RAY* DIFFRACTION PATTERN DATA ON HEXAMETHYLENEDIAMINE PICRATE

Spacing, d (Å)	Intensity, I/I_1	Spacing, d (Å)	Intensity, I/I_1
11.3	50	2.89	2
8.25	2	2.70	2
7.47	80	2.58	5
6.40	15	2.50	3
5.54	20	2.44	3
5.20	15	2.31	2
4.64	40	2.25	2
4.37	30	2.13	2
4.21	80	2.06	2
3.91	20	1.97	2
3.54	100	1.92	2
3.35	40	1.86	2
3.30	40	1.76	2
3.17	50		

*Wave length 1.5418 Å.

picrate by X-ray diffraction analysis (see Table II for list of diffraction lines from powder diagram and their relative intensities).

ACKNOWLEDGMENT

The author wishes to thank Dr. A. O. McIntosh for the X-ray diffraction work and Mr. R. J. Fabris for the elementary analyses.

REFERENCE

1. MOUREU, C. and BONGRAND, J. Ann. chim. 14: 47. 1920.

ALLOYS OF INDIUM: THE SYSTEM INDIUM–LEAD–TIN[1]

By A. N. Campbell, R. M. Screaton,[2]
T. P. Schaefer,[3] and C. M. Hovey[4]

ABSTRACT

There is no ternary eutectic in the system: indium–lead–tin: the eutectic trough extends from the lead–tin eutectic to the tin–indium eutectic. The liquidus surface has been outlined. The structures of all alloys of the above system have been investigated, at room temperature, by the X-ray and microscopic techniques. A one-phase region extends across the ternary diagram from the limits of the β-phase in the indium–tin system to the limits of the β-phase in the lead–indium system. This indicates that the intermetallic β-phases of the two systems (lead–indium and tin–indium) have the same lattice structure, viz. face-centered tetragonal. Heterogeneity has been detected by direct experiment in the system lead–indium, whereas it had previously only been deduced. Hardness tests, both Brinell and Vickers, have been made on the alloys.

The only previous work that has been reported on the above system is that of Grymko and Jaffee (5), who dealt primarily with the corrosion-resistance properties of the indium–lead–tin solders; they state, however, that the liquidus of one alloy containing 37.5 weight per cent lead, 37.5 weight per cent tin, and 25 weight per cent indium, lies at 181° C. and the solidus at 134° C. The component binary systems, viz.: lead–tin, indium–lead, and indium–tin, have all been investigated and very little remains in doubt. To save unnecessary discussion, the equilibrium diagrams are given in Figs. 1, 2,

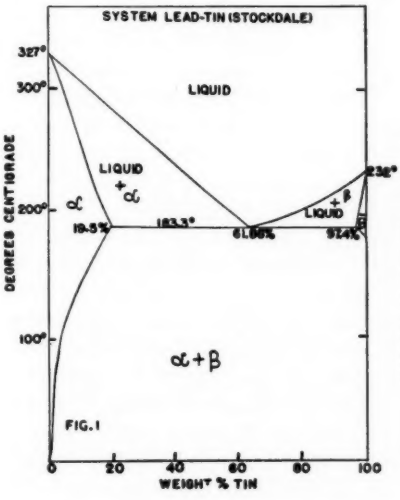

FIG. 1

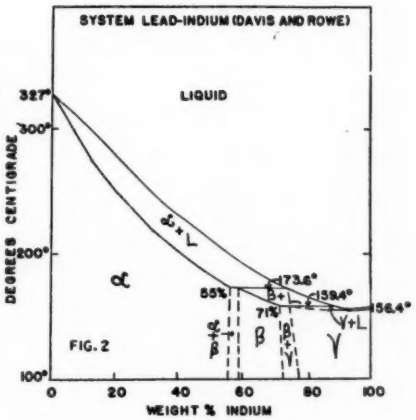

FIG. 2

[1]*Manuscript received November 8, 1954.*
Contribution from Department of Chemistry, University of Manitoba, Winnipeg, Manitoba.
[2]*Cominco Fellow, 1953–54.*
[3]*Holder of an N.R.C. Bursary, 1954–55.*
[4]*Professor of Civil Engineering, The University of Manitoba, Winnipeg, Man.*

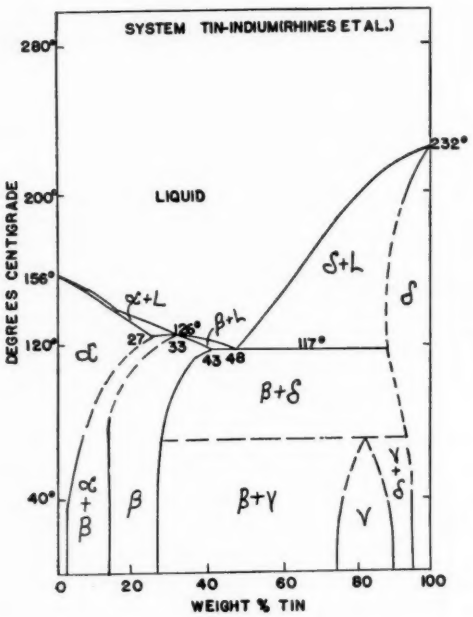

FIG. 3.

and 3. Fig. 1 is due to Stockdale (11) and represents the system lead–tin. The only point of interest in this system is a mysterious evolution of heat at 150° C., which occurs in all lead rich alloys; this is not due to any ordinary phase change.

Fig. 2 represents the system indium–lead: it is due to Davis and Rowe (1). This system shows a minimum freezing temperature, lying 1° C. below the melting point of pure indium, and three solid phases, an α-phase with the lead structure, a γ-phase with the indium structure, and an intermediate β-phase, for which Klemm (7) claims a face-centered tetragonal structure; further discussion of this structure is reserved until the discussion of our own work. The most complicated system is that of indium–tin (Fig. 3) due to Rhines (9). It is seen that this system exhibits four solid structures, one of which, however, the γ-phase, exists only at relatively low temperatures and therefore cannot be in equilibrium with melt. The α-phase possesses the structure of indium, the δ-phase that of tin, while the β-phase, according to Orlamunder (7) has a tetragonal, face-centered lattice. For the low-temperature γ-phase, Valentiner (12) proposed a body-centered tetragonal structure, but Fink (4) thought this phase was simple hexagonal: however, Ferguson and Screaton (3) believe it to be simple hexagonal with one atom per unit cell.

PART 1. THE LIQUIDUS SURFACE

Materials Used

The lead contained the following impurities:

Antimony	0.005%
Silver	0.002%
Total foreign metals	0.05%

The indium was given to us by the Consolidated Mining and Smelting Company of Canada Limited and had the following impurities:

Tin	0.015%
Nickel	0.0015%
Lead	0.015%
Copper	0.002%
Cadmium	0.001%
Iron	0.0005%

The tin analysis gave:

Iron	0.0020%
Antimony	0.0023%
Lead	Trace
Copper	Trace
Tin	99.9957% (by difference)

Methods of Chemical Analysis

The method of sampling differed in the study of the liquidus from that used in the study of the completely solid system. In no case did we rely on the original weighed composition since oxidation, though slight, is preferential, occurring chiefly to the lead. For the study of the liquidus, samples of liquid alloy were drawn up into a 1/16 in. diameter alundum tube. The alloy solidified in the tube after mounting a short distance; the tube was then broken and the whole of the sample analyzed, in case there should have been segregation of the alloy during solidification. Alloys with low indium content were dissolved, with the help of platinum foil, in hydrochloric acid, and the tin content determined by titration with iodine (10). Lead was estimated by the standard method of precipitation as sulphate. Prolonged attempts were made to determine indium directly, both polarographically and by precipitation with 8: 4 hydroxyquinoline but neither method was satisfactory in the presence of lead and tin. In the end, therefore, indium was obtained by difference. This may seem a doubtful procedure when the indium content is small but it should be remembered that the co nposition never differed much from that of the original weight composition. In alloys of high indium content, tin was determined as metastannic acid, which was subsequently ignited to the dioxide and weighed as such. All these analytical methods are well known.

Determination of Equilibrium Curves and Surfaces

The method of thermal analysis was used to determine these. The melts

were contained in alundum crucibles and temperature was measured with a mercury-in-glass thermometer, reading from 0 to 201° C. in 1/10°. The thermometer was calibrated against a standard platinum resistance thermometer: temperature was therefore accurate to ± 0.2° C.

The method of linear cooling was used, the rate of cooling being 1° per 1.5 minutes. The molten alloys were well stirred and kept at a temperature at which they were entirely liquid, for two hours, to ensure homogeneity. Starting with the composition of the lead–tin eutectic, as given by Stockdale (11), indium was added progressively and a cooling curve taken and an analysis made after each addition. An examination of the cooling curve showed whether or not the mixture had the trough composition. If it did not have, there was primary crystallization of a single phase and a preliminary point of inflection on the cooling curve. This was corrected, when necessary, by adding small quantities of tin (lead was never necessary). It soon became apparent that the eutectic trough, starting from the lead–tin eutectic, was heading smoothly for the indium–tin eutectic. Therefore, this was checked by starting from the indium–tin eutectic and adding lead. In this way, we were able to show that even the smallest addition of lead raised the solidification temperature of the indium–tin eutectic and therefore the possibility of a ternary eutectic lying very close to the indium–tin eutectic was excluded.

We thought it advisable to check the statement that there is a minimum freezing point in the lead–indium system, lying, according to the literature, 1° below the melting point of indium. For this purpose, we used a Beckmann thermometer with which we determined the freezing point of pure indium. Small weighed quantities of lead were then added and the freezing point determined each time. The procedure was repeated until a minimum freezing temperature was obtained. The freezing temperature of the lowest freezing alloy was then determined absolutely on the 200° thermometer. We obtained a depression of about 0.15° C. (constant) after the addition of 2.5 weight per cent lead.

Because of the occurrence of one peritectic in the lead–indium system and two in the indium–tin system, we expected peritectic halts along the eutectic trough of the ternary system. We first investigated the binary peritectics but we found the heat effects slight and difficult to observe, at least by our technique. When the third metal was added to these binary peritectic compositions, the heat effect was quenched entirely. Experimentally, then, we found no peritectic halt on the eutectic trough. Our investigation of the completely solid alloy at room temperature shows that there must be one, and only one, peritectic halt on the trough, but we do not know its temperature and composition.

To complete the study of the liquid surface, some points on the areas representing equilibrium of liquid with single solid phases were necessary (chiefly in the region where α-lead separates from the melt) and these were obtained by making up alloys of suitable composition and applying thermal analysis, using, however, a chromel–alumel thermocouple, since the temperatures involved were somewhat higher.

Experimental Results

TABLE I

DETERMINATION OF EUTECTIC TROUGH

Alloy No.	Solidification temperature (° C.)		Composition by weight		
	Start	Finish	Sn, %	In, %	Pb, %
Pb–Sn eutectic	183.3	183.3	61.9	—	38.1
1	177.6	174.8	59.5	2.9	37.6
2	170.7	164.5	57.0	5.8	37.2
3	164.7	159.1	56.1	7.7	36.2
4	147.7	134.9	54.1	17.3	28.6
7	135.9	130.8	51.8	25.9	22.3
8	134.3	129.4	51.5	27.4	21.1
9	132.7	128.0	51.1	28.9	20.0
10	131.2	126.4	50.9	30.3	18.8
11	130.0	126.0	51.1	31.1	17.8
12	129.0	126.0	50.7	32.2	17.1
13	128.3	125.7	50.2	33.5	16.3
14	127.1	125.1	50.1	34.6	15.3
15	125.9	124.5	50.3	36.6	13.1
16	124.9	123.6	49.8	38.0	12.2
17	124.5	121.5	49.4	38.9	11.7
18	118.7	118.7	48.7	51.3	—
19	118.9	118.7	48.4	51.1	00.5
20	119.6	118.8	47.4	50.0	2.6
21	120.3	119.6	46.8	49.3	3.9
22	121.7	120.0	45.8	48.3	5.9
23	122.6	121.4	48.1	42.8	9.1
25	123.9	122.5	48.2	42.0	—
26	118.8	118.8	48.7	51.3	—
27	118.8	118.8	48.7	51.2	0.1
30	150.3	133.3	53.2	15.8	31.0
31	147.1	133.8	53.4	18.2	28.4
32	144.6	132.8	53.5	20.0	26.5
33	142.0	131.9	53.6	21.8	24.6

TABLE II

EFFECT OF SMALL QUANTITIES OF LEAD ON THE MELTING POINT OF INDIUM

Alloy No.	Composition by weight		Freezing point
	In, %	Pb, %	
53	100.00	0	3.431
54	99.59	0.41	3.374
55	98.87	1.13	3.353
56	97.95	2.05	3.289
57	96.83	3.17	3.281
58	95.30	4.70	3.331
59	93.57	6.43	3.422

Beckmann setting of 3.422° = 156.5°C.
Melting point of pure indium was therefore = 156.5° C.

TABLE III

INVESTIGATION OF LIQUIDUS

Alloy No.	Solidification begins	Solidification ends	Trough temp.	Composition by weight %		
				Sn	In	Pb
39	157.9° C.	132.3° C.	145.6° C.	62.2	17.0	20.8
40	179.6	129.0	140.7	70.8	12.5	16.7
42	154.7	125.6	143.7	35.7	34.7	29.6
43	131.6	128.8	—	28.6	65.6	5.8
44	140.4	133.7	—	25.4	58.0	16.6
45	152.3	136.6	—	22.6	51.8	25.6
46	172.3	137.7	153.8	20.1	46.0	33.9
47	177.5	138.5	152.3	19.3	44.4	36.3
48	123.6	121.5	—	38.0	61.9	0.1
49	125.9	123.4	—	36.4	59.3	4.3
50	127.5	125.6	—	34.0	62.0	4.0
51	128.9	126.6	—	31.6	64.7	3.7
52	130.6	127.8	—	29.0	67.6	3.4
61	155.4	145.2	—	10.1	67.0	22.9
62	241.0	—	—	21.5	14.2	64.3

Discussion of the Liquidus Surface

The experimental results show that there is no ternary eutectic in this system; the eutectic trough extends from the lead–tin eutectic to the tin–indium eutectic.

Our value for the eutectic temperature of the binary system lead–tin, 183.3° C., is in good agreement with Stockdale's value (11). We have, however,

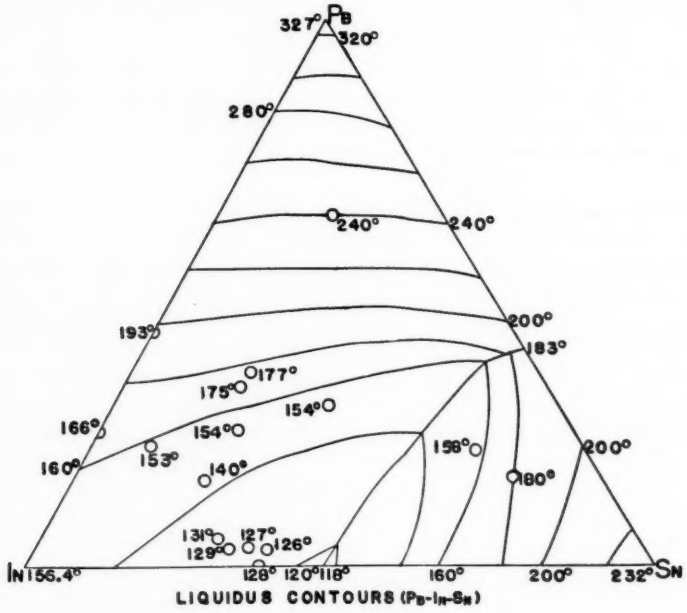

FIG. 4.

repeated the eutectic of the tin–indium system several times, using the composition given by Rhines (9) and we obtain values for this eutectic temperature lying between 118.7° C. and 118.9° C., as against Rhines's own value of 117° C. This may be due to our having had at our disposal very pure indium. In the lead–indium system, we confirm the existence of a minimum freezing temperature lying, however, only 0.15° C. below the melting point of pure indium.

Fig. 4 is a projection diagram of the liquid surface, with isothermal lines.

PART 2. ROOM TEMPERATURE ISOTHERM

The structure of the completely solidified alloy was studied by the X-ray and microscopic techniques. As a subsidiary aid in the study of structure and because of its intrinsic practical importance, the hardness was determined in various regions of the composition triangle: both Brinell and Vickers hardness tests were applied.

Experimental

All alloys were heat-treated by cooling them gradually over a period of twenty-four hours, from a temperature at which they were completely liquid down to room temperature. This was achieved by coupling a slow, constant speed, electric motor through a system of gears to a "Variac", which governed the input to the furnace. After the potential fell to zero, an automatic switch cut out the circuit. Twenty-three hours were required to rotate the Variac through its complete range. Obviously, such an apparatus does not decrease temperature linearly since the power input is proportional to the square of the voltage; in other words, cooling was more rapid at higher than at lower temperatures, but this is rather a desirable feature.

The purity of the materials is described under the first Section, where, also, it is stated that all alloys were analyzed and the methods of analysis are given. The method of treatment of alloys for the study of the solid system was as follows: A total weight of 40 gm. of the desired composition was charged into a crucible and preheated to about 60° above the liquidus temperature, as read from the appropriate equilibrium diagram (see preceding section). After fusion and repeated stirring with an alundum rod, the melt was cooled to roughly three degrees above the temperature of the liquidus surface, the whole process occupying about three hours. The continuous cooling mechanism was now set in motion and the alloy annealed down to room temperature.

From the ingot prepared as above the oxide film was removed with a lathe. A specimen for microscopic examination, approximately 7 mm. in width and 4 mm. thick, was also prepared on the lathe. Turnings for chemical analysis were taken from the immediate vicinity of the prepared surface. No demarcation marks, denoting gross phase separation during cooling, could ever be detected by a vertical saw-cut; moreover, the general agreement between final analysis and original composition of charge favors this conclusion.

A strip for X-ray examination was cut from the surface of the prepared specimen, with a sharp thin-bladed knife: it was possible to reduce the thickness of this strip as low as 0.2 mm. Powder pictures of such strips were taken on a North American Phillips X-ray unit, using a simple Debye camera of

57.3 mm. diameter. Copper radiation and a nickel filter were used. The exposure time varied from one to three hours depending on the composition and size of the specimen. The above procedure was necessary because indium and alloys rich in indium are almost as soft as putty. Filings could not be prepared readily because of the "smearing" properties of these alloys. The small degree of cold-working by the knife-edge would only cause a slightly preferred orientation of the grains and this effect was neutralized by rotation of the specimen during exposure to X rays.

Our treatment of the specimens prior to microscopic examination is described in detail, because no satisfactory methods of polishing and etching the indium alloys in question are to be found in the literature. Preparatory to polishing, the surface was lightly rubbed on a fine mill-file, held stationary, the teeth being cleaned after each stroke. The final polish was given on a wheel-driven silk cloth (selvyt), using the "light" variety of powdered magnesium oxide as polishing agent. If the sample contained large quantities of lead, tarnishing tended to occur but it was found that this could be prevented by the use of soap. Too much water on the cloth increased the tarnishing but a heavily tarnished layer could be removed by dabbing the surface with glacial acetic acid. Polishing was carried on close to the center of the wheel until the surface had a lustrous appearance, as far as possible scratch-free.

An etching reagent consisting of seven parts of glycerol, two parts of concentrated nitric acid, and one part of glacial acetic acid gave the best results over the whole concentration range, but the nitric acid content was varied for different samples to achieve the best effect. This reagent was described by Villela and Beregekoff (13) for lead alloys. Etching took place by immersion for 5 to 30 sec. at approximately 40° C. To ensure that the true structure of the sample did not remain latent, the specimen was alternately lightly polished and etched. This also decreased the danger of cold-working from overpolishing and the deterioration of a delicate microstructure from overetching.

Hardness tests were made by the Brinell ball and Vickers' diamond hardness tests. Because of the softness of these alloys, a special Brinell machine was constructed, which had a unit ratio of load in kgm. to the square of the diameter of the ball in mm., as specified in "Metals Handbook" (8). A load of 5.5 kilograms was applied to a steel ball of 2.35 mm. diameter, for 30 sec. The Vickers-Armstrong machine was of a standard type.

The method of procedure was as follows: Alloys, some fifteen in number, representing both the pure phases and the heterogeneous regions, of the binary systems, were prepared and, after heat-treatment in the manner described, the powder pattern and microstructure of each alloy were determined. A small quantity of third component was then added to each alloy; the alloy was then remelted, heat-treated, and examined by the two techniques mentioned, attention being directed to the appearance of a new phase. Because of the great similarities in lattice structure of β-lead–indium and β-tin–indium, it was thought that a continuous series of solid solutions might exist, forming a band over the diagram, and this was found to be the case.

Experimental Results

Table IV contains the compositions of all alloys studied, together with their hardness figures, on both scales. Table V gives approximate figures which will permit the single-phase, two-phase, and three-phase areas to be plotted.

TABLE IV

COMPOSITION AND HARDNESS

Sample No.	Composition by weight			Hardness	
	Pb	Sn	In	Bhn	DPH
1	—	100	—	3.9	5.8
1a	—	98.6	1.4	8.4	7.9
2	—	93.7	6.3	10.0	12.8
3	—	64.7	35.3	3.8	7.1
4	—	79.1	20.9	10.1	11.4
5	—	25.5	74.5	1.01	1.04
6	—	5.6	94.4	1.3	1.9
7	—	5.1	94.9	0.89	1.7
8	100.0	—	—	2.6	4.3
9	15.1	—	84.9	3.5	4.4
10	27.4	—	72.6	5.5	7.7
11	35.9	—	64.1	8.1	10.2
12	44.7	—	55.3	8.4	11.4
13	89.7	—	10.3	7.3	7.8
14	51.4	—	48.6	9.2	13.4
15	4.6	75.3	20.1	10.1	13.8
16	1.8	77.8	20.4	8.5	11.0
17	2.0	18.2	79.8	1.8	2.1
18	9.5	14.8	75.7	2.3	3.1
19	20.2	9.9	69.9	4.2	5.2
20	27.0	5.4	67.6	5.9	6.9
21	9.9	7.1	83.0	2.7	3.3
22	21.3	19.1	59.6	4.3	5.1
23	34.8	11.2	54.0	8.4	9.7
24	49.8	5.1	45.1	10.9	13.3
25	35.8	1.0	63.2	7.9	9.4
26	15.9	8.8	75.3	3.7	4.4
27	9.9	4.1	86.0	2.9	3.5
28	27.1	16.6	56.3	6.0	7.7
30	51.5	15.8	32.7	9.0	12.4
31	57.8	23.3	18.9	10.9	13.6
32	50.2	34.1	15.7	10.0	13.0
33	60.9	32.3	6.8	10.4	13.2
34	49.8	47.6	2.6	10.5	14.5
35	36.0	8.1	55.9	7.1	8.2
36	77.9	4.4	17.7	10.1	11.6
37	24.2	66.3	9.5	7.4	11.4
38	24.9	49.8	25.3	10.0	12.8
39	64.3	21.5	14.2	10.8	13.4

Fig. 5 is a graphical representation of these data—the room temperature isotherm. We give no X-ray data since no new phase occurs in the three component alloy and the X-ray data for all binary phases are now to be found in the literature. We reproduce, however, certain photomicrographs since, without them, a paper of this kind is practically valueless to workers in the field: the etching reagent was always that described previously, unless other-

wise stated. It will be noted on Fig. 5 that a single phase region extends across the isotherm from β-indium–tin to β-indium–lead. This is the most interesting of the results and it indicates that the two phases (of the binary systems) are of closely similar structure. The invariant triangle in which β-indium–tin, γ-indium–tin, and α-lead are in equilibrium occupies a large part of the isotherm.

In Fig. 6, the hardness numbers, both DPH and Bhn, are plotted for the binary systems designated. For the indium–tin system there is no indication of the formation of the intermediate β-phase but in the plot of the indium–tin alloys a maximum appears at the composition of the γ-phase. Fig. 7 is a plot of hardness contours for the ternary system.

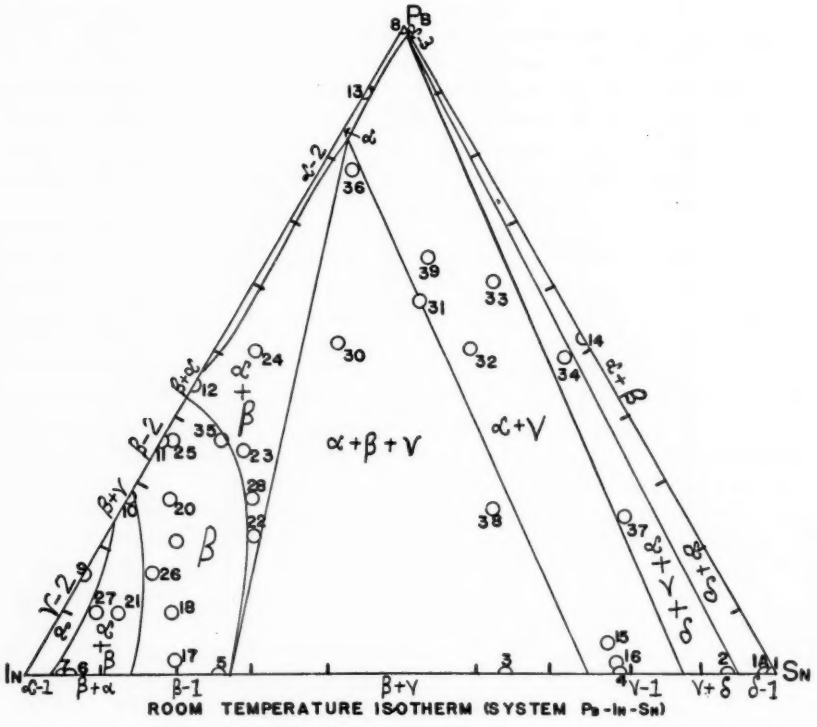

FIG. 5.

There follows a description of the individual photomicrographs. To facilitate discussion the phases designated by Greek letters are distinguished by Arabic numerals, thus, 1 for In–Sn, 2 for Pb–In, and 3 for Pb–Sn.

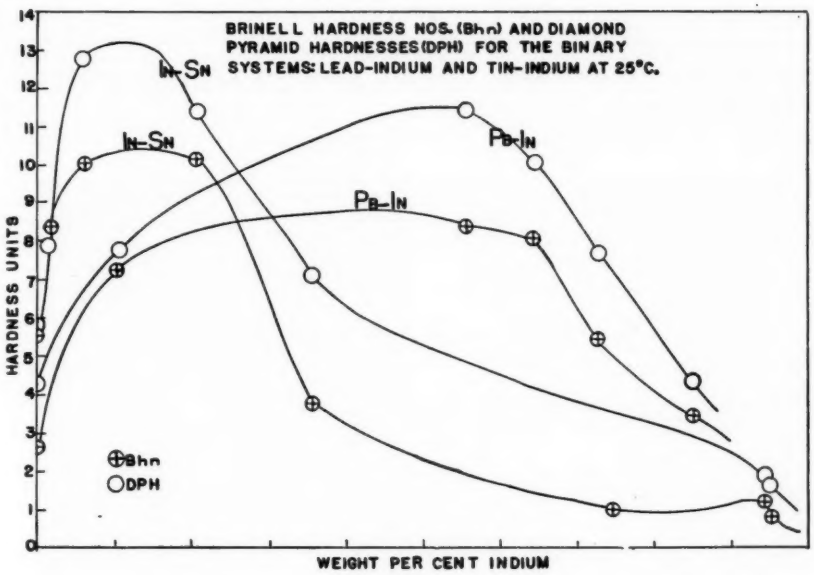
BRINELL HARDNESS NOS. (Bhn) AND DIAMOND PYRAMID HARDNESSES (DPH) FOR THE BINARY SYSTEMS: LEAD-INDIUM AND TIN-INDIUM AT 25°C.
In-Sn
In-Sn
Pb-In
Pb-In
⊕Bhn
○DPH
HARDNESS UNITS
WEIGHT PER CENT INDIUM

FIG. 6.

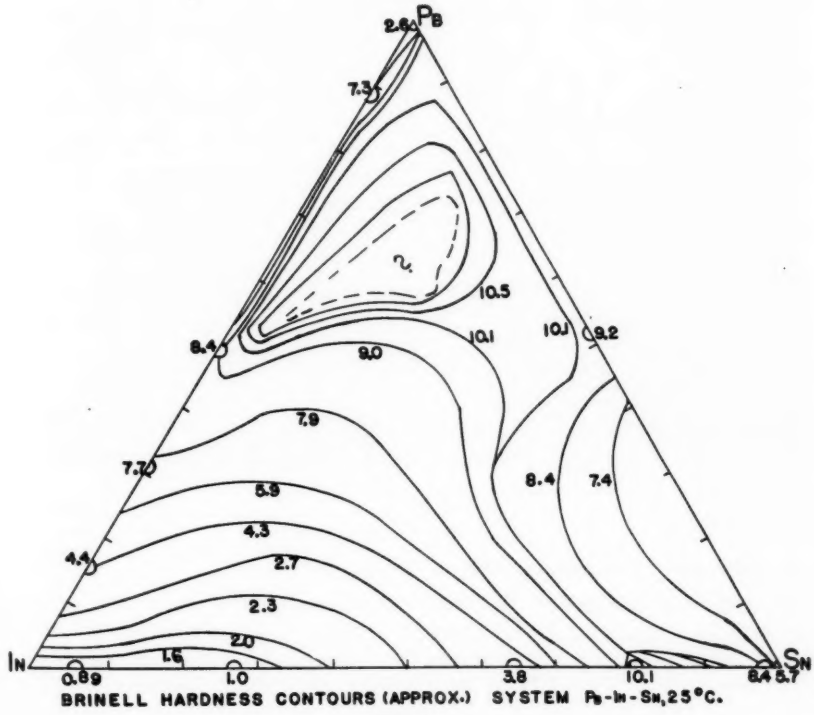
Pb
2.6
7.3
10.5
10.1
10.1
9.2
8.4
9.0
7.9
7.3
8.4
7.4
5.9
4.3
4.4
2.7
2.3
2.0
1.6
In
0.89
1.0
3.8
10.1
8.4 5.7
Sn
BRINELL HARDNESS CONTOURS (APPROX.) SYSTEM Pb-In-Sn, 25°C.

FIG. 7.

TABLE V

Nature of phase	Type of lattice	Composition of points defining area
Single-phase areas		
α-Lead	Face-centered cubic	(1) 1.5% Sn, 98.5% Pb (2) 53.1% In, 46.9% Pb (3) 1% Sn, 25% In, 74% Pb
δ-Tin	Body-centered tetragonal	Does not occur as a single phase in the ternary system; stable up to 5% In in In–Sn system
α-In	Face-centered tetragonal	(1) 3% Sn, 97% In (2) 23% Pb, 77% In (3) 3% Sn, 10% Pb, 87% In
γ-Tin–indium	Simple hexagonal	Does not occur as a single phase in the ternary system: (1) 75% Sn, 25% In (2) 88% Sn, 12% In
β-Lead-indium	Face-centered tetragonal	This phase extends down to β-In–Sn and is isostructural with it. The following points define the band: (1) 28% Pb, 72% In (2) 43% Pb, 57% In (3) 78% In, 13% Pb, 9% Sn (4) 14% Sn, 86% In (5) 27% Sn, 73% In (6) 61% In, 19% Sn, 20% Pb (7) 45% In, 8% Sn, 37% Pb
β-Tin–indium	Face-centered tetragonal	
Two-phase areas		
α-Lead + δ-Tin		(1) 100% Sn (2) 95% Sn, 5% In (3) 1.5% Sn, 97.5% Pb, 1% In
α-Lead + γ-Tin–indium		(1) 1.5% Sn, 97.5% Pb, 1.0% In (2) 95% Sn, 5% In (3) 88% Sn, 12% In (4) 16% In, 1% Sn, 83% Pb
α-Lead + β-Lead–tin		(1) 27% Sn, 73% In (2) 43% Pb, 57% In (3) 47% Pb, 53% In (4) 16% In, 1% Sn, 83% Pb
α-Indium + β-Lead–tin		(1) 14% Sn, 86% In (2) 3% Sn, 97% In (3) 3% Sn, 10% Pb, 87% In (4) 23% Pb, 77% In (5) 28% Pb, 72% In (6) 8% Sn, 77% In, 15% Pb
Three-phase areas		
α-Lead + δ-Tin + γ-Tin–indium		(1) 88% Sn, 12% In (2) 95% Sn, 5% In (3) 1.5% Sn, 97.5% Pb, 1% In
α-Lead + β-Lead–indium + γ-Tin–indium		(1) 75% Sn, 25% In (2) 27% Sn, 73% In (3) 23.5% Sn, 19% In, 57.5% Pb (4) 16% In, 1% Sn, 83% Pb

Interpretation of Photomicrographs

A number of representative photomicrographs are given, in order to indicate the type of microstructure obtained, and particularly such as are not to be found in the literature. Fig. 8 shows the difference in etching characteristics

between the γ-1 and δ-1 phases, the γ-1 being light, i.e. not attacked to the same extent as the δ-1 phase. Fig. 9 shows the grain boundaries in the γ-1 phase (the dark spots are probably spurious effects arising from polishing). That the γ-phase is the one actually present is proved by the powder photograph of this sample, which was identical with that obtained by Ferguson

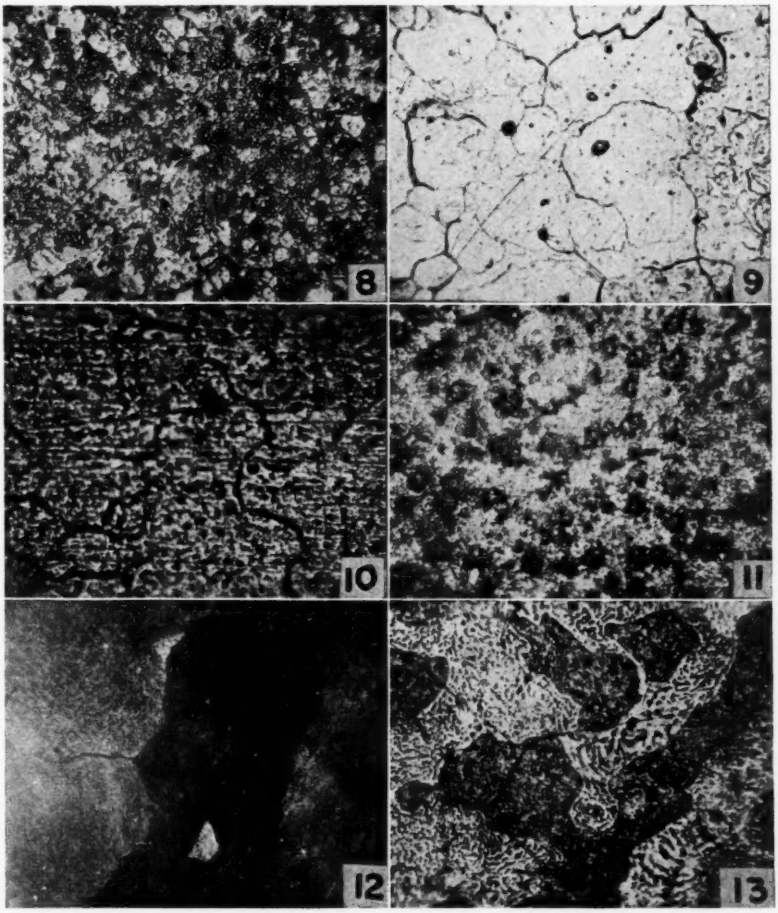

FIG. 8. Alloy 2, × 250. Note the difference in etching characteristics of γ-1 (light) and δ-1 (dark).

FIG. 9. Alloy 4, × 135. Grain boundaries in γ-1; black spots are probably spurious, although some β-1 may be present.

FIG. 10. Alloy 5, × 135. Grain boundaries in β-1, exhibiting the characteristic pitted appearance of this phase.

FIG. 11. Alloy 10, × 250. Repolished and re-etched after three months at room temperature; β-2 in a background of γ-2.

FIG. 12. Alloy 11, × 135. Repolished and re-etched after three months at room temperature; grain boundaries in β-2.

FIG. 13. Alloy 14, × 250. Lead grains (dark) in the Pb–Sn eutectic.

and Screaton (3) and showed the lines of the simple hexagonal lattice of γ-1. Grain boundaries in the β-1 phase are visible in Fig. 10 and were obtained by polishing in an electrolyte consisting of equal parts of 70% perchloric acid and

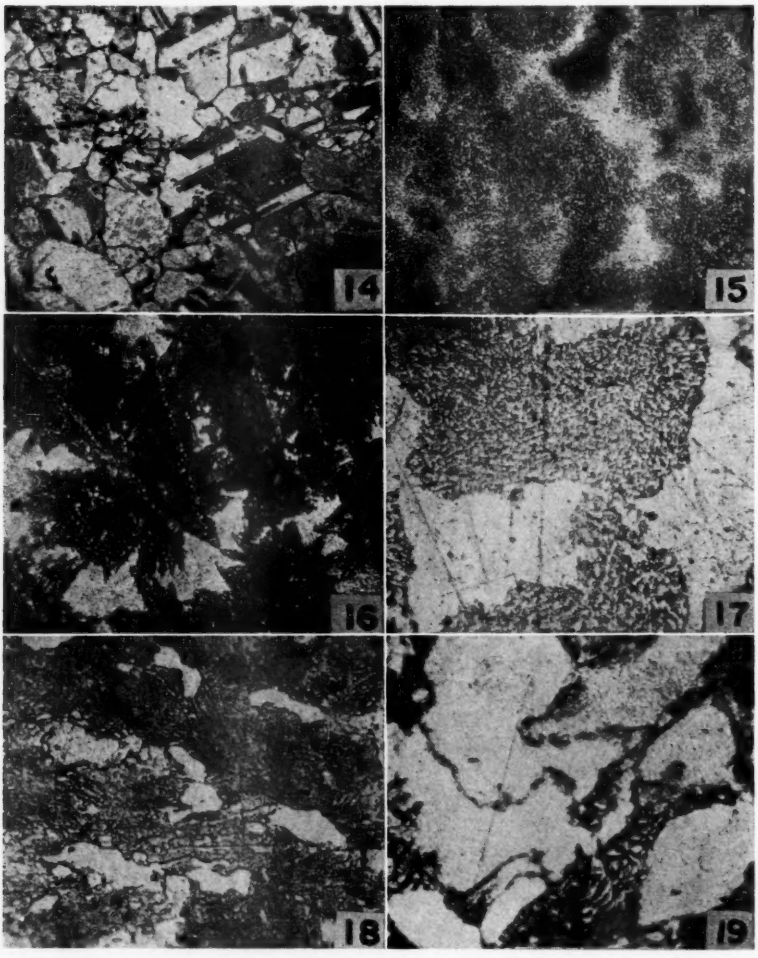

FIG. 14. Alloy 25, × 250. Repolished and re-etched after one month at room temperature; grains of β with twinning bands.

FIG. 15. Alloy 23, × 135. Repolished and re-etched after one month at room temperature; showing α-2 and β.

FIG. 16. Alloy 30, × 250. The dendritic growth of β is here well marked; α-2 and γ-1 are also present (light areas) as proved by X-ray photograph.

FIG. 17. Alloy 32, × 250. A region of the alloy where α-2 is present with eutectic of α-2 and δ-1; now breaking up with the disappearance of δ-1 and appearance of γ-1.

FIG. 18. Alloy 39, × 250. As cast; α-2 (light) in a eutectic matrix of α-2, and δ-1. Note difference (Fig. 13) in appearance of lead crystals when indium is present.

FIG. 19. Alloy 38, × 250. α-2 (light), β-(black), γ-1 (gray).

glacial acetic acid, the sample being made the anode with an aluminum plate serving as cathode (current density 0.3 amp. per cm.^{2}), followed by the usual etch. Note the pitted appearance of the surface. Fig. 11 shows the heterogeneity in alloy 10, Fig. 12 the grain boundaries in alloy 11. The eutectic in the lead–tin system (Fig. 13) has a lamellar structure, the lead etching darkly in the absence of indium. Twinning bands are to be seen in the grains of alloy 25, shown in Fig. 14: they arose from the cold-working caused by polishing. In Fig. 15, the microstructure of an alloy defining the phase boundary between the one- and two-phase regions, as seen on the isotherm, is exhibited. The interpretation is obvious, when one notes that the α-2 phase, lead structure, etches very weakly (appearing light) in the presence of indium. The X-ray photographs substantiate this argument. With alloy 30, Fig. 16, we enter the invariant triangle. The dendritic growth of the β-phase here manifests itself clearly, and this explains the difficulty in distinguishing it from certain other phases in the binary systems, as found by Davis and Rowe (9, in discussion). Such a growth can apparently produce interfluence between the phases. The γ-1 (gray) and α-2 (light) phases are also present and this is corroborated by the X-ray photograph.

As we leave the invariant triangle and enter the adjacent two-phase region where γ-1 and α-2 are stable, the microstructures take on the appearance of Fig. 17 which depicts a region of alloy 32 in which the eutectic (δ-1 and α-2) is in the process of breaking up into α-2 and γ-1. The structure of a cast alloy in this region is portrayed in Fig. 18, alloy 39; the X-ray photograph shows lines for α-2 and δ-1. Note that the lead phase appears light and is delineated by the dark structure of the eutectic. The three phases β (black), γ-1 (light gray), and α-2 (light) occur in Fig. 19, representing alloy 38.

DISCUSSION

Ferguson and Screaton (3) do not agree with Valentiner (12) on the structure of β-indium–tin but, since the lattice of β-indium–lead is established as face-centered tetragonal and since this is the stable lattice right across the diagram, it appears as if Valentiner's view is correct.

Previous workers have failed to detect, by microscopic examination, any evidence of heterogeneity in the lead–indium system, although they had deduced the existence of an intermediate β-phase from X-ray data. Our photomicrograph of alloy 10 (Fig. 11) shows the heterogeneity. The trouble is due to the fact that both α-indium and β-indium–lead have face-centered tetragonal lattices. Davis and Rowe (9, in discussion) do not state their etching reagent. It is probable that the acetic acid in ours was the factor of success, since it tends to remove tarnished films.

For stable intermetallic phases in an alloy the rule is that the intermetallic compound is usually harder than the hardest of its components. This is exemplified by the graph of hardness vs. composition for the indium–tin system, where the peak on the curve lies in the γ region: the β-phase is softer than pure tin and just slightly harder than pure indium. In general, an intermetallic "compound" has some composition within the boundaries of its stable

existence and corresponding to a definite chemical formula. Since compounds, according to Hume-Rothery (6) correspond to definite valence electron to atom ratios, one can hence attribute much of their hardness to their tendency to form homopolar bonds. The results support this view. The γ-phase, of simple hexagonal structure, is almost twice as hard as the body-centered tetragonal lattice of pure tin. Since the hexagonal lattice would have more planes for deformation slipping than the tetragonal, some other forces must be operative, e.g. homopolar bonding.

Alloys containing the γ-indium–tin phase could not be dissolved completely in acids, unless platinum was used to promote solution by galvanic action. Whatever the cause of this passivity, the phenomenon is interesting from the point of view of corrosion studies.

ACKNOWLEDGMENT

We are indebted to Professor R. B. Ferguson, Associate Professor of Crystallography, for much helpful advice in carrying out the X-ray measurements.

REFERENCES

1. DAVIS, H. M. Trans. Am. Soc. Metals, 39: 712. 1947.
2. EYRING, H. J. Phys. Chem. 57: 942. 1953.
3. FERGUSON, R. and SCREATON, R. Acta Cryst. 7: 364. 1954.
4. FINK, C. J., JETTE, E. R., KATZ, S., and SCHNETTLER, F. S. Trans. Electrochem. Soc. 75: 463. 1939; 88: 229. 1945.
5. GRYMKO, S. M. and JAFFEE, R. I. Materials & Methods, p. 59. March 1950.
6. HUME-ROTHERY, W. J. Inst. Metals, 35: 295. 1926.
7. KLEMM, W., KLEMM, LI, HOHMANN, E., VOLK, E., ORLAMUNDER, E., and KLEIN, H. A. Z. anorg. Chem. 256: 239. 1948.
8. METALS HANDBOOK. American Society for Metals. p. 93. 1948.
9. RHINES, F. N., URQUHART, N. M., and HOGE, H. R. Trans. Am. Soc. Metals, 39: 694. 1947.
10. SCOTT, W. W. Standard methods of chemical analysis. D. Van Nostrand Company, Inc., New York. 1927. p. 536.
11. STOCKDALE, D. J. Inst. Metals, 49: 267. 1932.
12. VALENTINER, S. Z. Metallkunde, 32: 31. 1940.
13. VILLELA, J. R. and BEREGEKOFF, D. Ind. Eng. Chem. 19: 1049. 1927.

HYDROGEN PEROXIDE AND ITS ANALOGUES

VI. INFRARED SPECTRA OF H_2O_2, D_2O_2, AND HDO_2 [1]

BY OSIAS BAIN[2] AND PAUL A. GIGUÈRE

ABSTRACT

The absorption spectrum of hydrogen peroxide was re-examined with a prism instrument in the region 1.5 to 25μ. A pair of well-resolved perpendicular bands arising from torsional oscillation of the OH groups were found centered about 460 and 575 cm.$^{-1}$. The overtone band at 3.8μ was shown to be a hybrid with prominent rotational structure and some indications of doubling. Its assignment to the combination $\nu_2+\nu_6$ implies a positive anharmonicity. Four new overtone bands were observed in liquid hydrogen peroxide. The infrared spectrum of deuterium peroxide was measured for the first time in the solid and vapor states. The vapor bands are quite different in appearance from those of hydrogen peroxide. One of the fundamentals, the asymmetric O—D stretching at 2661 cm.$^{-1}$, was resolved sufficiently to allow calculation of the rotational constants of the isotopic molecule. Mixtures of the two peroxides containing around 40% of HDO_2 were also investigated; from the results the frequency of the as yet unobserved symmetric modes ν_1 and ν_2 could be estimated with fair certainty. The O—O stretching vibration at 11μ was too weak to be located definitely in the spectra of the gaseous peroxides. The structural parameters of the H_2O_2 molecule are now established as follows:

$$r_{O—O} = 1.49 \pm 0.01 \text{ Å}$$
$$r_{O—H} = 0.97 \pm 0.01 \text{ Å}$$
$$\alpha_{OOH} = 100° \pm 2°$$

The O—H and O—D stretching bands were studied in solutions of the three isotopic peroxides in carbon tetrachloride.

Previous investigations of the molecular spectrum of hydrogen peroxide (2, 6, 10, 30, 34) have served to confirm the structure now accepted for that molecule but, otherwise, they have left unanswered a number of important questions, such as the assignment of the weak band at 3.8μ and the frequency of the four symmetric modes, especially ν_4 the torsional oscillation. In an effort to solve some of these problems the infrared spectrum of that compound was measured again under a wider range of conditions than covered heretofore. In addition, the completely deuterated peroxide was prepared and its spectrum in the vapor state was recorded for the first time. Mixtures of these two isotopic peroxides were used to obtain valuable information on the hybrid molecule HDO_2. Unfortunately, study of the latter was severely limited by interference from the parent molecules H_2O_2 and D_2O_2, always present in large proportions, in addition to traces of H_2O, D_2O, and HDO. Finally the spectra of the three peroxides dissolved in a non-polar solvent have helped elucidate the region of the O—H and O—D stretching fundamentals. While the subject remains far from exhausted the new results have made possible calculation of the force constants of the molecule (11) and an appreciable refinement in our knowledge of the structural parameters.

EXPERIMENTAL

The material used for obtaining the spectra was prepared as described before;

[1]*Manuscript received November 22, 1954.*
Contribution from the Department of Chemistry, Laval University, Quebec, with financial assistance from the National Research Council of Canada.
[2]*Present address: C.A.R.D.E., Valcartier, Que.*

the hydrogen peroxide, 99.5%, by fractional distillation of Becco's 90% commercial product, and the deuterium peroxide, 90–93%, by dissociation of heavy water vapor, 99.6% pure, in the electrodeless discharge (16). The tendency of these peroxides to decompose spontaneously gave rise to numerous difficulties in selecting suitable containers and window material. For the latter, plates of highly polished silver chloride were found to be quite satisfactory. Spectra of the solid peroxides were studied without too much difficulty because of the slower decomposition rate at low temperature. An absorption cell of the type described by Wagner and Hornig (31) was used. One drop of liquid peroxide was squeezed between two precooled silver chloride plates and the whole was quickly inserted in the holder. After the cell was evacuated the temperature was lowered further with dry ice and acetone. Atmospheric humidity had to be kept low enough to prevent condensation on the windows.

The liquid peroxides could not be studied so easily. Even with very smooth silver chloride plates some slight decomposition always occurred at room temperature and the oxygen produced forced out the thin film of liquid. In the overtone region glass spacers were used and the thickness, measured by an interference method (28), was about 0.1 mm. Below 1μ a glass cell 1 cm. thick was used so that four new combination bands could be detected in both hydrogen and deuterium peroxides (Table I). Solutions in carbon tetrachloride could only be studied in the near infrared up to approximately 4μ where the solvent is still sufficiently transparent. A very thick absorption cell was needed then because of the low solubility of the peroxides. (No data are available on the solubility of hydrogen peroxide in carbon tetrachloride but, from the relative intensity of the various absorption bands, it seems to be of the same magnitude as that of water (7), namely 8–10 mgm. per 100 gm. of solvent.) A glass tube, 10 cm. long, closed by silver chloride windows made tight by means of Koroseal gaskets was entirely satisfactory. For the vapor a Perkin-Elmer 1-meter multiple reflection cell made of cast aluminum was tried at first. In practice the sample of liquid peroxides could not be heated much above 70°C., where the vapor pressure is of the order of 30 mm. Hg. To prevent condensation on the mirrors and windows the cell had to be kept at 90°C. Under such conditions, decomposition was so rapid, even with a flow system, that a steady concentration of peroxide could not be secured and the water vapor produced blotted large sections of the spectrum. Therefore a glass cell of 1.25 meter path-length was built as shown in Fig. 1.

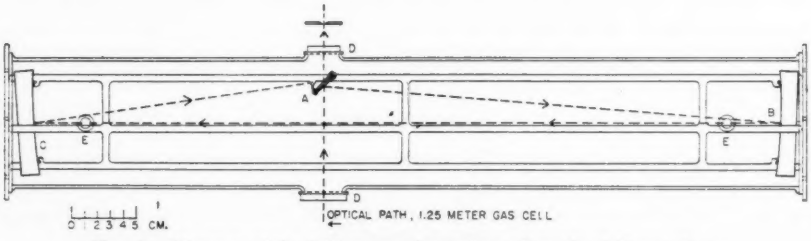

FIG. 1. Diagram of the 1.25 meter absorption cell made of Pyrex glass.

TABLE I

INFRARED SPECTRA OF HYDROGEN AND DEUTERIUM PEROXIDES

H_2O_2				D_2O_2				
Vapor		Liquid, cm.$^{-1}$	Solid, cm.$^{-1}$	Vapor		Liquid, cm.$^{-1}$	Solid, cm.$^{-1}$	Assignment
cm.$^{-1}$	(a)*			cm.$^{-1}$	(a)*			
465 575	0.07	635 m.†	472 v.w.† 660 s. 792 w.			538 m.†	480 m.	$\nu_4(a)$
890(?)	0.007	878 m.w.	878 m.w.			878 m.w.†	880 m.w.	$\nu_3(a)$
1266	0.38	1350 s.	1380 s.	923 947	0.45	1004 s.†	1000 s.	$\nu_6(b)$
			1430 w.†	1007(?)				$\nu_3(a)$
2647	0.065	2780 m.	2840 m. 2930 w.	1985	0.02	2087 m.w.†	2090 m.w.	$\nu_2+\nu_6(B)$
3610	0.24	3360 v.s.†	3320 v.s.†	2661	0.25	2482 v.s.†	2470 v.s.	$\nu_5(b)$
4465	0.004	4290 v.w.						$\nu_3+\nu_5(B)$
4835 4955	0.007	4770 w.	4595 v.w.†			3430 w.		$\nu_1+\nu_6(B)$ $\nu_2+\nu_5(B)$
		6100 v.w.						
7036.6 7041.6		6805 w.		5240	0.03	4980 v.w.		$\nu_1+\nu_5(B)$
		8040 v.w.				6110 v.w.		$2\nu_5+\nu_6(B)$
10283.7 10291.1		9950 v.w.				7215 v.w.		$2\nu_1+\nu_5(B)$, $3\nu_5(B)$

*$(a) = (1/pl) \log I_0/I$, with p in atm. and l in cm.
†From reference (30).

The cell proper is made out of a 60 cm. length of Pyrex tube 10 cm. diameter. The ends, slightly flared and ground flat, are closed by disks of 1S aluminum, 3 mm. thick and well polished. (Very pure aluminum, when properly cleaned, is fairly inert towards hydrogen peroxide.) The two front-aluminized, spherical mirrors, B and C, 8 cm. diameter and 117.5 cm. focal length (such as used in the Perkin-Elmer spectrometer) are mounted in a frame of three thick glass rods held together by rings of bent glass rods. Light, stainless steel springs press the spherical mirrors against lumps of glass fused onto the main rods. Two small plane mirrors, 1.8 × 2.5 cm. cut from microscope slides and bevelled on one side, are mounted diagonally and back-to-back in a holder of thin glass rods fused onto the glass frame. (They could be replaced by a single wedge-shape piece.)

The optical alignment proved to be a delicate operation, but once made it was permanent. To that end the optical assembly was taken out of the glass tube and placed at right angle in the convergent beam of the spectrometer. Mirrors A and B were first lined up so that the reflected beam was collimated and centered about the main axis of the cell. This was achieved by a trial and error method. The lumps of glass, against which the spherical mirrors rest, were softened with a torch and "worked" to the correct position. Mirror C was then similarly adjusted so as to focus the reflected beam on the entrance slit of the monochromator after reflection on the other face of the "wedge" mirror, A. Such an arrangement does not alter appreciably the convergence of the infrared beam. With the optimum alignment of the mirrors, as much as 80% of the incident light was transmitted after traversing the cell. The openings of the cell, closed either by the aluminum disks or by silver chloride windows, D, could be made tight without difficulty by means of Koroseal gaskets. However, this material is somewhat troublesome in that the plasticizer (a mixture of tritolyl phosphates) distills off on heating *in vacuo*. These esters were identified by their infrared spectra (8) in the 11–15μ region. By keeping the pressure above 15 mm. Hg in the cell at all times this undesirable phenomenon could be reduced appreciably.

To keep the cell at 85–90°C. it was wrapped with insulated nichrome wire and covered with asbestos paper and aluminum foil. The extent of decomposition of the peroxide vapor after one passage through this cell was of the order of 15%, as compared with 85% with the all-metal cell. Various techniques were tried to introduce the peroxide vapor. A static system with the liquid peroxide in a side tube and the absorption cell evacuated was unsatisfactory on account of decomposition. Continuous pumping of the cell through a dry-ice trap and a reducing valve adjusted so that the pressure in the cell remained at 15 mm. Hg resulted in a steady state as indicated by the reproducibility of the intensity spectra. Evacuation of the absorption cell was not necessary, however. The device shown in Fig. 2 was found useful: the sample of liquid peroxide in tube A is surrounded by a vapor jacket B in which a suitable liquid (for instance carbon tetrachloride) is boiled under atmospheric pressure. A regulated stream of dry nitrogen is bubbled through a small tube closed by a fritted glass disk. The stream of gas saturated with peroxide vapor is passed at constant rate

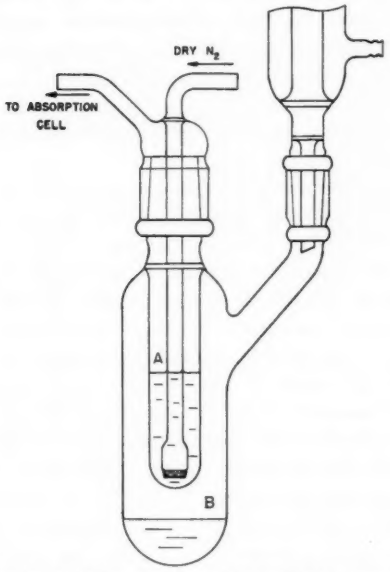

FIG. 2. Device for filling the absorption cell with peroxide vapor.

through the absorption cell and then through a dry-ice trap. The infrared spectrometer was a Perkin-Elmer, model 12C, with automatic scanning and recording on a Speedomax. During this investigation the monochromator was converted to double-pass with notable increase of resolving power and reduction of scattered light. Absorption by atmospheric gases was kept at a tolerable level by circulation of dry nitrogen through the two housings of the instrument.

INTERPRETATION OF THE SPECTRA

From the structural point of view the molecules H_2O_2 and D_2O_2 may be described as slightly asymmetric, prolate tops. The degree of prolateness is characterized by the function

$$\beta = (I_{B,C}/I_A) - 1, \qquad [1]$$

where $I_{B,C}$ is the harmonic mean of the two large moments of inertia and I_A is the minor moment of inertia of the molecule. The rotational constants of H_2O_2 have been measured previously (10, 34) and from these, β turns out to be 11.2. Similar calculations for D_2O_2, assuming the same structural parameters, lead to $\beta = 6.4$. As for their asymmetry (I_B/I_C), it cannot be evaluated with the same certainty because of insufficient data, but estimates of the individual moments of inertia (3, 10) show that it must be less than 5%, even in the case of D_2O_2, unless the azimuthal angle ϕ is very different from 90°. The spectra of these molecules will therefore exhibit two different types of band structures; (*a*) perpendicular bands, corresponding to the symmetric vibrations, ν_1 to ν_4, (10) for which the change of electric moment is essentially perpendicular to the

top axis, and, (*b*) hybrid bands of predominantly parallel character arising from the asymmetric vibrations ν_5 and ν_6. The former, presumably rather weak in infrared, will have a single broad maximum with a rotational structure easily resolvable under the dispersion of a prism instrument. Indeed, the spacing of their rotational levels is 18 cm.$^{-1}$ for H_2O_2 and about half as much for D_2O_2.

On the other hand, the strong parallel component of the hybrid bands will show separate *P*, *Q*, and *R* branches but the rotational structure will not be perceptible because of too fine spacing: 1.65 cm.$^{-1}$ for H_2O_2 and 1.47 cm.$^{-1}$ for D_2O_2. The contour of these bands may be predicted from the equation of Gerhard and Dennison (9). Thus the separation of the *P* and *R* maxima, dependent on the various moments of inertia and the temperature, is calculated to be 43 and 45 cm.$^{-1}$ respectively for H_2O_2 and D_2O_2 at 70°C. Similarly the intensity of the zero *Q* branch relative to the total intensity of the parallel band should be 9% for H_2O_2 and 12% for D_2O_2. Finally, the perpendicular component of these hybrid bands may be expected to alter the over-all intensity distribution, particularly near the center, with more or less definite indications of a coarse rotational structure.

Spectra of the Vapor

(A) *The Torsional Oscillation Mode*

The outstanding feature in the present study of hydrogen peroxide vapor is certainly the band system of medium intensity extending from 16μ to beyond the transmission limit of KBr optics. For deuterium peroxide the corresponding band lies mostly outside the present range of our instrument; we hope to investigate it soon with CsBr optics. The tracing shown in Fig. 3 was recorded with a

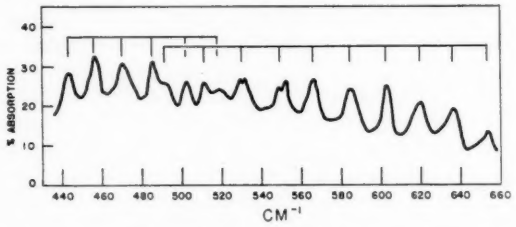

FIG. 3. The torsional oscillation band in hydrogen peroxide vapor.

slit equivalent to a resolved width of frequency band ranging from 4.4 to 6.7 cm.$^{-1}$. On the basis of location and relative intensity there is little doubt that this band arises from the torsional oscillation, or hindered internal rotation, mode ν_4. Qualitatively this oscillation may be expected to result in a fairly large change of the electric moment of the molecule perpendicular to the top axis. Analysis of the rotational structure (Table II) shows a spacing averaging 18 cm.$^{-1}$ on the short wavelength side, dropping suddenly to 16–15 cm.$^{-1}$ somewhere around 480 cm.$^{-1}$. This convergence is in opposite direction to that in the second (10) and third harmonics (34) of the O—H stretching vibrations and, for that reason, it is unlikely that we have here a single, or unsplit

TABLE II

APPROXIMATE FREQUENCIES AND TENTATIVE ASSIGNMENTS OF THE PRINCIPAL MAXIMA IN THE 17–22μ BANDS OF HYDROGEN PEROXIDE

	High frequency band				
K	$^{P}Q_K$	$^{R}Q_K$	$\frac{^{R}Q_K - {}^{P}Q_K}{4K}$	$\frac{^{R}Q_{K-1} - {}^{P}Q_{K+1}}{4K}$	Low frequency band
	cm.$^{-1}$	cm.$^{-1}$	cm.$^{-1}$	cm.$^{-1}$	cm.$^{-1}$
0		585			519
1	567	603	9.0	8.5	503
2	551	620	8.6	9.1	486
3	530	637	8.9	9.1	470
4	511	653	8.8	9.1	456
5	492				443

vibrational transition. This, coupled with the irregular spacing observed between 485 and 520 cm.$^{-1}$, points strongly to the presence of two separate bands. From intensity distribution the center of the short wavelength component is tentatively located at 575 cm.$^{-1}$ and the other, around 465 cm.$^{-1}$. Obviously these figures, especially the latter, are rather uncertain because of the low intensity of incident radiation and the small number of maxima observed.

That this band is doubled confirms the previous interpretation of a similar feature in overtone bands namely, a double minimum in the torsional oscillation. Indeed, the other explanations considered seem most unlikely. For instance, it is doubtful that one of the two bands could be due to transition from an excited state such as $2\nu_4 - \nu_4$ because both components have about the same intensity and "borrowing" by coupling of levels is not expected in this case. Also, the high-frequency band is too intense to be an harmonic of some fundamental situated in the far infrared. The large doublet splitting, about 110 cm.$^{-1}$, is not surprising as the torsional oscillation is much more closely associated with the double minimum than the other vibrational levels. (Compare the inversion splitting of ν_1 and ν_2 in NH_3 (18) for instance.) It also confirms that one of the potential barriers must be fairly low. According to the model of Penney and Sutherland (26) rotation of the two O—H groups about the O—O bond is restricted by an asymmetric potential function having a high and low barrier in the *cis*- and *trans*-positions respectively. The height of the first, V_1, was estimated by them at 1 electron volt and that of the second V_2, at about half of that value. No complete theoretical treatment of the asymmetric potential function has been reported yet although various approximations have been suggested (22, 27). From electron density calculations Lassettre and Dean (19) arrived at values of 94° to 113° for ϕ, the azimuthal angle, with heights of potential barriers ranging from 8 to 21 kcal./mole for V_1 and from 2 to 10 kcal./mole for V_2. Therefore, the potential function generally assumed for the torsional oscillation in molecules such as ethylene,

$$V = \tfrac{1}{2} V_0(1-\cos 2\phi), \qquad [2]$$

where V_0 is the barrier of periodicity π, is not strictly applicable to the case of

hydrogen peroxide. If a periodicity of 2π is to be preserved, then a cosine function of the following form is the simplest possible one:

[3] $$V = \tfrac{1}{2}(V_1 - V_2)\cos\phi + \tfrac{1}{2}(V_1 + V_2)\cos^2\phi.$$

From this the position of the minima is given by

[4] $$\phi \text{ min.} = 2n\pi \pm \cos^{-1}[(V_2 - V_1)/2(V_2 + V_1)],$$

and a ratio of V_1/V_2 of about 3 is required to make $\phi = 105°$, the average estimated by Lassettre and Dean. In principle the energy levels could be found by replacing the potential function in the Schrödinger equation by V from [3], and would be given by the periodic eigenvalues of "a" in the following Mathieu-type equation:

[5] $$(d^2M/dx^2) + (a - b\cos 2x - c\cos^2 2x)M = 0,$$

[6] where $$a = 32\pi^2 I_r E/h^2,$$

[7] $$b = (16\pi^2 I_r/h^2)(V_1 - V_2),$$

[8] and $$c = (16\pi^2 I_r/h^2)(V_1 + V_2).$$

At present the lengthy calculations to determine how the eigenvalues of "a" depend on V_1 and V_2 do not seem justified for lack of enough accurate data.

Pending rigorous solution of the wave equation for the asymmetric function [3] various simplifications are necessary in correlating the experimental results. Thus, assuming a symmetrical twofold barrier [2], an average value of 520 cm.$^{-1}$ for the torsional frequency leads, through solution of the Mathieu equation, to a value of $V_0 = 6$ kcal./mole. About the same value was obtained from the perturbed oscillator treatment (20). A recent investigation of the microwave spectrum of hydrogen peroxide (24) has yielded a much lower value, *ca.* 320 cal./mole, also on the assumption of a symmetrical potential function. It is possible that this spectrum could be interpreted as well in terms of a function with a high and a low barrier.

On the other hand the difference between the calorimetric entropy at 25°C. and the calculated statistical entropy of hydrogen peroxide (13) corresponds to an hypothetical barrier $V_0 = 3.5$ kcal./mole. On the same basis the treatment suggested by Pitzer (27) for molecules with slightly asymmetric tops attached to a rigid frame yields the more reliable value 4.7 kcal./mole. Thus it appears fairly certain that the *trans*-barrier is appreciably lower than the *cis*-one. However, it could hardly be as low as suggested by the microwave spectrum because then an important fraction of the H_2O_2 molecules would possess a torsional energy greater than V_2 at moderate temperatures, and their symmetry would be effectively C_{2h} (23). In that respect it is unfortunate that the low volatility and thermal unstability of hydrogen peroxide make it impossible to measure the infrared spectrum or the heat capacity of the vapor as a function of temperature.

(*B*) *The O—O Stretching Mode*

Repeated scrutiny of the 11μ region in the spectrum of H_2O_2 vapor has failed to reveal any definite indication of the O—O vibration ν_3. Under the maximum

equivalent path-length attainable, absorption amounted to less than 3% in the range 830–920 cm.$^{-1}$ while it was complete for ν_6, the OH bending mode. (In D_2O_2 and HDO_2 the situation is less favorable because of the strong ν_6 band near by.) This remarkable fact, which, alone, is sufficient to rule out any tautomeric form of the molecule such as H_2O—O, has not been fully appreciated in previous investigations. One of us (10) reported a very weak maximum "hardly noticeable" in the vapor and assigned to it a value of 877 cm.$^{-1}$ largely on the faith of the corresponding Raman shift (6). As for the band of medium intensity found by Bailey and Gordon at 870 cm.$^{-1}$ (2), it must have resulted from condensation on the windows of the absorption cell as confirmed otherwise (10) by the resemblance of their spectra in both phases.

Indeed, it is a peculiarity of this frequency that it is much stronger, relatively speaking, in the condensed states than in the vapor. Such enhanced activity must be due to strong molecular association as it is not likely that the configuration of the free molecule is appreciably different from that in the liquid or the solid. X-ray investigations of the crystal structure of hydrogen peroxide (1) and its addition compound with urea (21) have shown azimuthal angles of about 94° and 106° respectively. Even when the hydrogen atoms of H_2O_2 are replaced by much heavier groups, as in SF_5—O—O—SF_5, the azimuthal angle remains nearly the same (107°±5° (17) from electron diffraction by the vapor). According to the C_2 model of H_2O_2 ν_3 must yield a perpendicular band with a single maximum, which makes its location still more problematic. The intensity, at any rate relatively low, would depend on the azimuthal angle, becoming zero for $\phi = 180°$. A consequence of this situation is that the frequency of ν_3 is not yet known accurately, having been measured so far only in the liquid and solid where it may be altered slightly by molecular interaction. Cf. the case of hydroxylamine (12). For that reason measurement of the Raman spectrum of hydrogen peroxide vapor would be a desirable, if difficult investigation.

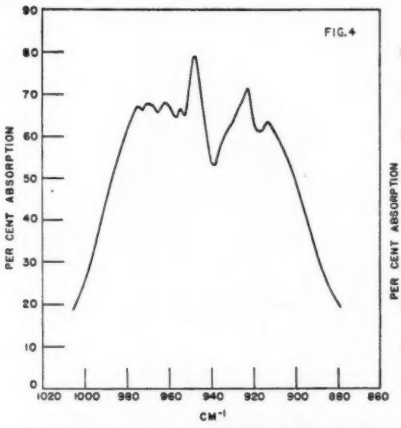

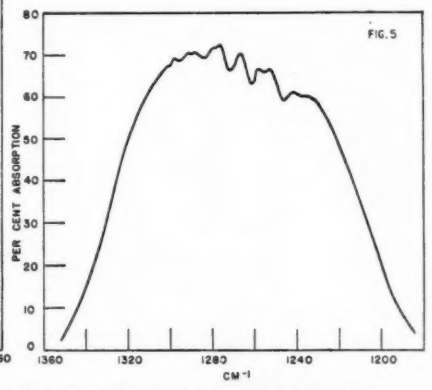

FIG. 4. The asymmetric OD bending frequency in deuterium peroxide vapor.
FIG. 5. The OH bending vibration ν_6 in gaseous hydrogen peroxide.

(C) The OH and OD Bending Modes

The asymmetric bending modes ν_6 are the most intense in the spectra of both peroxides, their central Q branch occurring at 1266 cm.$^{-1}$ in H_2O_2 and 947 cm.$^{-1}$ in D_2O_2. The first one was recorded with a fluorite prism and the second, with a rock salt prism; in both cases the resolution was about 4 cm.$^{-1}$. As predicted by the equation of Gerhard and Dennison (9) the Q branch is much stronger in D_2O_2 (Fig. 4) than in H_2O_2 (Fig. 5). It was not possible to evaluate the separation of the P and R maxima because of some coarse structure arising presumably from the perpendicular component. No regularity could be detected in this rotational structure, possibly on account of doubling of the bands. The prominent maxima on the low frequency side, specially in the case of D_2O_2, at 923 cm.$^{-1}$, resemble the satellite bands reported by Williams (32) in his study of formic acid. In general appearance both bands show pronounced asymmetry, the intensity gap between the P and Q branches missing in D_2O_2. Since other bands of both peroxides feature the same unequal intensity distribution it is doubtful if it arises from another coincident vibration, ν_2 in this case. Rather we believe there is an appreciable frequency difference between ν_2 and ν_6 on the basis of the following indirect evidence.

The spectrum of HDO_2 measured in that region showed very clearly the Q branch of the OOD bending vibration at 981 cm.$^{-1}$. By analogy with the

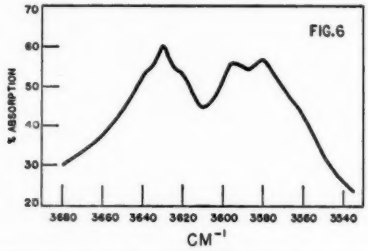

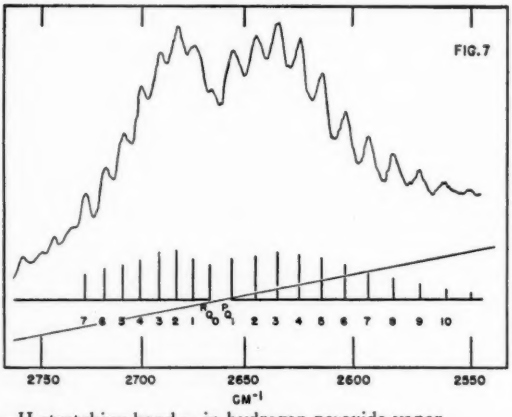

FIG. 6. The O—H stretching band ν_5 in hydrogen peroxide vapor.
FIG. 7. Rotational structure of the stretching band ν_5 in deuterium peroxide. (The sloping line corresponds roughly to the background.)

bending frequency in HDO, which occurs about halfway between those in H_2O and D_2O, we infer that ν_2 should be around $981+(981-947) = 1015$ cm.$^{-1}$ in D_2O_2. In fact a slight absorption was noticeable at 1007 cm.$^{-1}$ in the vapor of both D_2O_2 and HDO_2. The corresponding OOH bending mode could not be identified with certainty in H_2O_2 but, from the isotope shift, it may be expected to lie around 1350 cm.$^{-1}$ in that molecule. Consideration of various combination bands leads to the same conclusion, as explained below.

(D) The O—H and O—D Stretching Modes

Recording of the asymmetric stretching bands ν_5 was done under medium absorption with a LiF prism and a spectral half-width resolution of 9.7 cm.$^{-1}$ for H_2O_2 (Fig. 6) and 4.9 cm.$^{-1}$ for D_2O_2 (Fig. 7). Here the two peroxides show still greater differences than for the bending modes. While both bands have the same parallel contour, the coarse rotational structure of the perpendicular component is prominent in D_2O_2 but is missing completely in H_2O_2 although the resolution was sufficient to bring it out. This situation is reminiscent of the overtone band of hydrogen peroxide $\nu_1+\nu_5$ under high dispersion (10) in contrast with the corresponding band finely resolved in hydrogen persulphide (33). Still, the present circumstance may be fortuitous—overlapping by water vapor bands or doublet splitting—as there is no obvious reason why the perpendicular component should be much stronger in D_2O_2 than in H_2O_2.

The frequencies of the various maxima in Fig. 7 are listed in Table III together with the calculated rotational constants A′ and A″. The accuracy of these figures is estimated to be 4%. The band center was found from the equation of Dieke and Kistiakowsky (5) to be at 2661 cm.$^{-1}$. For the H_2O_2 band the center was taken at the absorption minimum, 3610 ± 5 cm.$^{-1}$. Like the others these values are not corrected for vacuum.

TABLE III

ROTATIONAL ANALYSIS OF THE 2661 CM.$^{-1}$ BAND OF D_2O_2

K	^PQ_K	^RQ_K	$\frac{^RQ_K-{}^PQ_K}{4K}$	$\frac{^RQ_{K-1}-{}^PQ_{K+1}}{4K}$	ν_0
	cm.$^{-1}$	cm.$^{-1}$	cm.$^{-1}$	cm.$^{-1}$	cm.$^{-1}$
0		2667.6			
1	2657.6	2676.5			
2	2646.6	2685.1	4.81	5.13	2662.4
3	2635.5	2693.5	4.84	4.98	2660.7
4	2625.4	2702.5	4.82	4.91	2660.6
5	2614.9	2711.2	4.81	4.94	2661.5
6	2603.7	2720.3	4.86	4.90	2658.7
7	2593.7	2729.4	4.85	4.92	2660.2
8	2582.6			4.95	
9	2571.2	Average	4.83	4.93	2661.
10	2560.0				

(E) Overtone Bands

An interesting result of this investigation is the resolution of the hybrid band at 3.8μ in H_2O_2 vapor, the origin of which had remained uncertain until

now. With its definite parallel-type contour and prominent rotational structure (Fig. 8) it can only arise from combination of the two bending modes $\nu_2+\nu_6$ since both $2\nu_2$ and $2\nu_6$ would be predominantly perpendicular. Besides

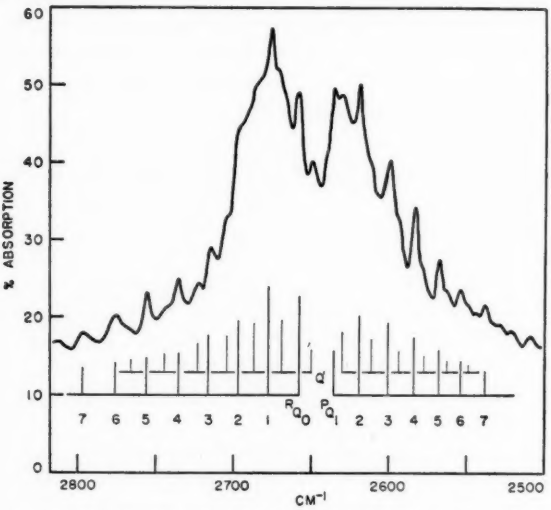

FIG. 8. Overtone band at 3.8μ in gaseous hydrogen peroxide.

they should be very weak, and for different reasons: $2\nu_6$, because even harmonics of unsymmetrical frequencies are usually missing in non-linear molecules, and $2\nu_2$, because of the weakness of its first harmonic. The present assignment leads to an unexpected anharmonicity as the frequency of the combination band, 2647 cm.$^{-1}$, is higher, instead of lower, than the sum of its components, about 2615 cm.$^{-1}$ if the above deduced value for ν_2 is correct. The difference cannot be due entirely to uncertainty in the latter estimate. Indeed, an increase of more than 30 cm.$^{-1}$, making ν_2 greater than 1380 cm.$^{-1}$, would hardly leave any shift for this frequency in the condensed phases. In fact it has been observed at 1400 cm.$^{-1}$ in the Raman effect of the pure liquid (29). That the unusual anharmonicity associated with $\nu_2+\nu_6$ is real is further confirmed by the frequency of this band in the Raman spectrum, *ca.* 2815 cm.$^{-1}$ (29).

Recordings of this band made under maximum absorption revealed some secondary peaks between the main ^PQ and ^RQ sub-bands particularly at 2650 and 2723 cm.$^{-1}$. These could be due to absorption from the first excited level of ν_4 although we are inclined to consider them as indications of doubling in view of their fair intensity and the presence of the same feature in the other two resolved overtones. The separation of the doublet at the center, 10 cm.$^{-1}$ from the minima of intensity, seems plausible in that conjecture. The irregular convergence of the rotational structure (Table IV) is probably exaggerated by the low resolving power available. Consequently the rotational constants derived therefrom would be much less accurate than those from the two over-

TABLE IV

FREQUENCIES OF THE PRINCIPAL MAXIMA IN THE 3.8μ BAND OF H_2O_2

K	${}^{P}Q_K$	${}^{R}Q_K$	${}^{P}Q'_K$	${}^{R}Q'_K$
	cm.$^{-1}$	cm.$^{-1}$	cm.$^{-1}$	cm.$^{-1}$
0		2658		2650
1	2636	2678	2630	2670(?)
2	2619	—	2612(?)	2686(?)
3	2601	2716	2593(?)	2704
4	2584	2736	2577(?)	2723
5	2568	2755	2562(?)	2744
6	2554	2776	2545(?)	2766(?)
7	2538.5	2797.5		

Note: The primed symbols refer to the secondary band.

tones of the O—H stretching frequencies (10, 34). Incidentally when the latter are compared with the present band the difference in general appearance is striking. In particular no ${}^{P}Q$ or ${}^{R}Q$ branches are missing near the center (Fig. 8). The reason for such differences is not clear at present. For the corresponding band in D_2O_2 at 5μ absorption was too low to reveal any structure. Similarly, the combination $\nu_1+\nu_5$ appeared as a hybrid band at 5240 cm.$^{-1}$. Finally a few very weak maxima were noticed in H_2O_2 vapor at 4465, 4835, and 4955 cm.$^{-1}$. The first of these can be assigned unambiguously to $\nu_3+\nu_5$ which gives a reasonable anharmonicity, 35 cm.$^{-1}$. As for the other two, their separation is far too great for the P and R branches of a single band, so that they must arise from different combinations among the various possibilities listed in Table I.

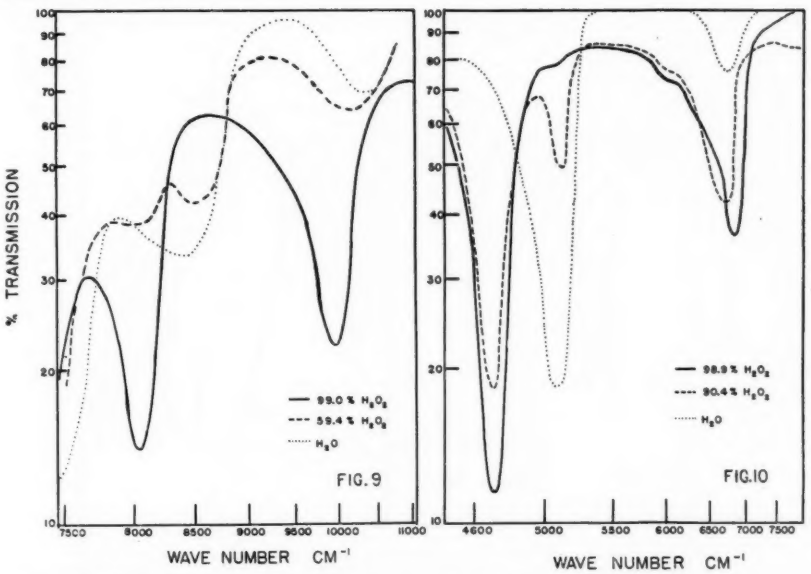

FIG. 9. Absorption spectra of aqueous hydrogen peroxide solutions in the 1μ region.
FIG. 10. Infrared spectra of liquid hydrogen peroxide and water between 1.2 and 2μ.

Spectra of the Condensed States

(F) Liquid and Solid

Strong molecular association in the peroxides makes a spectroscopic study of their condensed states of special interest. On the other hand, and for the same reason, little information may be expected from it in connection with the structure of the free molecule. In the region covered by the LiF prism six weak maxima were found in liquid H_2O_2 (Figs. 9 and 10) and four in liquid D_2O_2 (Table I). Of the latter, two are rather uncertain (at 6110 and 7215 cm.$^{-1}$) as they were observed in a dilute solution (15–20%) and the maxima are probably shifted appreciably by dilution (compare Figs. 9 and 10). For crystalline H_2O_2 the present measurements agree quite well with those of Taylor (30) except for the combination band reported by him at about 2740 cm.$^{-1}$ which we found at a higher frequency and resolved into two peaks at 2840 and 2930 cm.$^{-1}$. Thus the temperature shift is really in the same direction as for the fundamentals ν_2 and ν_6 so there is no objection to an assignment to that combination; this leads to a positive anharmonicity as for the vapor band. The weaker component at 2930 cm.$^{-1}$ may be due to $2\nu_2$ and/or to a ternary combination with a lattice mode. In crystalline D_2O_2 the frequency of ν_4 shows the normal isotope shift with the low-frequency band in H_2O_2. Therefore it is likely that the value given by Taylor for this mode in liquid D_2O_2, (538 cm.$^{-1}$) is too high. Attempts to check this point were unsuccessful. No splitting of the bending OD frequencies could be detected contrary to H_2O_2, although the peak at 1000 cm.$^{-1}$ (Fig. 11) appears slightly asymmetric.

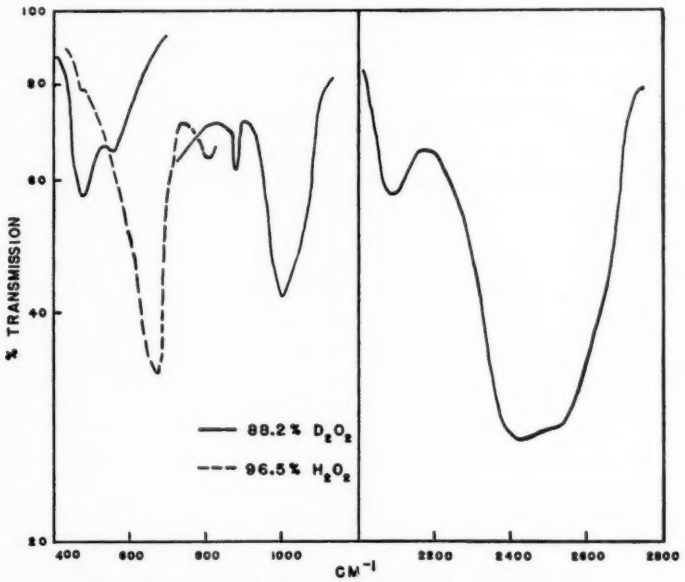

FIG. 11. Absorption spectra of crystalline H_2O_2 and D_2O_2.

(G) Solutions in Carbon Tetrachloride

Just as in the case of water (7) the absorption spectra of H_2O_2 and D_2O_2 dissolved in a non-polar solvent have provided valuable information on the O—H and O—D stretching modes. Mixtures of the two peroxides were particularly useful in that respect. It must be remembered here that an equimolar mixture of H_2O_2 and D_2O_2 will contain approximately 25 mole % of each constituent along with the hybrid compound HDO_2. In addition the molecular species H_2O, D_2O, and HDO will also be present in various amounts depending on the initial concentration of the peroxides. The H_2O_2 used was over 99% pure and the D_2O_2, about 50% in D_2O; the CCl_4 always contained some H_2O.

The results, shown in Table V and Figs. 12 and 13, lead to some interesting correlations the most striking of which is the exact coincidence of the O—H stretching frequency in HDO_2 with ν_5 in H_2O_2 and similarly, of the O—D

TABLE V

INFRARED BANDS OF ISOTOPIC WATER AND PEROXIDE MOLECULES IN SOLUTION IN CCl_4

cm.$^{-1}$	H_2O_2	D_2O_2	HDO_2	H_2O	D_2O	HDO
2628 v.s.		ν_5, (ν_1)	ν_{O-D}			
2646†	$\nu_2+\nu_6$				ν_1	
2696 s.						ν_{O-D}
2753 s.					ν_3	
3554 v.s.	ν_5, (ν_1)	$\nu_5+\nu_6$	ν_{O-H}			
3565 v.w.		$\nu_1+\nu_6$				
3615 w.				ν_1		
3666 s.		$\nu_2+\nu_5$(?)				ν_{O-H}
3714 s.				ν_3		
4414 v.w.	$\nu_3+\nu_5$					
4818 v.w.	$\nu_1+\nu_6$					
4919 v.w.	$\nu_2+\nu_5$					
5172 v.w.		$\nu_1+\nu_5$				

†*Weak in solutions of D_2O, and medium in solutions of H_2O_2.*

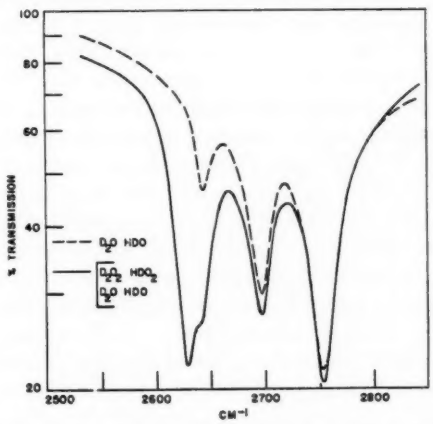

FIG. 12. Absorption by water and peroxide molecules in solution in carbon tetrachloride.

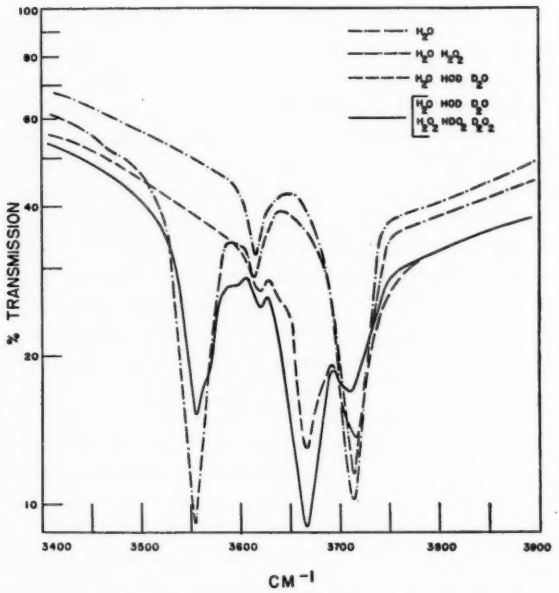

FIG. 13. Absorption bands due to various peroxide and water molecules in carbon tetrachloride solutions.

frequency in HDO_2 with ν_5 in D_2O_2. In HDO the O—H and O—D frequencies occur midway between the symmetric and asymmetric vibrations of the corresponding parent molecules.* By analogy the same relationship may be expected to abide in the peroxide molecules from which, therefore, it follows that the symmetric and asymmetric modes ν_1 and ν_5 should have nearly the same frequency. This conclusion, in harmony with the loose coupling between these two modes, explains why only one O—H stretching vibration has been observed so far, even in the crystal at low temperatures. The weak band found by Taylor (30) shifted some 135 cm.$^{-1}$ from the main O—H band in the Raman spectrum of the crystal was correctly assigned by him to a combination with a lattice vibration since the same difference appears between other frequencies in the solid. It may be noted here that assignment of the two H_2O_2 bands at 4818 and 4919 cm.$^{-1}$ to combination of one stretching with one bending mode is consistent with the previous conclusions, $\nu_1 \approx \nu_5$ and $\nu_2 \approx \nu_6 + 90$ cm.$^{-1}$.

It is instructive to compare the shifts of the various frequencies in the condensed states of the peroxide molecules with those of water. The figures summarized in Table VI are only approximate on account of the width of the absorption maxima. That the shifts of the O—H stretching frequency in peroxides are only half of those in water molecules might be considered an indication of weaker hydrogen bonds in the former. Other physical properties

**The present results for D_2O and HDO dissolved in carbon tetrachloride agree with those of a recent investigation of HDO vapor (4) as regards the frequency of ν_1 in that molecule.*

TABLE VI

FREQUENCY SHIFTS (IN CM.$^{-1}$) FOR WATER AND PEROXIDE MOLECULES IN CONDENSED PHASES

	H_2O_2	D_2O_2	H_2O	D_2O
Vapor – crystal (at −70°C.)				
ν bend.	−115	−53	−55	−30
ν stretch.	290	190	515	350
Vapor – solution in CCl_4				
ν stretch.	56	50	37	30

have been interpreted in the sense of nearly equal energy of these bonds in both compounds (15, 25). Judging from the shortest O—H · · · O distances in the crystals the difference cannot be very large since these distances are 2.78 Å in solid H_2O_2 (1) and 2.76 Å in ice. However, whereas in the latter all the hydrogen bonds are of equal length and tetrahedrally oriented, in H_2O_2 there are two slightly longer O—H · · · O distances per molecule, namely 2.90 Å. Comparison between the two types of molecules is further complicated by the fact that the shifts of the bending frequency are about twice as great in peroxides as in water. On the other hand the shifts in a non-polar solvent involve mainly van der Waals forces and this is confirmed by the observation that for peroxide and water solutions in carbon tetrachloride the shifts are roughly in the same ratio as the polarizability of the two molecules, 2.31 and 1.48 × 10^{-24} cm.^{3} (15).

Structural Parameters

The above data were used to calculate the force constants and bond lengths and angles in the peroxide molecule. All these have been published elsewhere (11) except for the two following points: First, the resolution of the rotational structure of a D_2O_2 band (Table III) makes possible some refinement of the molecular parameters. Thus the locus of points corresponding to the X_{01}

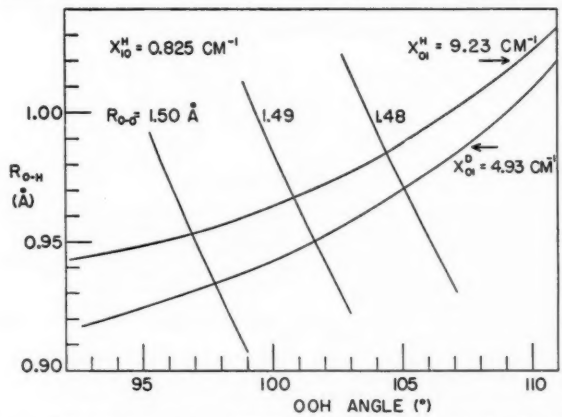

FIG. 14. Locus of O—H distances and OOH angles fitting the rotational constants of H_2O_2 and D_2O_2.

rotational constant for D_2O_2, 4.93 cm.$^{-1}$, has been added to the already published graph in Fig. 14. From the nearness of loci for the two isotopic molecules it is clear that more accuracy is needed for the D_2O_2 constant X_{01} in order to improve the situation significantly. The other point concerns the second rotational constant of H_2O_2 in the ground state, $X_{10} = 0.825$ cm.$^{-1}$ (34) contribution of which was not included in the published calculations. Since it corresponds to the harmonic mean of the two large moments of inertia it is very sensitive to changes in the O—O distance. Calculated values of this constant for $r_{O-O} = 1.48$, 1.49, and 1.50 Å have been plotted in Fig. 14 against r_{O-H} and α_{OOH}, the azimuthal angle being taken as 90°. The intersection of these curves shows that $r_{O-O} = 1.49 \pm 0.01$ Å in exact agreement with the X-ray data on the crystal (1) and within the limits of accuracy of the electron diffraction results (14). This datum is of special interest in connection with the single bond covalent radius of oxygen.

RÉSUMÉ

Le spectre infrarouge du peroxyde d'hydrogène a été mesuré de nouveau avec un appareil à prisme couvrant la région de 1.5 à 25μ. Une bande double, dont les centres sont situés aux environs de 460 et 575 cm.$^{-1}$, apparaît dans la vapeur due à la torsion des groupes OH. La bande rapportée précédemment à 3.8μ a été résolue; elle est attribuée à la combination des modes de déformation $\nu_2+\nu_6$, ce qui implique une anharmonicité positive. Dans le spectre d'absorption du liquide on a observé quatre nouvelles bandes.

On a également mesuré le spectre du peroxyde de deutérium dans les mêmes conditions. On a réussi à résoudre la structure fine d'une des fondamentales, ν_5, à 2661 cm.$^{-1}$, ce qui a permis de calculer les constantes de rotation de la molécule isotopique. Des mélanges des deux peroxydes contenant environ 45% de la molécule hybride HDO_2 ont aussi été étudiés. Enfin on a mesuré l'absorption de ces trois molécules en solutions diluées dans un solvant non polaire. A partir des nouvelles données on a obtenu les constantes de force des diverses liaisons ainsi que les paramètres suivants:

$$r_{O-O} = 1.49 \pm 0.01 \text{ Å},$$
$$r_{O-H} = 0.97 \pm 0.01 \text{ Å},$$
$$\alpha_{OOH} = 100 \pm 2°.$$

REFERENCES

1. Abrahams, S. C., Collin, R. L., and Lipscomb, W. N. Acta Cryst. 4: 15. 1951.
2. Bailey, C. R. and Gordon, R. R. Trans. Faraday Soc. 34: 1133. 1938.
3. Bain, O. Ph.D. Thesis, Laval University, Quebec. 1953.
4. Benedict, W. S., Gailar, N., and Plyler, E. K. J. Chem. Phys. 21: 1302. 1953.
5. Dieke, G. H. and Kistiakowsky, G. B. Phys. Rev. 45: 4. 1934.
6. Fehér, F. Ber. 72: 1778. 1939.
7. Fox, J. J. and Martin, A. E. Proc. Roy. Soc. (London), A, 174: 234. 1940.
8. Ganz, E. Helv. Chim. Acta, 28: 1580. 1945.
9. Gerhard, S. L. and Dennison, D. M. Phys. Rev. 43: 197. 1933.
10. Giguère, P. A. J. Chem. Phys. 18: 88. 1950.
11. Giguère, P. A. and Bain, O. J. Phys. Chem. 56: 340. 1952.
12. Giguère, P. A. and Liu, I. D. Can. J. Chem. 30: 948. 1952.
13. Giguère, P. A., Liu, I. D., Dugdale, J. S., and Morrison, J. A. Can. J. Chem. 32: 117. 1954.

14. GIGUÈRE, P. A. and SCHOMAKER, V. J. Am. Chem. Soc. 65: 2025. 1943.
15. GIGUÈRE, P. A. and SECCO, E. A. Can. J. Chem. 32: 550. 1954.
16. GIGUÈRE, P. A., SECCO, E. A., and EATON, R. S. Discussions Faraday Soc. 14: 104. 1953.
17. HARVEY, R. B. and BAUER, S. H. J. Am. Chem. Soc. 76: 859. 1954.
18. HERZBERG, G. Infrared and Raman spectra of polyatomic molecules. D. Van Nostrand Company, Inc., New York. 1945.
19. LASSETTRE, E. N. and DEAN, L. B. J. Chem. Phys. 17: 317. 1949.
20. LIU, I. D. Ph.D. Thesis, Laval University, Quebec. 1954.
21. LU, C. S., HUGHES, E. W., and GIGUÈRE, P. A. J. Am. Chem. Soc. 63: 1507. 1941.
22. LUFT, N. W. J. Chem. Phys. 21: 179. 1953.
23. LUFT, N. W. Private communication.
24. MASSEY, J. T. and BIANCO, D. R. J. Chem. Phys. 22: 442. 1954.
25. PAULING, L. Nature of the chemical bond. Cornell Univ. Press, Ithaca, N.Y. 1939.
26. PENNEY, W. G. and SUTHERLAND, G. B. B. M. J. Chem. Phys. 2: 492. 1934.
27. PITZER, K. S. J. Chem. Phys. 14: 239. 1946.
28. SUTHERLAND, G. B. B. M. and WILLIS, H. A. Trans. Faraday Soc. 41: 174. 1945.
29. TAYLOR, R. C. Ph.D. Thesis, Brown University, Providence, R.I. 1947.
30. TAYLOR, R. C. J. Chem. Phys. 18: 898. 1950.
31. WAGNER, E. L. and HORNIG, D. F. J. Chem. Phys. 18: 296. 1950.
32. WILLIAMS, V. Z. J. Chem. Phys. 15: 243. 1947.
33. WILSON, M. K. and BADGER, R. M. J. Chem. Phys. 17: 1232. 1949.
34. ZUMWALT, L. R. and GIGUÈRE, P. A. J. Chem. Phys. 9: 458. 1941.

A COMPARATIVE STUDY OF THE DEHYDRATION KINETICS OF SEVERAL HYDRATED SALTS[1]

By R. C. Wheeler[2] and G. B. Frost

ABSTRACT

Rates of dehydration under full vacuum, and also as the pressure of water vapor due to the dehydration process was allowed to increase, have been determined for a number of hydrated salts. The dehydration of manganous sulphate tetrahydrate, zinc sulphate heptahydrate, nickel sulphate hexahydrate, and magnesium sulphate heptahydrate has been found to proceed through the formation of amorphous intermediates, the last two of these being very stable. The dehydration of nickel nitrate hexahydrate, magnesium nitrate hexahydrate, and probably of ferrous sulphate heptahydrate and cobalt chloride hexahydrate at very low pressures takes place with the formation of crystalline intermediates. The results obtained are discussed in relation to the dependence of rate of dehydration on water vapor pressure previously reported for copper sulphate pentahydrate and for manganous oxalate dihydrate.

INTRODUCTION

It has been shown in an earlier paper (3) that when powdered samples of copper sulphate pentahydrate are dehydrated under vacuum at moderate temperatures, the dehydration proceeds to the monohydrate stage with a gradual decrease in rate. The product is amorphous in the sense that it does not diffract X-rays. However, if similar samples are placed in a closed and initially evacuated space, and the water vapor pressure due to the dissociation of the hydrate allowed to increase in the vessel, the rate of dehydration at first decreases to a minimum value, then increases to a value much larger than the minimum rate, this being followed, in turn, by a decline. The end product formed under these conditions is crystalline.

The minimum in rate occurs at a water vapor pressure of approximately 0.25 mm. and the periods of acceleration and decline, over a range in pressure of only a few millimeters, these pressures being far below those corresponding to possible phase equilibria. This marked effect of water vapor in a very narrow region of pressure has been observed also by carrying out dehydrations at a series of controlled pressures. The dehydration curves obtained for pressures below 0.25 mm. are quite different than for those above this value, the former showing a gradual loss in weight with time, while the latter show induction periods, the duration of which depends on the pressure.

The behavior of copper sulphate pentahydrate in this respect is similar to that of manganous oxalate dihydrate (6, 7), which for many years was regarded as unique in the dependence of its rate of dehydration on water vapor pressure. On vacuum dehydration this salt hydrate also yields a product which does not diffract X-rays.

Explanations of the form of these rate curves have been discussed elsewhere (1, 3, 4). The initial fall in rate is probably due to the retarding effect of water

[1]*Manuscript received November 16, 1954.*
Contribution from the Department of Chemistry, Queen's University, Kingston, Ontario.
[2]*Present address: Imperial Oil Fellow in Chemistry, Cambridge University.*

vapor on diffusion through a transition layer of amorphous material formed during the initial stages of dehydration, and the intermediate acceleration in rate, to an increase in porosity occurring on crystallization of the amorphous product in the presence of adsorbed water. The final decline is probably due to the gradually increasing impedance of the crystalline layer.

The purpose of the present work has been to survey the dehydration kinetics of a number of hydrated salts in order to obtain information regarding the generality of these effects. Rate determinations have been carried out for dehydrations at pressures of 10^{-5} mm. or less (designated as vacuum dehydrations in the following) and also while the pressure due to the liberated water vapor increased. For convenience, these latter are referred to as "increasing pressure" dehydrations. Determinations of rates of dehydration at externally controlled and constant pressures of water vapor have not been made in this work, although they give much more detailed information regarding the nature of the processes involved. However, such experiments are very time consuming, and it was desired to obtain comparative data for as many salts as possible.

EXPERIMENTAL METHOD

The salts used were reagent grade materials, recrystallized twice, air-dried, and screened, the "through 60 mesh on 80 mesh" fraction being used.

The essential features of the apparatus have been described (3). Powdered samples were placed in a small basket made of 100-mesh copper gauze, and suspended from a quartz spiral. The water vapor pressure in the system was measured by means of an oil manometer which had a conventional vertical arm and also an inclined arm for fine sensitivity in low pressure ranges. Readings of spiral extension and of pressure were made with a rigidly mounted cathetometer.

Vacuum dehydrations were carried out by allowing small samples (approximately 50 mgm. in most cases) to dehydrate while the pumps were in operation. Readings were plotted as weight-loss versus time. For several salts these curves were found to present points of interest, but they also served to establish the composition of the dehydration product. Increasing pressure dehydrations were carried out in the following manner. The samples were nucleated by allowing dehydration to proceed under vacuum to 10% of the total possible weight loss as determined by vacuum dehydration. The spiral case was then closed off from the pumps and the samples allowed to dehydrate and slowly build up a pressure of water vapor in the system. Readings of weight-loss were commenced at the beginning of the nucleation period, and those of pressure, at the time of closing off the spiral case, both of these being continued at a series of times for several hours. Determinations of rates of dehydration were made by evaluating tangents to the weight-loss versus time curves at a series of time values.

X-ray powder photographs were made using copper K_α radiation. For convenience, the term "X-ray amorphous" is used to describe products for which no diffraction lines were observed.

RESULTS

(1) *Manganous Sulphate Tetrahydrate*

Vacuum dehydration at 40°C. resulted in the smooth continuous weight-loss versus time curve shown in Fig. 1 (lower curve) the end product being of the monohydrate composition.

The results obtained on dehydration at 50°C. as the pressure of water vapor in the system increased are shown in Fig. 2.

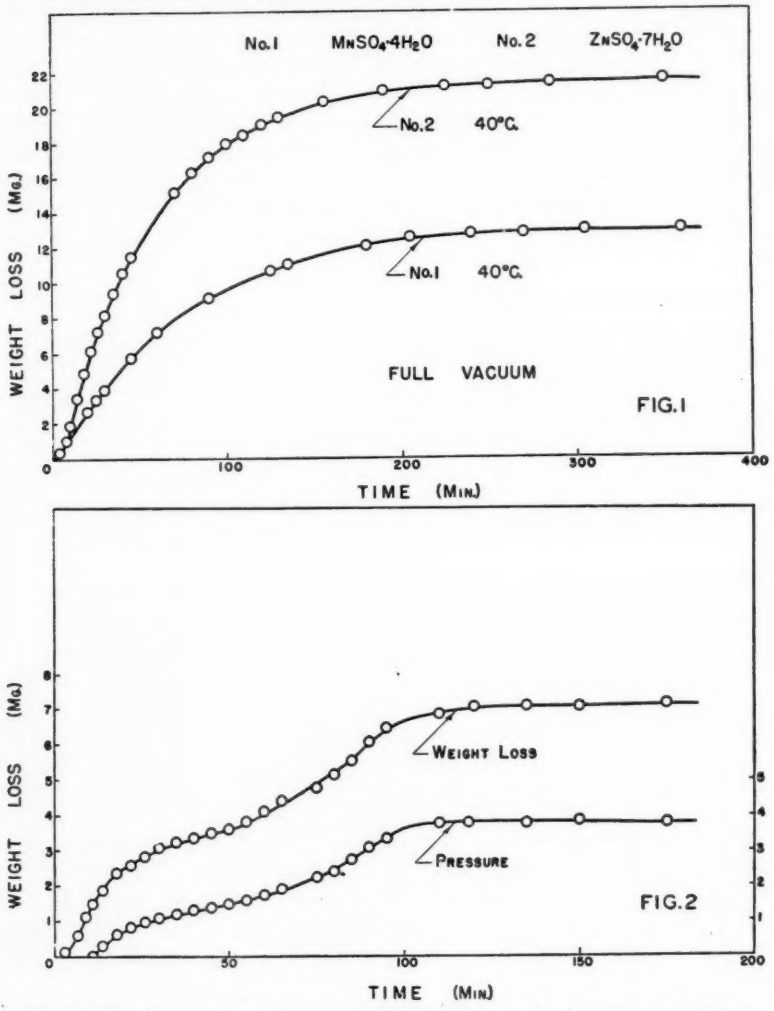

FIG. 1. The dehydration of zinc sulphate heptahydrate and of manganous sulphate tetrahydrate under vacuum.

FIG. 2. The dehydration of manganous sulphate tetrahydrate with increasing pressure of water vapor.

Following the period of nucleation under vacuum, the slope of the weight-loss curve gradually decreases as the pressure in the system becomes greater. The curve flattens somewhat at a weight-loss of about 3.5 mgm. which corresponds roughly to the trihydrate composition. An accelerated rate is then observed followed by a decline, the slope becoming zero at the dihydrate stage. These rates of dehydration plotted against the pressure, are shown in Fig. 3. Although the decline in rate to a minimum value, followed by an accelerated period, is similar to that reported for copper sulphate pentahydrate and for manganous oxalate dihydrate, the actual weight-loss versus time curve (Fig. 2) is slightly different in that a fairly rapid weight-loss persists for some time after the sample is exposed to water vapor, whereas with copper sulphate pentahydrate an induction period occurs almost immediately.

Unfortunately, X-ray data could not be obtained for this salt with the copper target available, since the absorption of the radiation was strong, resulting in fluorescent radiation.

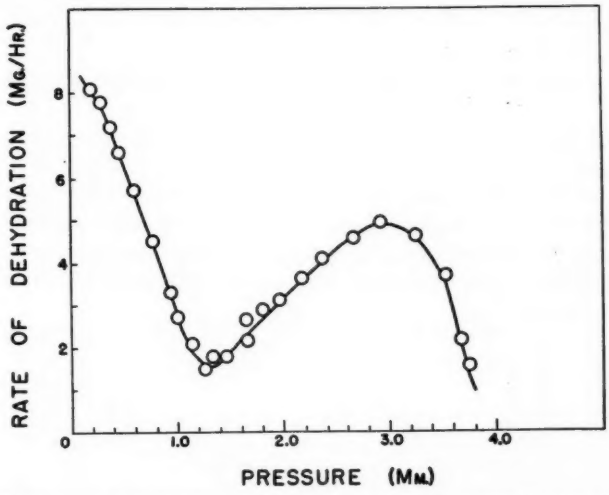

FIG. 3. The change in rate of dehydration of manganous sulphate tetrahydrate with pressure increase.

(2) *Zinc Sulphate Heptahydrate*

Vacuum dehydration at 40°C. again resulted in a smooth continuous curve (upper curve, Fig. 1), the end product being stoichiometrically of the monohydrate composition, and X-ray amorphous.

Measurements made at increasing pressure, and at 40°C., are shown in Fig. 4.

A small but reproducible induction period occurred immediately after nucleation, corresponding to the longer induction period observed for copper sulphate pentahydrate. Following this, the weight-loss curve has a slightly concave portion followed by a slightly convex portion, there being no clearly

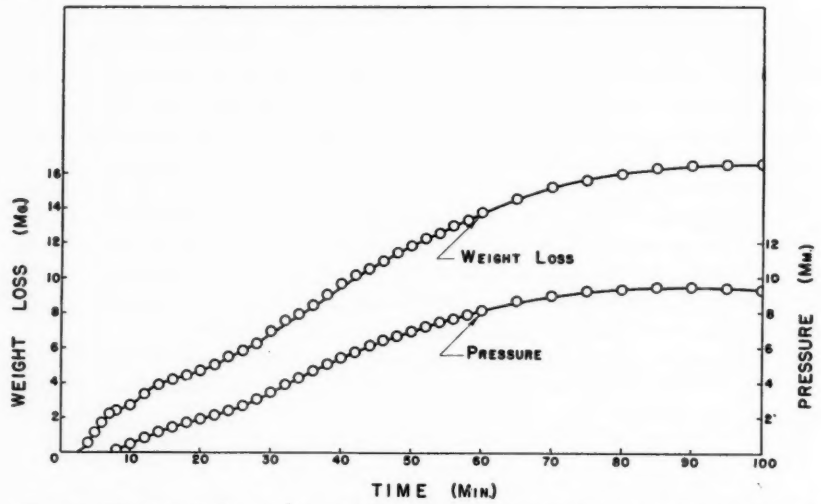

FIG. 4. The dehydration of zinc sulphate heptahydrate with increasing pressure of water vapor.

defined induction period. This resulted in two minima being obtained when the rate of dehydration was plotted against the pressure, as shown in Fig. 5.

X-ray powder photographs of the products obtained from these increasing pressure dehydrations showed a clearly defined diffraction pattern of monohydrate lines. Patterns identical with these were obtained when sealed samples of the amorphous product formed on vacuum dehydration were allowed to stand for several days.

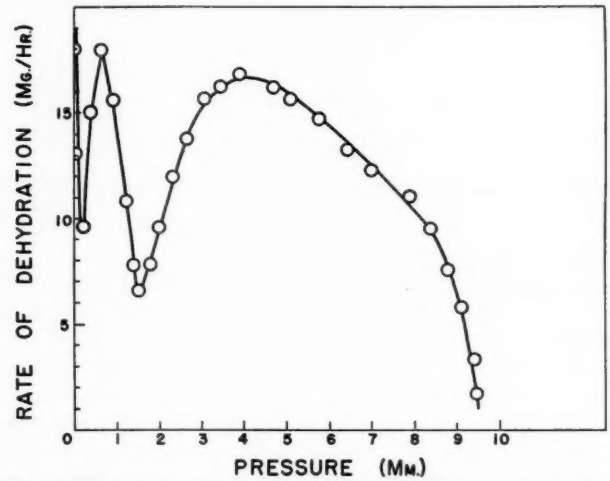

FIG. 5. The change in rate of dehydration of zinc sulphate heptahydrate with pressure increase.

(3) *Ferrous Sulphate Heptahydrate*

Dehydration under vacuum again exhibited a continuous loss of water from the heptahydrate to the monohydrate, the curve being similar to those shown in Fig. 1.

The weight-loss curve obtained on dehydration at increasing pressure at 60°C. is shown in Fig. 6.

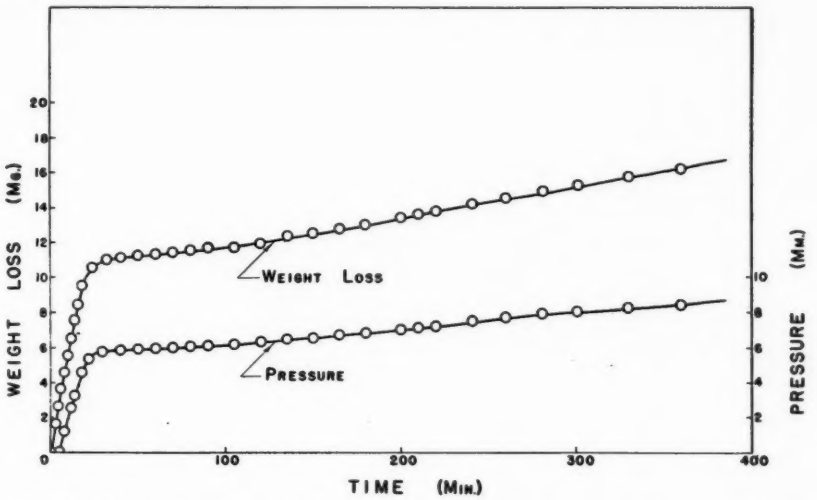

FIG. 6. The dehydration of ferrous sulphate heptahydrate with increasing pressure of water vapor.

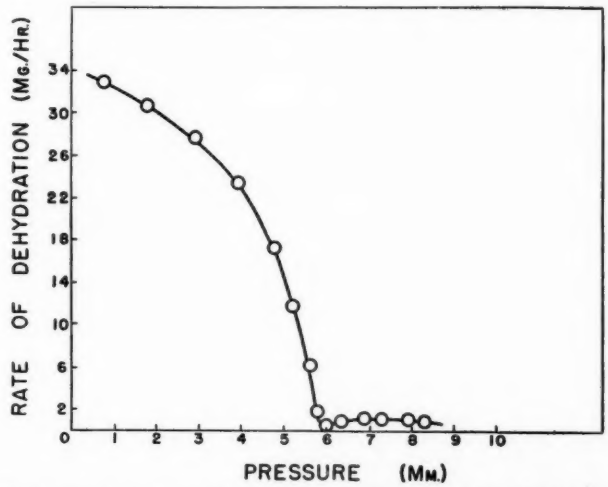

FIG. 7. The change in rate of dehydration of ferrous sulphate heptahydrate with pressure increase.

Following nucleation, rapid dehydration continued to somewhat beyond the tetrahydrate composition where an induction period set in followed by a slow increase in rate. This increase was diminished as the dehydration temperature was lowered, no increase being observed in a 21 hr. period at 40°C. The rate of dehydration at 60°C., plotted against the water vapor pressure, is shown in Fig. 7.

The curve is similar in character to that shown in Fig. 3, although the secondary increase in rate is much smaller, and the minimum occurs at a much higher pressure. It was not possible to obtain X-ray diffraction patterns for this salt for the reason that has been mentioned for manganous sulphate.

(4) *Nickel Nitrate Hexahydrate*

Vacuum dehydrations at several temperatures resulted in curves of different character than those described in the foregoing; the curve obtained at 40°C. is shown in Fig. 8, those obtained at other temperatures being similar. The initial loss of water is rapid and the rate nearly linear. After a weight-loss of about 6 mgm., the curve transforms to a second region which is also nearly linear, and then declines. If the two linear sections are extended to point A (Fig. 8), the point of intersection is found to be at approximately the tetrahydrate composition. The slopes of these linear portions were found to increase with temperature.

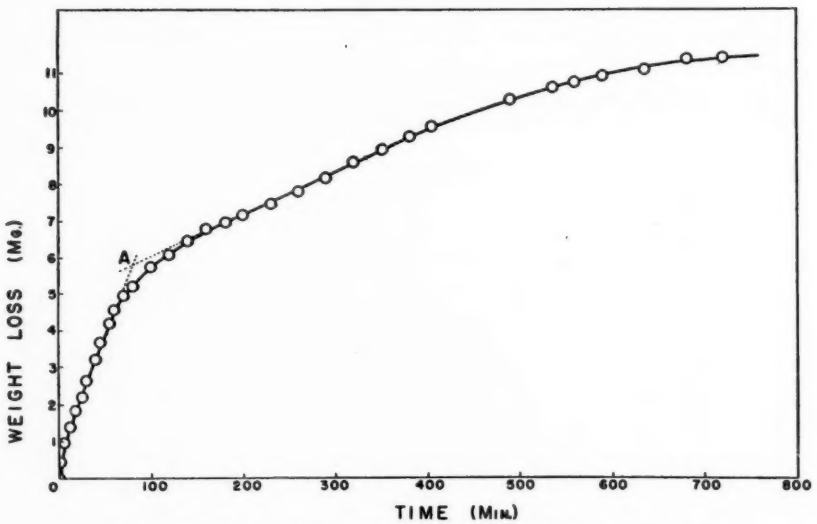

FIG. 8. The dehydration of nickel nitrate hexahydrate under vacuum.

The end product had the dihydrate composition. It appears, therefore, that under vacuum, dehydration takes place fairly rapidly to the tetrahydrate state, followed by the dehydration of this intermediate product to the dihydrate.

Unlike the examples reported in the foregoing, the end product of vacuum dehydration gave a definite X-ray diffraction pattern. However, if the time of preparation for the exposure were made as short as possible, the diffraction lines were very faint. It is possible that an amorphous material of very low stability was produced, subsequent handling being sufficient to cause the commencement of crystallization.

For dehydrations carried out at increasing pressure, an induction period was observed at the tetrahydrate stage followed by a slow and gradual increase in rate, the curves resembling closely those obtained for ferrous sulphate heptahydrate. Close examination of X-ray diffraction patterns obtained indicated the presence of tetrahydrate and dihydrate lines. It appears therefore that the first step in this process is the formation of crystalline tetrahydrate which then nucleates and forms crystalline dihydrate at a much slower rate. The rate of dehydration plotted against pressure is shown in Fig. 9, the curve again resembling that obtained for ferrous sulphate heptahydrate.

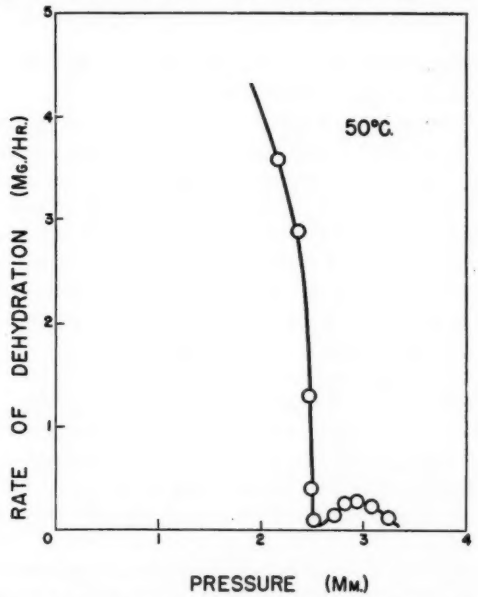

FIG. 9. The change in rate of dehydration of nickel nitrate hexahydrate with pressure increase.

The possibility of the formation of a basic salt in the dehydration process has been disregarded since it was found that the product formed both on vacuum and increasing pressure dehydration gave a pattern of only hexahydrate lines after standing in the room atmosphere for a few hours.

(5) *Magnesium Nitrate Hexahydrate*

Preliminary experiments with this salt indicated that effects occurred which were quite different from those observed for the other salts studied. Conse-

quently a number of dehydrations were carried out at several temperatures. The details of the experiments are given in Table I.

TABLE I

DEHYDRATION DATA FOR MAGNESIUM NITRATE HEXAHYDRATE

Expt. No.	Temp., °C.	Type of dehydration	Time of dehydration, min.	Sample wt., mgm.	Moles water lost per formula-wt.
1	30	Vacuum	1150	34.7	3.80
2	35	Vacuum	1166	40.2	3.92
3	40	Vacuum	1300	39.8	4.05
4	45	Vacuum	580	37.1	3.93
5	50	Vacuum	772	37.0	3.70
6	50	Vacuum	1370	37.3	3.98
7	55	Vacuum	510	38.9	2.39
8	40	Increasing pressure	1230	40.8	1.95
9	50	Increasing pressure	1415	35.4	3.42
10	40	Vacuum	35	32.3	1.89

Weight-loss versus time curves for the vacuum dehydration experiments Nos. 1, 3, 5, and 7 of Table I are shown in Fig. 10.

These dehydrations all displayed an induction period setting in at the tetrahydrate composition. These vacuum dehydration curves are, therefore, of the type which has been previously associated with dehydrations at increasing pressure. Furthermore, the period of acceleration following the induction period shows an interesting temperature dependence, the rate at 40°C. being higher than that at 30°C. and then declining as the temperature is raised.

Rate curves plotted against time, for these temperatures, are shown in Fig. 11. These curves show the minima and accelerated rates associated with increasing pressure dehydrations in the foregoing.

The end product of the vacuum dehydrations was found to be crystalline dihydrate, well defined and characteristic diffraction patterns being obtained. Clearly defined tetrahydrate lines were obtained with samples (Expt. 10) partially dehydrated to this stage. It appears quite definite, therefore, that on vacuum dehydration this salt forms crystalline tetrahydrate which then nucleates and forms crystalline dihydrate at rates which are markedly temperature dependent.

Experiments 8 and 9 of Table I were carried out at increasing pressure. Dehydration was observed to take place rapidly to the tetrahydrate stage at which an induction period set in, followed at 50°C. by a slow increase in rate, while at 40°C. no increase could be detected. The rate versus pressure curve obtained at 50°C. was found to be similar to that reported above for nickel nitrate hexahydrate.

Although many basic hydrated salts of magnesium have been reported, the formation of these takes place at dehydration temperatures exceeding 150°C. When the crystalline products obtained in the present experiments were allowed to stand in the humidity of the ordinary room atmosphere reversion to the hexahydrate crystalline form occurred.

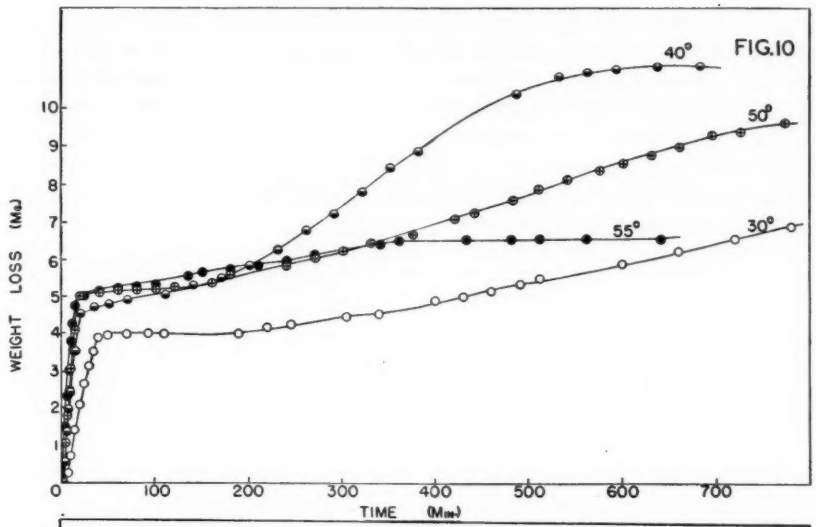

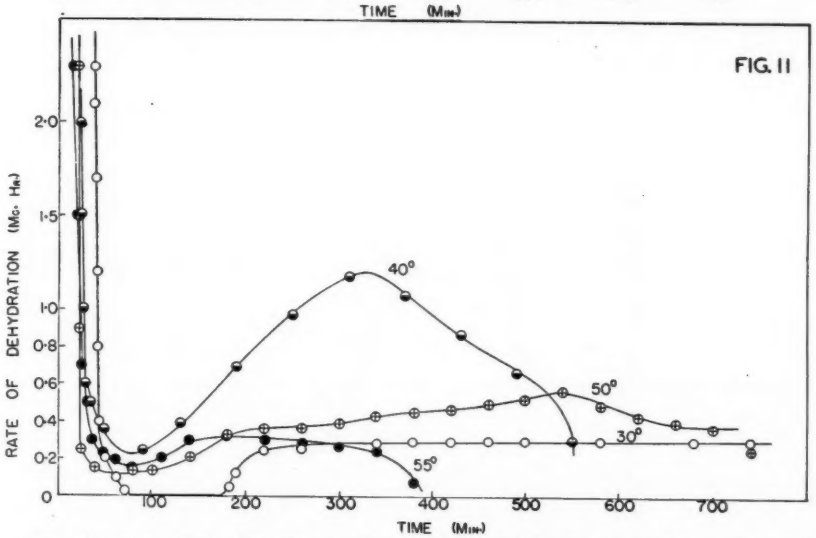

FIG. 10. The dehydration of magnesium nitrate hexahydrate under vacuum at several temperatures.

FIG. 11. The change in rate of dehydration of magnesium nitrate hexahydrate at several temperatures.

Since the dehydration from the tetrahydrate to the dihydrate stage has a temperature coefficient exhibiting a maximum in the region of 40°C., a careful survey of the rates in the temperature range from 30°C. to 55°C. was carried out. In order to make a comparison, the maximum rate of dehydration was found from the rate versus time curves (or from rate versus percentage decomposition curves) and converted to a rate per milligram of sample. (The com-

parison of maximum rates rather than rates obtained at the same percentage decomposition has been made in view of a suggestion by Colvin and Hume (1) that the maximum rates correspond to approximately the same interfacial conditions.) The results of these calculations are given in Table II and are

TABLE II

CALCULATED MAXIMUM RATES

Expt. No.	Temp., °C.	Maximum rate, mgm./hr./mgm.	Point Fig. 12
1	30.4	10.06	A
2	35.1	44.62	B
3	40.2	48.20	C
4	45.0	37.81	D
5	49.0	21.10	E
6	50.1	22.70	F
7	55.1	12.06	G

plotted in Fig. 12. From this figure it is clear that at temperatures above approximately 40°C., the mechanism of the dehydration process is in some way adversely affected by increase in temperature, the rate of dehydration becoming negligible above approximately 55°C.

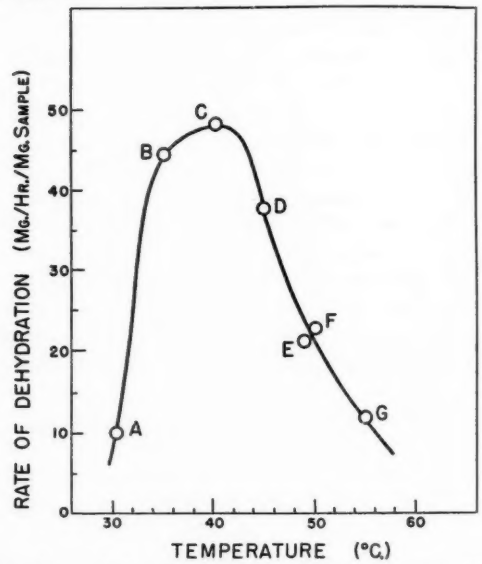

FIG. 12. The dependence of the second stage of the rate process on temperature for magnesium nitrate hexahydrate.

(6) *Magnesium Sulphate Heptahydrate*

Vacuum dehydration of this salt resulted in a smooth continuous curve of the same type as those shown in Fig. 1. The end product had the monohydrate

composition and was X-ray amorphous. Lines characteristic of the crystalline monohydrate appeared when amorphous samples were sealed and heated for two days at 130°C.

However, the behavior of this salt on dehydrating at increasing pressure was very different from that of any of the salts mentioned in the foregoing. It was found that the rate of dehydration gradually decreased with corresponding increase in pressure, no induction periods being observed. The product obtained was X-ray amorphous. The change of rate with pressure increase is shown in Fig. 13.

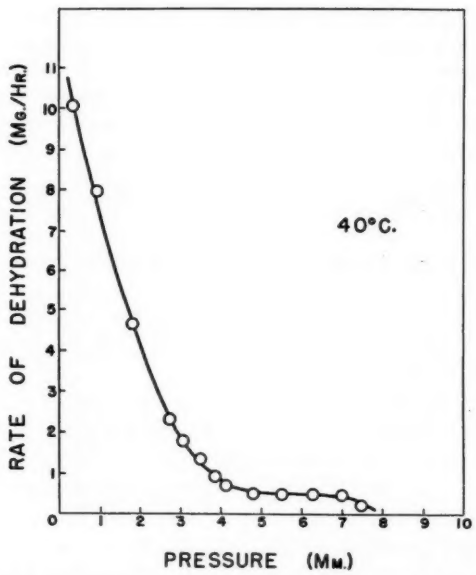

FIG. 13. The change in rate of dehydration of magnesium sulphate heptahydrate with pressure increase.

(7) *Nickel Sulphate Hexahydrate*

This salt was found to behave in similar manner to magnesium sulphate heptahydrate. The product of vacuum dehydration had the monohydrate composition and was X-ray amorphous. The effect of increasing water vapor pressure on the dehydration rate is similar to that shown in Fig. 13. Faint hexahydrate lines were obtained in this sample, indicating incomplete dehydration.

(8) *Cobalt Chloride Hexahydrate*

Vacuum dehydration resulted in curves similar to those obtained for nickel nitrate hexahydrate. These are shown in Fig. 14.

The rate of dehydration proceeds rapidly to the dihydrate stage followed by a much slower rate. Prolonged dehydration yields a product having the mono-

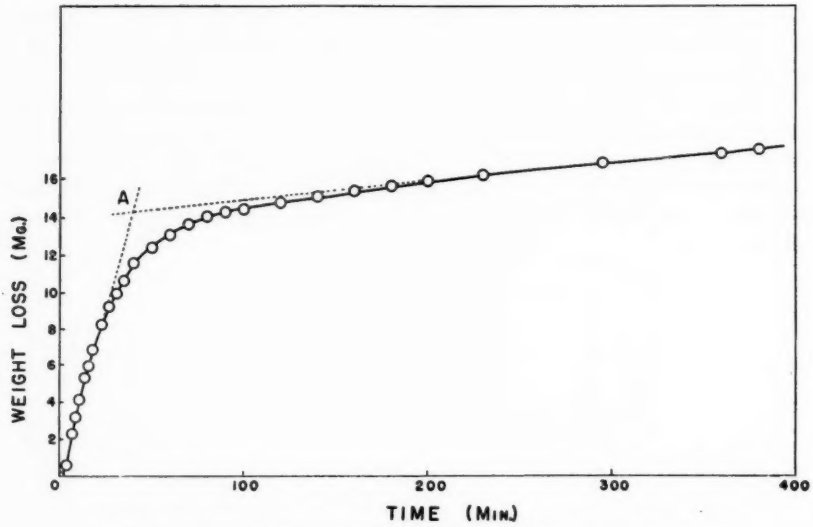

FIG. 14. The dehydration of cobalt chloride hexahydrate under vacuum.

hydrate composition. Unfortunately, the crystalline or amorphous character of the end product could not be definitely determined by X-ray diffraction for reasons which have been mentioned.

On dehydrating at increasing pressure, a rapid loss of water occurred to approximately the dihydrate composition, beyond which no change was observed. The change in rate with pressure increase is shown in Fig. 15.

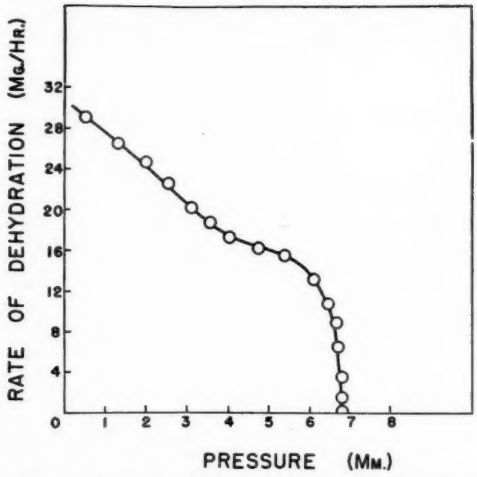

FIG. 15. The change in rate of dehydration of cobalt chloride hexahydrate with pressure increase.

DISCUSSION

Although it has not been possible to determine from X-ray evidence whether or not the product obtained from the vacuum dehydration of manganous sulphate tetrahydrate is amorphous, the similarity of the dehydration curves to those previously reported for copper sulphate pentahydrate (3) and for manganous oxalate dihydrate (6, 7) suggests that the dehydration process is the same in each case and is subject to the same interpretation. However, the minimum in the rate curve for the manganous salt occurs at about 1.2 mm., whereas for copper sulphate pentahydrate it occurs at about 0.25 mm., and for manganous oxalate dihydrate at less than 0.2 mm.

The dehydration process for zinc sulphate heptahydrate is more complex. Since an X-ray amorphous product is formed on vacuum dehydration, it is certain that this forms during the nucleation period. It is possible that the short induction period following nucleation (or therefore the first minimum in the rate curve) is due to the crystallization of this product at very low pressure. No adequate interpretation can be made of the second minimum at higher pressure on the basis of the present data and a more comprehensive study of the dehydration kinetics of this salt hydrate should be made.

Magnesium sulphate heptahydrate is of particular interest in that the dehydration curves obtained indicate that an X-ray amorphous product is formed not only on vacuum dehydration but also in the presence of water vapor at a pressure much higher than those observed for the other salts. The amorphous product is therefore very stable. This result suggests that this salt might be found to behave in a manner similar to copper sulphate pentahydrate if investigated over a wide range of controlled and constant pressures of water vapor. Experiments of this type are being carried out in this laboratory and will be reported in a later paper. The data given for nickel sulphate hexahydrate suggest a similar type of behavior.

The formation of crystalline products in the vacuum dehydration of nickel nitrate hexahydrate and magnesium nitrate hexahydrate indicates that if an amorphous product is formed at all, it must crystallize at extremely low water vapor pressures. Although the decomposition products obtained from ferrous sulphate heptahydrate could not be characterized by X-ray diffraction, the similarity of the dehydration curves to those obtained for nickel nitrate hexahydrate suggests that these products may be also crystalline. The minima observed in the rate versus pressure curves for these salts must be interpreted therefore in a somewhat different manner than has been done for copper sulphate pentahydrate. Instead of a process involving the crystallization of amorphous material, it must be assumed that as nuclei develop on the surfaces of the crystalline intermediates, the development of macrocrystalline aggregates is catalyzed by adsorbed water molecules.

The curves obtained for the dehydration of cobalt chloride hexahydrate are also similar to those obtained for nickel nitrate hexahydrate and it is probable that this dehydration also proceeds through the formation of a crystalline intermediate. However, with this salt the dehydration at increasing pressure does not proceed past the dihydrate stage, the corresponding pressure being

much lower than the equilibrium pressure reported by Derby and Yngve (2) for the hexahydrate – dihydrate – water vapor equilibrium. The behavior of this salt is of interest in comparison with that of magnesium sulphate heptahydrate, and a more comprehensive study of its dehydration kinetics is in progress.

The dehydration of magnesium nitrate hexahydrate is of particular interest, since the sequence of changes occurring on vacuum dehydration is that which is observed for other salts as the pressure of water vapor increases. Dehydration takes place rapidly with the formation of crystalline tetrahydrate which then nucleates and forms crystalline dihydrate. If it is assumed that the development of macrocrystals from these nuclei is catalyzed by water vapor, then this process must occur at the very low pressures prevailing in the transition layer as the water molecules liberated from the hexahydrate lattice pass through the crystalline tetrahydrate layer into the external evacuated space. The rate of escape of water molecules from the dehydrating tetrahydrate lattice will increase with temperature. However, any slight adsorption in the transition layer will decrease with the temperature. The opposition of these two effects may qualitatively explain the over-all dependence of rate on temperature which has been observed. However, any such explanation must be regarded as highly tentative in view of the lack of more comprehensive data. It will be observed from Fig. 10 that the rate of dehydration of the primary hexahydrate lattice increases with temperature in the normal manner, as also does both the primary and secondary rate for nickel nitrate hexahydrate.

It is clear from all the data presented in the foregoing that the effect of water vapor in first decreasing and then accelerating the over-all rate of dehydration, first observed by Topley and Smith for the decomposition of manganous oxalate dihydrate, is quite general and is always associated with an induction period in which a crystalline lower hydrate is formed from an intermediate. The intermediate may be an X-ray amorphous product or it may be crystalline. The nature of the X-ray amorphous product is, therefore, of interest. It may consist of an aggregate of microcrystals with dimensions of only a few unit cells, these being below the limiting size required for X-ray diffraction (about 100 Å). If this is so, the nature of the process whereby macrocrystals are formed in the presence of water molecules from X-ray amorphous intermediates does not differ in any essential way from that in which macrocrystals of the end product are formed from a nucleated crystalline intermediate. However, the heats of transition from the X-ray amorphous to the crystalline states which have been reported for the monohydrates of copper and zinc sulphate (4) are higher than might be expected from consideration of surface energy only, and it is possible that, for these salts at least, some condition other than high state of division results from low pressure dehydration of the primary lattices. The determination of such heats of transition for other salts is in progress.

The limiting pressure of water vapor above which amorphous products crystallize varies greatly from one salt hydrate to another, being virtually zero for nickel nitrate, magnesium nitrate, and cobalt chloride, and ranging to

presumably relatively high values for magnesium sulphate and nickel sulphate. Experiments carried out in this laboratory suggest that this effect is related to differences in the surface areas and capillary structures of the transition layer, although the nature of the amorphous material itself may also be a factor (5).

ACKNOWLEDGMENTS

Financial assistance given by the National Research Council of Canada during the progress of this work is gratefully acknowledged. One of the authors (R. C. W.) wishes to thank the Research Council of Ontario for a Scholarship held during part of this work.

REFERENCES

1. COLVIN, J. and HUME, J. Trans. Faraday Soc. 34: 969. 1938.
2. DERBY, I. H. and YNGVE, V. J. Am. Chem. Soc. 38: 1439. 1916.
3. FROST, G. B. and CAMPBELL, R. A. Can. J. Chem. 31: 107. 1953.
4. FROST, G. B., MOON, K. A., and TOMPKINS, E. H. Can. J. Chem. 29: 604. 1951.
5. QUINN, H. W., MISSEN, R. W., and FROST, G. B. Can. J. Chem. 33: 286. 1955.
6. TOPLEY, B. and SMITH, M. L. J. Chem. Soc. 321. 1935.
7. VOLMER, M. and SEYDEL, G. Z. physik. Chem. A, 179: 153. 1937.

NOTES

INTERDIFFUSION OF POLYISOBUTYLENE AND CYCLOHEXANE

By J. Kelly and A. T. Hutcheon

Prior to a more extensive study of the diffusion in dilute solutions of polyvinylacetate in acetone, results are reported here for one sample of polyisobutylene in interdiffusion with cyclohexane. The measurements were intended to be an experimental test for this system of the equation (5).

[1] $$D = \frac{RTP^{-1}\Phi^{\frac{1}{3}}}{\eta_0 N(M[\eta])^{\frac{1}{3}}}$$

in which the product $P^{-1}\,\Phi^{\frac{1}{3}}$ is claimed to be a constant for all polymer systems and the other symbols have their usual significance. Furthermore, the dependence of the diffusion coefficient on concentration serves as a test of the equation (4).

[2] $$Y = \frac{1+2\Gamma_2 c+3\Gamma_3 c^2}{D} = \frac{1+k_s c}{D_0}$$

since Γ_2 has been obtained from osmotic pressure measurements (2), and k_s from sedimentation (6) data assuming a linear dependence of the frictional coefficient on concentration.

EXPERIMENTAL

The diffusion was carried out in a Neurath cell (7) at 30°C. ±0.02 in a constant temperature air bath on a vibration-free mounting. The diffusion coefficients were calculated by the area-maximum ordinate method (3) from measurements of the refractive index gradient obtained by the scale method of Lamm (10).

The diffusion coefficient was measured at three different initial concentrations and at time intervals of several hours for each concentration, as shown in Table I. Average values of D_A are given for concentrations 0.2636 and 0.3660 gm./100 ml. For the concentration 0.5676 gm./100 ml., there was a decided gradual decrease in the value of D_A with time and for this experiment a corrected value of D was obtained by extrapolation to infinite time of the plot of D versus 1/time. This procedure is necessary when the boundary is not initially sharp (8).

The average and corrected values of D_A and the value of $\Gamma_2 = 0.63$ (2) were used in plotting the function

$$Y = (1+2\Gamma_2 c+3\Gamma_3 c^2)/D$$

against the mean concentration $c_0/2$ in Fig. 1 for $\Gamma_3 = \frac{5}{8}\,.\,\Gamma_2^2$ and $\Gamma_3 = \frac{1}{4}\,.\,\Gamma_2^2$. From the intercept, $1/D_0$, D_0 is calculated to be 3.3×10^{-7} cm.^{2} sec^{-1}.

TABLE I

DIFFUSION COEFFICIENTS, D_A, FOR POLYISOBUTYLENE IN CYCLOHEXANE AT 30°C.—MOLECULAR WEIGHT 86,700

Concentration, gm./100 ml.	Time (sec.)	$D_A \times 10^7$, cm.²/sec. (Area-maximum ordinate method)
0.2636	63,270	3.31
0.2636	122,550	3.23
	Average value	3.27±0.04
0.3660	22,350	3.27
0.3660	30,177	3.23
0.3660	58,895	3.28
0.3660	86,430	3.23
	Average value	3.25±0.03
0.5676	28,020	3.48
0.5676	41,516	3.41
0.5676	82,183	3.35
0.5676	104,940	3.34
	Corrected value	3.29

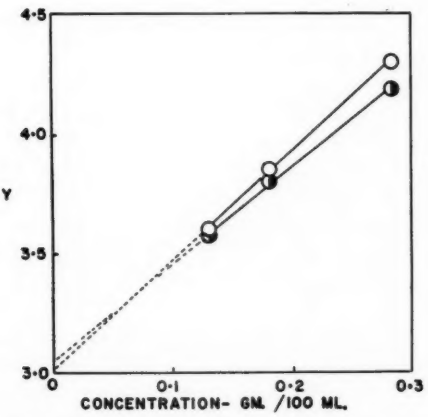

FIG. 1. $Y = (1+2\Gamma_2 c+3\Gamma_3 c^2)/D = (1+k_d c)/D_0$ as a function of concentration $c_0/2$, in gm./100 ml.

○ — $\Gamma_3 = \frac{5}{8}.\Gamma_2^2$
◑ — $\Gamma_3 = \frac{1}{4}.\Gamma_2^2$

DISCUSSION

This experimental value may be compared with that calculated from equation 1. Using Flory's data (6)—$\eta_0 = 9.7 \times 10^{-3}$ poises, $[\eta] = 2.76\times10^{-4} M^{0.69}$, $M = 86{,}700$, and $P^{-1}\Phi^{\frac{1}{3}} = 2.65 \times 10^{-6}$ for this particular fraction—D_0 is calculated to be 2.8×10^{-7} cm.²/sec. at 20°C. The value of $D_0 = 3.4 \times 10^{-7}$ cm.²/sec. at 30°C. is obtained from the relation (7)

$$D_0^{30} = D_0^{20} \frac{T_{30}\eta_{20}}{T_{20}\eta_{30}}$$

where T is the absolute temperature and η the viscosity of the solvent. This is in good agreement with the experimental value and better agreement would be obtained using the average value of $P^{-1}\,\Phi^{\frac{1}{3}}$ reported as 2.5×10^6 (1).

From equation 2, the slope of the plot of Y versus concentration is equal to k_s/D_0. From the data of Flory *et al.* on sedimentation (2), k_s is equal to 1.28 for this fraction of polyisobutylene, hence, using the calculated value of D_0, the predicted slope would be $1.28/(3.4 \times 10^{-7}) = 3.8 \times 10^6$. If the observed value of D_0 equal to 3.3×10^{-7} were used, the slope would be 3.9×10^6. The observed slopes in Fig. 1 are 4.6×10^6 for $\Gamma_3 = \frac{5}{8}.\Gamma_2^2$ and 4.1×10^6 for $\Gamma_3 = \frac{1}{4}.\Gamma_2^2$ when Y is plotted against $c_0/2$ from Table II. The suggestion

TABLE II

VALUES OF $Y = (1+2\Gamma_2 c+3\Gamma_3 c^2)/D = (1+k_s c)/D_0$ AS A FUNCTION OF CONCENTRATION

Concentration $c_0/2$, gm./100 ml.	$D_0 \times 10^7$ cm.²/sec.	$Y \times 10^{-6}$ for $\Gamma_3 = \frac{5}{8}.\Gamma_2^2$	$Y \times 10^{-6}$ for $\Gamma_3 = \frac{1}{4}.\Gamma_2^2$
0.132	3.27	3.61	3.58
0.183	3.25	3.86	3.81
0.284	3.29	4.31	4.20

that the third virial coefficient should be less than $\frac{5}{8}.\Gamma_2^2$ (9) and that it is $\frac{1}{4}.\Gamma_2^2$ (2) is therefore supported by these data.

The values of D at the concentration of 0.2636 gm./100 ml. were least precise and if the other values at 0.3660 and 0.5676 gm./100 ml. are weighted more in drawing the lines in Fig. 1, the slope of the line for $\Gamma_3 = \frac{1}{4}.\Gamma_2^2$ would be 3.96×10^6 and D_0 would be 3.23×10^{-7} cm.²/sec., which corresponds to $P^{-1}\,\Phi^{\frac{1}{3}} = 2.5 \times 10^6$ in equation 1, in agreement with Flory's best average value (1). The data are not sufficiently precise to contend for exact values of $P^{-1}\,\Phi^{\frac{1}{3}}$ or Γ_3, but the conclusion that $\Gamma_3 = \frac{1}{4}.\Gamma_2^2$ is more nearly correct than $\Gamma_3 = \frac{5}{8}.\Gamma_2^2$ is inescapable and that it *may* be exactly $\frac{1}{4}.\Gamma_2^2$ is not contradicted by these results.

The above good agreement between theory and experiment is for the diffusion coefficient calculated by the area-maximum ordinate method; there is some discrepancy, in these experiments, between D_A and D_σ (second moment method (6)) unlike the results of Schulz and Meyerhoff (8). The D_σ values generally lie *below* those for the area-maximum ordinate method. The reasons for this discrepancy are not known and will be discussed more fully in a future publication.

ACKNOWLEDGMENT

The authors are much indebted to Doctors Krigbaum and Flory for the sample of polyisobutylene and to the National Research Council of Canada for financial assistance.

1. FLORY, P. J. Principles of polymer chemistry. Cornell Univ. Press, Ithaca, N.Y. 1953. p. 628.
2. KRIGBAUM, W. R. and FLORY, P. J. J. Am. Chem. Soc. 75: 1775. 1953.
KRIGBAUM, W. R. Private communication.

3. LAMM, O. Nova Acta Regiae Soc. Sci. Upsaliensis, 10(4): 6. 1937.
4. MANDELKERN, L. and FLORY, P. J. J. Chem. Phys. 19: 984. 1951.
5. MANDELKERN, L. and FLORY, P. J. J. Chem. Phys. 20: 212. 1952.
6. MANDELKERN, L., KRIGBAUM, W. R., SCHERAGA, H. A., and FLORY, P. J. J. Chem. Phys. 20: 1392. 1952.
7. NEURATH, H. Chem. Revs. 30: 357. 1942.
8. SCHULZ, G. V. and MEYERHOFF, G. Makromol. Chem. 7: 294. 1952.
9. STOCKMAYER, W. H. and CASASSA, E. F. J. Chem. Phys. 20: 1560. 1952.
10. SVEDBERG, T. The ultracentrifuge. Oxford University Press, Toronto. 1940. p. 253.

RECEIVED NOVEMBER 3, 1954.
DEPARTMENT OF CHEMISTRY,
MCMASTER UNIVERSITY,
HAMILTON, ONTARIO.

UNIT CELL, SPACE GROUP, AND INDEXED X-RAY DIFFRACTION POWDER DATA FOR CERTAIN NARCOTICS
VII. MORPHINE HYDROCHLORIDE TRIHYDRATE, AND THE DIHYDRATES OF MORPHINE HYDROBROMIDE, MORPHINE HYDRIODIDE, CODEINE HYDROCHLORIDE, CODEINE HYDROBROMIDE, CODEINE HYDRIODIDE[1]

BY W. H. BARNES AND JUNE M. LINDSEY[2]

Morphine hydrochloride (anhydrous, and trihydrate) and morphine hydriodide dihydrate were the only hydrohalide salts of morphine or of codeine included in the collection of X-ray diffraction powder data completed in this laboratory some time ago as an aid to the identification of certain narcotics (1, 3). It was realized at the time of this survey that morphine hydrobromide, and the hydrochloride, hydrobromide, and hydriodide of codeine should be examined at some future date. Through the kindness of Dr. C. G. Farmilo, specimens of all four hydrohalide salts (in the form of the dihydrates) were obtained in due course, and their unit cell constants, space groups, and powder patterns (indexed for $d > \backsim 3$ Å), together with single-crystal data for morphine hydrochloride trihydrate and for morphine hydriodide dihydrate, have now been determined. At the same time the powder patterns for the last two salts, which are recorded in full elsewhere (3), have been indexed for those reflections corresponding to $d > \backsim 3$ Å. The experimental methods have been described in detail previously (1, 2, 3).

Of the various narcotics studied during the powder-data survey (3), morphine, codeine, and thebaine were selected as the first to be considered for complete structural investigation because of the widespread interest in their stereochemical configuration (11). In view of the fact, however, that their molecules are asymmetric, it was decided to use the corresponding hydrohalide salts in an application of the isomorphous-replacement method to the problem. This eliminated thebaine for which only the free base and the hydrochloride were immediately available.

The six salts of morphine and codeine, which are the subject of the present note, crystallized from water in rosettes, and in sheaves, of needles, elongated

[1]*Issued as N.R.C. No. 3524.*
[2]*National Research Laboratories Postdoctorate Fellow.*

in the direction of the *c*-axis. Individual crystals of the codeine hydrohalides, however, were somewhat larger, and of better form, than those of the corresponding salts of morphine. They were of almost square cross-section and could be cut readily to cubical shape of suitable size for single-crystal study. Primarily for these reasons, therefore, codeine hydrobromide dihydrate was selected for the investigation of the structure of the codeine molecule, and the isomorphous codeine hydriodide dihydrate was employed to provide data of assistance in the allocation of signs to the observed structure amplitudes. A brief account of the results of this investigation has been given elsewhere (7) and full details will be published later (8).

An interesting feature of the hydrohalide salts of morphine and of codeine is that the phase normally available from commercial sources (and obtained by crystallization from water or dilute alcohol at ordinary temperatures) is the dihydrate in all cases with the exception of morphine hydrochloride, which crystallizes as the trihydrate. The existence of other hydrates, and of the anhydrous salts, has been reported in the literature (10), and an extensive series of hydration–dehydration studies is now in progress in this laboratory. It is hoped to report X-ray diffraction data for some of these other hydrate phases in a subsequent note in order to supplement existing powder data for *anhydrous* morphine hydrochloride (3).

Single-crystal data, obtained from precession photographs (Cu K_α, λ = 1.5418 Å), for morphine hydrochloride trihydrate, morphine hydrobromide dihydrate, morphine hydriodide dihydrate, and the dihydrates of codeine hydrochloride, hydrobromide, and hydriodide, are summarized in Table I;

TABLE I

SINGLE CRYSTAL DATA (M = MORPHINE, $C_{17}H_{19}O_3N$; C = CODEINE, $C_{18}H_{21}O_3N$)

	M.HCl.3H$_2$O	M.HBr.2H$_2$O	M.HI.2H$_2$O	C.HCl.2H$_2$O	C.HBr.2H$_2$O	C.HI.2H$_2$O
a(Å)	13.04	12.75	13.04	12.93	13.10	13.44
b(Å)	20.78	20.04	20.34	20.47	20.86	21.38
c(Å)	6.92$_1$	6.92$_3$	6.87$_4$	6.82$_3$	6.81$_8$	6.83$_6$
S.G.	$P2_12_12_1$	$P2_12_12_1$	$P2_12_12_1$	$P2_12_12_1$	$P2_12_12_1$	$P2_12_12_1$
Z(mols. per cell)	4	4	4	4	4	4
ρ(gm./ml.)						
(calc.)	1.335	1.511	1.637	1.368	1.483	1.568
(obs.)	1.334	1.518	1.641	1.368	1.489	1.565

the accuracy of the unit cell dimensions is about ±0.3%. The powder data (Co K_α, λ = 1.790 Å; camera diameter, 114.6 mm.) for the six salts are given in Table II, where B and BB identify lines that were broader and much broader, respectively, than the general average for a particular film, and an asterisk (under d(Obs.)) indicates the probable presence of a line the intensity of which was too low ($I/I_1 < 1$) for accurate measurement. Only the indexed data are shown for morphine hydrochloride trihydrate and for morphine hydriodide dihydrate because a complete list of observed spacings and relative intensities for each of these salts has already been recorded (3). The powder photographs of morphine hydrobromide dihydrate, codeine hydrochloride

dihydrate, codeine hydrobromide dihydrate, and codeine hydriodide dihydrate are reproduced in Fig. 1 for comparison with those of morphine hydrochloride

TABLE II

X-RAY DIFFRACTION POWDER DATA (INDEXED FOR $d > \sim 3$ Å)

I/I_1	d(Å) Obs.	d(Å) Calc.	hkl	I/I_1	d(Å) Obs.	d(Å) Calc.	hkl	I/I_1	d(Å) Obs.	d(Å) Calc.	hkl
					Morphine hydrochloride trihydrate						
1	11.1	11.0	110	1	4.59	4.63	211		*	3.35	160
85	10.4	10.4	020			4.58	131			3.34	102
75	8.11	8.12	120	20	4.32	4.32	221	10	3.33	3.33	340
	*	6.57	011	—	—	4.25	310			3.30	112
		6.52	200	20	4.15	4.15	041			3.28	022
		6.22	210		*	4.06	240		*	3.26	400
100	6.11	6.12	130	—	—	4.01	320			3.25	331
		6.11	101	100	3.95	3.96	141,150	—	—	3.22	410
85	5.80	5.86	111			3.91	231	10	3.19	3.18	122
		5.76	021			3.68	301,330			3.13	251
	*	5.52	220	10B	3.63	3.62	311	70	3.11	3.11	420
50	5.22	5.27	121			3.56	051			3.10	032,061
		5.19	040	60	3.50	3.50	241,250	—	—	3.06	202,260
40	4.87	4.90	031			3.47	321			3.02	212
		4.83	140			3.46	002,060	50	3.01	3.01	132,161
50	4.76	4.75	230	30B	3.42	3.44	151			3.00	341,350
		4.74	201			3.41	012				
					Morphine hydrobromide dihydrate						
3	10.8	10.8	110		*	3.47	051	15	2.25		
20	10.0	10.0	020			3.46	002	25	2.23		
30	7.87	7.88	120			3.42	241	25	2.19		
2	6.50	6.54	011	75	3.41	3.41	012,321	25	2.15		
25	6.37	6.38	200			3.39	250	10	2.12		
40	6.11	6.08	101	1	3.35	3.35	151	20	2.09		
		6.07	210			3.34	060,102	1	2.07		
60	5.89	5.92	130			3.29	112	20	2.03		
		5.82	111	20B	3.26	3.27	022	3	2.01		
60	5.69	5.69	021			3.24	340	2	1.94		
1	5.38	5.38	220			3.23	160	30	1.90		
50	5.21	5.20	121			3.19	400	5	1.88		
20	5.03	5.01	040	20	3.17	3.18	331	3BB	1.82		
	*	4.81	031			3.17	122	3	1.76		
60	4.70	4.69	201			3.15	410	5	1.74		
		4.66	140	—	—	3.07	032	5	1.71		
		4.61	230	45	3.05	3.05	251	3	1.70		
30B	4.59	4.57	211			3.04	202,420	10	1.66		
		4.50	131		*	3.01	061,212	2BB	1.61		
25	4.25	4.25	221			2.99	132	5	1.58		
	*	4.16	310	50	2.91			2	1.56		
15	4.06	4.06	041	10	2.89			3	1.54		
	*	3.94	240	20	2.79			3	1.52		
		3.91	320	15	2.69			2	1.50		
100	3.87	3.87	141	15	2.63			2	1.45		
		3.84	231	15	2.59			1	1.43		
	*	3.82	150	5B	2.48			1	1.42		
—	—	3.62	301	30	2.38			3	1.40		
		3.59	330	15	2.33						
30	3.57	3.56	311	10	2.28						
					Morphine hydriodide dihydrate						
50	11.0	11.0	110	3	4.57	4.61	211	30	3.38	3.39	012,060
	*	10.2	020			4.53	131			3.38	151
1	8.04	8.02	120	10	4.27	4.29	221			3.32	102
35	6.49	6.52	200			4.25	310			3.30	340
		6.51	011	1	4.10	4.09	041	10B	3.27	3.28	112,160
—	—	6.21	210		*	4.01	240			3.26	022,400
		6.08	101			4.00	320			3.23	331
60	6.03	6.02	130	100	3.89	3.90	141			3.22	410
		5.83	111			3.88	150,231	5	3.15	3.16	122
20B	5.75	5.70	021	—	—	3.67	301			3.10	420
1	5.47	5.49	220			5.66	330	40	3.09	3.08	251
60	5.21	5.22	121	20	3.60	3.61	311			3.07	032
	*	5.09	040	—	—	3.50	051				
—	—	4.83	031			3.46	241				
		4.74	140	40	3.45	3.45	250,321				
70	4.72	4.73	201			3.44	002				
		4.70	230								

TABLE II (*Concluded*)

I/I_1	d(Å) Obs.	d(Å) Calc.	hkl	I/I_1	d(Å) Obs.	d(Å) Calc.	hkl	I/I_1	d(Å) Obs.	d(Å) Calc.	hkl
Codeine hydrochloride dihydrate											
10	11.0	10.9	110	—	—	3.64	301,330	5	2.67		
30	10.2	10.2	020	5	3.58	3.59	311	5B	2.57		
70	8.04	8.03	120	—	—	3.51	051	5	2.48		
—	—	6.47	011,200	5	3.45	3.46	241,250	10	2.42		
—	—	6.16	210			3.43	321	5B	2.35		
55	6.03	6.03	101,130	—	—	3.41	002,060	1	2.28		
—	—	5.79	111			3.39	151	2	2.24		
75	5.68	5.68	021	20	3.36	3.36	012	5	2.20		
	*	5.47	220	2	3.30	3.30	102,160	1	2.16		
30	5.17	5.20	121				340	10	2.13		
		5.12	040			3.26	112	2	2.11		
		4.82	031	2	3.24	3.24	022	10	2.05		
30B	4.75	4.76	140			3.23	400	2B	2.01		
		4.69	201,230	—	—	3.21	331	20	1.97		
		4.57	211			3.19	410	1	1.93		
1	4.54	4.52	131	10	3.13	3.14	122	1	1.90		
2	4.27	4.27	221	25	3.08	3.08	251,420	2	1.88		
—	—	4.22	310		*	3.05	032,061	10	1.84		
2	4.10	4.09	041	—	—	3.02	202,260	1	1.78		
	*	4.01	240	20	2.97						
		3.97	320	8	2.89						
100	3.91	3.90	141,150	1	2.84						
		3.87	231	20	2.76						
Codeine hydrobromide dihydrate											
	*	11.1	110	—	—	3.70	330	15	2.90		
25	10.4	10.4	020			3.68	301	2	2.84		
20	8.16	8.16	120	20	3.61	3.62	311	25B	2.78		
		6.55	200			3.56	051	25	2.71		
5	6.52	6.48	011	—	—	3.52	250	25	2.59		
5	6.24	6.25	210			3.50	241	2	2.51		
—	—	6.14	130	20	3.48	3.48	060	5B	2.44		
45	6.04	6.05	101			3.47	321	15	2.38		
		5.81	111		*	3.43	151	1	2.35		
30B	5.75	5.71	021			3.41	002	2	2.23		
—	—	5.55	220	40	3.35	3.36	012,160	1	2.21		
		5.23	121			3.35	340	18	2.13		
75	5.22	5.21	040			3.30	102	5	2.08		
		4.87	031			3.28	400	5	2.04		
25	4.84	4.85	140	5B	3.25	3.26	112	20	1.99		
—	—	4.77	230			3.25	331	5	1.90		
40	4.71	4.72	201			3.24	022,410	10	1.86		
		4.61	211			3.15	122	5	1.78		
5	4.58	4.56	131	35	3.13	3.13	251,420	5	1.76		
	*	4.30	221			3.10	061	2B	1.71		
		4.27	310			3.07	260	1	1.47		
10	4.14	4.14	041	1	3.06	3.06	032	1	1.42		
—	—	4.08	240			3.02	202,350				
1	4.03	4.03	320			3.01	161,341				
	..	3.98	150	15B	2.99	2.99	212				
100	3.95	3.95	141			2.98	132				
		3.91	231			2.96	430				
Codeine hydriodide dihydrate											
30	11.5	11.4	110			3.57	241	15	2.61		
10	10.7	10.7	020	30	3.56	3.56	060	1	2.57		
5	8.34	8.37	120			3.54	321	5	2.52		
—	—	6.72	200		*	3.50	151	2B	2.46		
		6.51	011	—	—	3.44	160	20	2.43		
25	6.43	6.41	210			3.43	340	5B	2.38		
—	—	6.30	130	25	3.42	3.42	002	20	2.29		
45	6.09	6.09	101	30	3.36	3.37	012	1	2.26		
50	5.86	5.86	111			3.36	400	15	2.24		
1	5.76	5.76	021		*	3.32	331,410	30	2.14		
—	—	5.69	220			3.31	102	20	2.02		
—	—	5.34	040		*	3.27	112	1	1.99		
85	5.29	5.29	121			3.26	022	5	1.95		
		4.97	140			3.20	420	5	1.93		
25	4.94	4.93	031	25B	3.18	3.19	251	15	1.89		
	*	4.89	230			3.16	061,122	2	1.82		
75	4.78	4.79	201			3.15	260	2	1.80		
—	—	4.68	211			3.09	350	1BB	1.73		
10	4.64	4.63	131	20	3.08	3.08	032,161	1BB	1.68		
		4.38	310			3.07	341	5	1.63		
5	4.37	4.37	221	—	—	3.05	202	5B	1.59		
		4.21	041			3.04	430	1	1.56		
5	4.20	4.18	240			3.02	212	1	1.54		
		4.13	320			3.01	401	1	1.51		
5	4.10	4.07	150	10B	3.00	3.00	132	1	1.49		
		4.02	141			2.99	411	1	1.47		
100	4.01	3.98	231			2.98	170	2	1.44		
—	—	3.79	330	20	2.92						
—	—	3.75	301	25	2.85						
30	3.68	3.69	311	25BB	2.78						
	*	3.62	051	1	2.72						
		3.61	250	15	2.66						

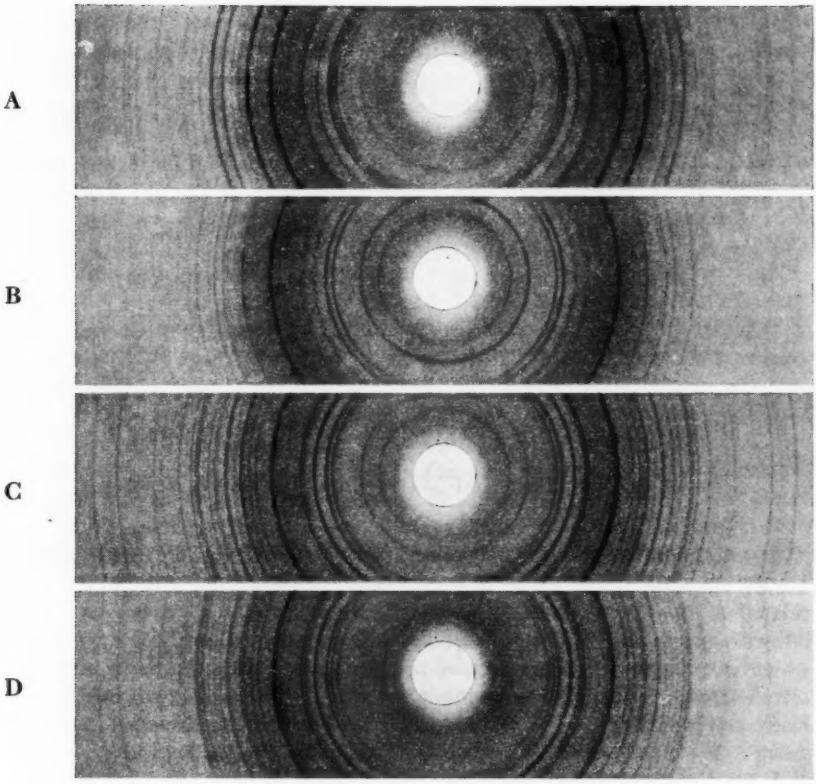

FIG. 1. X-ray diffraction powder photographs of A, morphine hydrobromide dihydrate; B, codeine hydrochloride dihydrate; C, codeine hydrobromide dihydrate; D, codeine hydriodide dihydrate. (Camera diameter: 114.6 mm.; radiation: Co K_α, $\lambda = 1.790$ Å).

trihydrate and morphine hydrobromide dihydrate, which will be found elsewhere (3).

It should be mentioned that the orientation chosen for the unit cells is $c < a < b$ in conformity with the convention recommended in Dana's *System of Mineralogy* (4) and in *Crystal Data* (5), and with that adopted for codeine (anhydrous free base) and for codeine monohydrate (free base) in *Barker's Index* (9) and by Groth (6).

Mr. B. J. Cowick assisted with the powder investigations.

1. BARNES, W. H. Bull. Narcotics U.N. Dept. Social Affairs, 6(1): 20. 1954.
2. BARNES, W. H. and FORSYTH, W. J. Can. J. Chem. 32: 984. 1954.
3. BARNES, W. H. and SHEPPARD, H. M. Bull. Narcotics U.N. Dept. Social Affairs, 6(2): 27. 1954.
4. DANA, J. D. and DANA, E. S. System of mineralogy. 7th ed. Vol. 1. *By* C. Palache, H. Berman, and C. Frondel. John Wiley & Sons, Inc., New York. 1944. p. 6.

5. DONNAY, J. D. H. and NOWACKI, W. Crystal data. Geol. Soc. Amer., Mem. No. 60. 1954. p. 138.
6. GROTH, P. Chemische Krystallographie. Vol. 5. W. Engelmann, Leipzig. 1919. pp. 964, 965.
7. LINDSEY, J. M. Acta Cryst. 7: 651. 1954.
8. LINDSEY, J. M. and BARNES, W. H. Acta Cryst. In press.
9. PORTER, M. W. and SPILLER, R. C. The Barker index of crystals. W. Heffer and Sons, Ltd., Cambridge, England. 1951. Index Nos. O.2059, O.2060.
10. SMALL, L. F. Chemistry of the opium alkaloids. Suppl. No. 103. Public Health Service, Washington. 1932. pp. 150, 189.
11. STORK, G. *In* The alkaloids. Vol. 2. *Edited by* R. H. F. Manske and H. L. Holmes. Academic Press, Inc., New York. 1952. p. 171. Rapoport, H. and Lavigne, J. B. J. Am. Chem. Soc. 75: 5329. 1953. Ginsburg, D. Bull. Narcotics U.N. Dept. Social Affairs, 6(1): 32. 1954.

RECEIVED NOVEMBER 17, 1954.
DIVISION OF PHYSICS,
NATIONAL RESEARCH COUNCIL,
OTTAWA, CANADA.

THE IDENTITY OF CRYPTOCAVINE AND CRYPTOPINE[1]

BY A. F. THOMAS,[2] LÉO MARION, AND R. H. F. MANSKE

Cryptocavine ($C_{21}H_{23}O_5N$) has been reported to occur in various fumariaceous plants (2) and to be different from, but isomeric with and closely related to cryptopine I. Its structure IV was deduced (3) from the Emde reduction of the methosulphate followed by dehydration with acetyl chloride which gave anhydrotetrahydromethylcryptocavine, very similar to anhydrotetrahydromethylcryptopine II obtained in the same way from cryptopine (4). Both anhydrotetrahydro derivatives, on oxidation with potassium permanganate, gave the same products, i.e., 5,6-methylenedioxy-*o*-toluic aldehyde and 4,5-dimethoxy-2-β-dimethylaminoethylbenzaldehyde. The slight difference between the anhydrotetrahydro compounds was ascribed to geometrical isomerism (3).

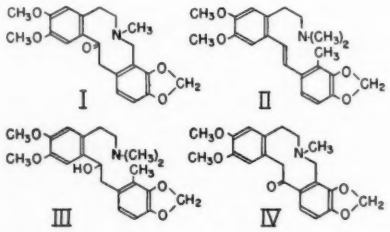

Construction of models of II showed that the *cis*-form would be highly strained with the aromatic rings partly overlapping. Examination, however, of the specimen originally obtained from cryptocavine and one freshly prepared from pure cryptopine showed that the two were identical. Both crystallized from dilute methanol as long colorless silky needles, m.p. 110°, undepressed on

[1]*Issued as N.R.C. No. 3522.*
[2]*National Research Council of Canada Postdoctorate Fellow.*

admixture, and both possessed the same absorption in the ultraviolet ($\lambda_{max.}$ 330 mμ, log ϵ, 4.38; $\lambda_{min.}$ 264 mμ, log ϵ, 3.91) and in the infrared. It is perhaps significant that at no time were we able to crystallize Perkin's tetrahydromethylcryptopine III although several preparations were made, and it is noteworthy that Perkin states that II contains solvent of crystallization when freshly prepared, and that the melting points of both II and III were the same (4).

The apparent confirmation of structure IV for cryptocavine (3) made it of interest to examine the *trans*-annular amide formation of this molecule. The perchlorate was prepared (crystallized from aqueous methanol, m.p. 226–228°, dec. Calc. for $C_{21}H_{23}O_5N.HClO_4$: Cl, 7.55. Found: Cl, 7.36, 7.42%), but was found to have an infrared absorption spectrum identical with that of cryptopine perchlorate. The free bases had the same pK_a value (8.09) which was higher than expected in view of the fact that cryptopine had been reported to be a weak base (1). Debye-Scherrer powder photographs of the two bases were the same, as were the infrared absorption spectra in various media. The melting point of a mixture of cryptocavine and cryptopine was not lowered provided that pure cryptopine was used, but it was found that any mixture of the pure bases with the cryptopine sample originally used (3) was indeed liquid at 205° as reported (3). Furthermore, both the Debye-Scherrer photograph and the infrared absorption spectrum of this sample contained all the characteristics of the corresponding photograph and spectrum of pure cryptopine, together with a few minor additional lines and peaks. The latter were all present in the Debye-Scherrer photograph and the infrared spectrum of protopine. Hence the sample of cryptopine originally used for comparison was contaminated with protopine. The melting point of this sample was taken again and found to be not 221°, but 204–208°. It must, therefore, be concluded that cryptocavine is identical with cryptopine, and the designation cryptocavine should be deleted from the literature.

ACKNOWLEDGMENTS

The pure cryptopine used in this work was obtained from the Dyson Perrins Laboratory, through Dr. A. S. Bailey whose courtesy we acknowledge. Our thanks are also due to Mr. R. Lauzon and Dr. R. N. Jones for the infrared spectra and to Dr. Maria Przybylska for the Debye-Scherrer photographs.

1. ANET, F. A. L., BAILEY, A. S., and ROBINSON, R. Chemistry & Industry, 944. 1953.
2. MANSKE, R. H. F. Can. J. Research, B, 15: 274. 1937; B, 16: 438. 1938; B, 17: 51. 1939; B, 18: 75. 1940.
3. MANSKE, R. H. F. and MARION, L. J. Am. Chem. Soc. 62: 2042. 1940.
4. PERKIN, W. H. J. Chem. Soc. 109: 815. 1916.

RECEIVED DECEMBER 9, 1954.
DIVISION OF PURE CHEMISTRY,
NATIONAL RESEARCH COUNCIL,
OTTAWA, CANADA.

CANADIAN JOURNAL OF CHEMISTRY

Notes to Contributors

Manuscripts

(i) ***General.*** Manuscripts, in English or French, should be typewritten, double spaced, on paper 8½×11 in. **The original and one copy are to be submitted.** Tables and captions for the figures should be placed at the end of the manuscript. Every sheet of the manuscript should be numbered.

Style, arrangement, spelling, and abbreviations should conform to the usage of this journal. Names of all simple compounds, rather than their formulas, should be used in the text. Greek letters or unusual signs should be written plainly or explained by marginal notes. Superscripts and subscripts must be legible and carefully placed.

Manuscripts should be carefully checked before they are submitted; authors will be charged for changes made in the proof that are considered excessive.

(ii) ***Abstract.*** An abstract of not more than about 200 words, indicating the scope of the work and the principal findings, is required, except in Notes.

(iii) ***References.*** References should be listed **alphabetically by authors' names,** numbered, and typed after the text. The form of the citations should be that used in this journal; in references to papers in periodicals, titles should not be given and only initial page numbers are required. All citations should be checked with the original articles and each one referred to in the text by the key number.

(iv) ***Tables.*** Tables should be numbered in roman numerals and each table referred to in the text. Titles should always be given but should be brief; column headings should be brief and descriptive matter in the tables confined to a minimum. Vertical rules should be used only when they are essential. Numerous small tables should be avoided.

Illustrations

(i) ***General.*** All figures (including each figure of the plates) should be numbered consecutively from 1 up, in arabic numerals, and each figure referred to in the text. The author's name, title of the paper, and figure number should be written in the lower left corner of the sheets on which the illustrations appear. Captions should not be written on the illustrations (see Manuscripts (i)).

(ii) ***Line Drawings.*** Drawings should be carefully made with India ink on white drawing paper, blue tracing linen, or co-ordinate paper ruled in blue only; any co-ordinate lines that are to appear in the reproduction should be ruled in black ink. Paper ruled in green, yellow, or red should not be used unless it is desired to have all the co-ordinate lines show. All lines should be of sufficient thickness to reproduce well. Decimal points, periods, and stippled dots should be solid black circles large enough to be reduced if necessary. Letters and numerals should be neatly made, preferably with a stencil (**do NOT use typewriting**) and be of such size that the smallest lettering will be not less than 1 mm. high when reproduced in a cut 3 in. wide.

Many drawings are made too large; originals should not be more than 2 or 3 times the size of the desired reproduction. In large drawings or groups of drawings the ratio of height to width should conform to that of a journal page but the height should be adjusted to make allowance for the caption.

The original drawings and one set of clear copies (e.g. small photographs) are to be submitted.

(iii) ***Photographs.*** Prints should be made on glossy paper, with strong contrasts. They should be trimmed so that essential features only are shown and mounted carefully, with rubber cement, on white cardboard with no space or only a **very** small space (less than 1 mm.) between them. In mounting, full use of the space available should be made (to reduce the number of cuts required) and the ratio of height to width should correspond to that of a journal page (4¾ × 7½ in.); however, allowance must be made for the captions. Photographs or groups of photographs should not be more than 2 or 3 times the size of the desired reproduction.

Photographs are to be submitted in duplicate; if they are to be reproduced in groups one set should be mounted, the duplicate set unmounted.

Reprints

A total of 50 reprints of each paper, without covers, are supplied free. Additional reprints, with or without covers, may be purchased.

Charges for reprints are based on the number of printed pages, which may be calculated approximately by multiplying by 0.6 the number of manuscript pages (double-spaced typewritten sheets, 8½ × 11 in.) and including the space occupied by illustrations. An additional charge is made for illustrations that appear as coated inserts. The cost per page is given on the reprint requisition which accompanies the galley.

Any reprints required in addition to those requested on the author's reprint requisition form must be ordered officially as soon as the paper has been accepted for publication.

Contents

Page

Organic Fluorine Compounds. I. An Improved Synthesis of Hexafluoroacetone—*A. T. Morse, P. B. Ayscough, and L. C. Leitch* 453

The Synthesis of Hemopyrrole-dicarboxylic Acid and of Some Dipyrromethenes—*S. F. MacDonald and R. J. Stedman* - - 458

Simple Pyrroles as Bases—*R. J. Stedman and S. F. MacDonald* - 468

Photolysis of Acetone in the Presence of Mercury Dimethyl—*H. G. Oswin, R. Rebbert, and E. W. R. Steacie* - - - - - - - 472

Studies on Carrageenin: Comparison of Fractions Obtained with Potassium Chloride and by Successive Extraction at Elevated Temperatures—*D. A. I. Goring and E. Gordon Young* - - - 480

The Photo-oxidation of Azomethane—*G. R. Hoey and K. O. Kutschke* - - - - - - - - - - - - - - - - 496

The Preparation of Dicyanodiacetylene—*F. J. Brockman* - - - 507

Alloys of Indium: The System Indium-Lead-Tin—*A. N. Campbell, R. M. Screaton, T. P. Schaefer, and C. M. Hovey* - - - - - 511

Hydrogen Peroxide and its Analogues. VI. Infrared Spectra of H_2O_2, D_2O_2, and HDO_2—*Osias Bain and Paul A. Giguère* - - - 527

A Comparative Study of the Dehydration Kinetics of Several Hydrated Salts—*R. C. Wheeler and G. B. Frost* - - - - - 546

Interdiffusion of Polyisobutylene and Cyclohexane—*J. Kelly and A. T. Hutcheon* - - - - - - - - - - - - - - - - 562

Unit Cell, Space Group, and Indexed X-ray Diffraction Powder Data for Certain Narcotics. VII. Morphine Hydrochloride Trihydrate, and the Dihydrates of Morphine Hydrobromide, Morphine Hydriodide, Codeine Hydrochloride, Codeine Hydrobromide, Codeine Hydriodide—*W. H. Barnes and June M. Lindsey* - 565

The Identity of Cryptocavine and Cryptopine—*A. F. Thomas, Léo Marion, and R. H. F. Manske* - - - - - - - - - - 570

Printed in Canada *by* University of Toronto Press